COMPUTER-ASSISTED IMAGE ANALYSIS OF HUMAN OVARIAN FOLLICLES: IMAGING PHYSIOLOGIC SELECTION

A Thesis Submitted to the College of

Graduate Studies and Research

In Partial Fulfillment of the Requirements

For the Degree of Master's of Science

In Interdisciplinary Studies

University of Saskatchewan

Saskatoon

By

ELHAM REZAEISARLAK

PERMISSION TO USE

In presenting this thesis in partial fulfilment of the requirements for a Postgraduate degree from the University of Saskatchewan, I agree that the Libraries of this University may make it freely available for inspection. I further agree that permission for copying of this thesis in any manner, in whole or in part, for scholarly purposes may be granted by the professor or professors who supervised my thesis work or, in their absence, by the Head of the Department of Obstetrics, Gynaecology and Reproductive sciences or the Dean of the College of Medicine. It is understood that any copying, publication, or use of this thesis or parts thereof for financial gain shall not be allowed without my written permission. It is also understood that due recognition shall be given to me and to the University of Saskatchewan in any scholarly use which may be made of any material in my thesis.

Requests for permission to copy or to make other use of material in this thesis in whole or part should be addressed to:

Head of the Department of Obstetrics, Gynaecology and Reproductive Sciences

College of Medicine

University of Saskatchewan

Saskatoon, SK

S7N 0W8

GENERAL ABSTRACT

Antral ovarian folliculogenesis involves recruitment of a cohort of small follicles, physiological selection of a dominant follicle, and ovulation. The mechanism of selection has not been precisely determined. Identification of the timing of preovulatory selection is a key component in understanding natural and peri-menopausal ovarian function, ovarian suppression for contraception, and improvement of ovarian stimulation protocols. Morphologic characteristics obtained by ultrasonography cannot be precisely quantitated by the human eye. Computer-assisted image analysis overcomes subjective human evaluation of ultrasonographic images.

The objectives of this research were to assess ultrasound image attributes of human dominant (DF) and 1st subordinate (SF1) ovarian follicles during natural menstrual cycles and following discontinuation of conventional and continuous oral contraceptives (OC). We utilized sophisticated computer algorithms to elucidate an association between image attributes and physiologic status of follicles. Transvaginal ultrasonographic images obtained in 2 previous studies were used to quantify changes that occur in ovarian follicles.

We detected quantitative differences between the dominant and largest subordinate follicles of ovulatory and major anovulatory follicular waves, as well as during the first wave following OC discontinuation. Differences in ultrasonographic image attributes were associated with the physiological status of follicles. Evidence of follicular dominance in follicles which develop during major ovulatory waves or following OC discontinuation can be detected prior to the time of selection manifest by differences in dominant and subordinate follicle diameters. In addition, differences in quantitative image attributes were detected between ovulatory and anovulatory DF. Follicles that develop following conventional and continuous OC administration schemes exhibit the same image characteristics.

Further research is necessary to elucidate the exact correlation of follicle image attributes during all stages of development with histological characteristics, prediction of the timing of DF selection and the effects of different OC formulations on follicle development during and following OC cessation. Computer-assisted image analysis of ultrasound images has the potential to develop into a diagnostic, prognostic, and research tool for the in vivo evaluation of ovarian physiology and pathology and elucidate biologically important times such as physiologic selection, ovulation of DF and characterization of abnormal follicles (i.e., follicular cysts, luteinized unovulated follicles).

ACKNOWLEDGMENTS

This research project would not have been achievable without the support of many people. In the first place, the author wishes to express her gratitude to her supervisor, Dr. Roger A. Pierson who was abundantly helpful and offered invaluable assistance, support and guidance. He has provided for an optimum working environment at the Obstetrics and Gynecology Department, where a lack of resources is something unimaginable due to his managerial skills and foresight. I am also indebted to Dr. Marla Lujan, who has been a source of enthusiasm and encouragement over these years. I also would like to express my sincere appreciation to her excellent guidance, teaching, endless support, friendship, and the time she devoted to me.

Deepest gratitude are also due to the members of the supervisory committee, Drs. Olufemi (Femi) A. Olatunbosun, Gregg Adams, Jaswant Singh, and Angela R. Baerwald, without whose knowledge and assistance this study would not have been successful. I wish convey my deepest regard to Mr. John Deptuch for his continual computer expertise and technical support. To all members of the group I am very grateful for the cooperative spirit and the excellent working atmosphere, creating a unique setting for intellectual explorations.

I wish to express love and gratitude to my beloved family; Afsoun and Afshin, for their understanding & endless love through the duration of my study. Afsoun, thank you for understanding if I couldn't help you much with your school work because, I was too busy with my thesis.

Finally, I owe special gratitude to my parents, brothers, and my sister, for their continuous and unconditional support and encouragement.

DEDICATED TO

My parents, who offered me unconditional love and put inside me all the right stuff including adventure and freedom.

TABLE OF CONTENTS

LIST OF FIGURES

LIST OF ABBREVIATIONS

AMH = anti-mullerian hormone

BDNF = brain-derived neurotrophic factor

BMP-15 = bone morphogenetic protein 15

cAMP = cyclic adenosine monophasphate

CC = cumulus cells

CL = corpus luteum

COC = cumulus oocyte complex

DF = dominant follicle

E2 = estrogens

E-A = estrogen active

EE = ethinyl estradiol

EGF = epidermal growth factors

E-I = estrogen inactive

ER = Elham Rezaei

FGF = fibroblast growth factors

FSH = follicle stimulating hormone

FGF-7 = fibroblast growth factor-7

GH = growth hormone

GSV = gray-scale values

GDF-9 = growth differentiation factor 9

GC = granulosa cells

HA = hyaluronin

HAF = hemorrhagic anovulatory follicles

HFI = hormone free interval

IGF = insulin-like growth factors

IOI = interovulatory interval

LH = luteinizing hormone

LUF = luteinized unruptured follicles

MGC = mural granulosa cells

NGF = nerve growth factor

NPV = numerical pixel value

OMI = oocyte maturation inhibitor

OCT3/4 = Octamer3/4

PH = pixel heterogeneity

PLAP = placental/germ-like cell alkaline phosphatises

PAF = plasminogen activation factor

PA = plasminogen activator

PG = prostaglandins

RSV = region selected volume

RAP = Roger Allen Pierson

SF1 = 1st subordinate follicle

TGF-β = transforming growth factor β

TGF = transforming growth factors

TNFRsf = tumour necrosis factor receptor superfamily

TNF-α = tumour necrosis factor-α

TA = transabdominal

TV = transvaginal

ZP = zona pellucida glycoproteins

VEGF = vascular endothelial growth factor

Chapter 1

1. GENERAL INTRODUCTION

1.1 Human ovarian follicular dynamics

The first concepts of human reproduction were described in the Aristotelian doctrine. Aristotle believed that the egg was formed in the uterus as a consequence of menstrual blood activation by the male semen. During the seventeenth century, Jan Swammerdam and Johannes Van Horne of Leiden and Niels Stensen of Copenhangen independently developed the new idea that the female "testes", like the ovaries of birds, were the sites of egg formation [1]. Their works were never formally published. Later, a Dutch anatomist, named Regnier de Graaf (1641-1673) provided the first descriptions of the mammalian female gonad after making a comprehensive study. He wrote:

> *The common function of the female testicles is to generate eggs, foster them and bring them to maturity. Thus, in women, they perform the same task as do the ovaries of birds. Hence they should be called women's ovaries rather than testicles, especially as they bear no similarity either in shape or content to the male testicles properly so-called. On account of this lack of similarity they have been regarded by many as bodies without function; quite wrongly, because they are absolutely essential for generation* [2].

Albrecht von Haller (1708-1777) subsequently named the ovarian follicle after de Graaf despite the fact that he made an error in defining of the fluid-filled follicle as an egg. Later in 1827, Carl Ernst von Baer described the true ova of mammals as the follicle-enclosed "ovulum". The history of reproductive research shows that considerable progress was made in spite of the technical limitations and erroneous observation, and that these early studies have provided the foundation for this field.

1.1.1 Human ovarian anatomy

The ovaries are dull white, paired ovoid structures which have an average volume of 11 cm^3 in reproductively mature women [3]. The ovary develops from the genital ridge (the ventral cranial mesonephrone) in vertebrate embryos. Germ cells originate in the yolk sac, then migrate to the ovary during early gestation (6 weeks) [1]. In embryonic and early fetal life, the ovaries are located in the lumbar region. They gradually descend to the lesser pelvis, and lie on each side of uterus close to the lateral wall. Each ovary has lateral and medial surfaces, superior and inferior extremities, and anterior and posterior borders. The suspensory ligament, a peritoneal fold of the ovary, is attached to the upper part of the lateral surface of the ovary and contains the ovarian vessels and nerves. The ovarian ligament attaches the medial aspects of the ovary to the lateral angle of the uterus and contains some smooth muscle cells. The ovarian ligament is continuous with the medial border of the round ligament. The mesoovarium, a short peritoneal fold, attaches the ovary to the back of the broad ligament and carries blood vessels and nerves to the ovarian hilum. Thus, the ovary nestles in the posterior wall of the broad ligament and is connected to the fimbriated end of the fallopian tubes [1].

The ovarian arteries originate from the abdominal aorta below the renal arteries and supply the ovaries, the uterine tubes, the labium majus and the inguinal region [3]. The ovarian veins emerge from the ovary as a plexus then form 2 ovarian veins which ascend with the ovarian arteries. They enter the inferior vena cava on the right side and into the renal vein on the left side. Lymph vessels ascend along the ovarian arteries to preaortic and lateral nodes via 3 main routes. The ovarian neural plexuses are comprised of postganglionic sympathetic, parasympathetic and visceral afferent fibres. Efferent sympathetic fibres emerge from the tenth and eleventh thoracic spinal segment and are vasoconstrictory. Parasympathetic fibres are derived from the inferior hypogastric

plexuses and are probably vasodilatory. The nerves follow the ovarian artery to the ovary and uterine tube [3].

The mature human ovary consists of an outer zone, the cortex, and an inner zone, the medulla. A specialized mesothelium (the surface epithelium) covers the ovarian cortex. It contains an outer strip of connective tissue, the tunica albuginea and an inner zone that contains the follicles [3]. After puberty in a young female, the ovary consists of: 1) surface epithelium; 2) cortex; and, 3) medulla. The major part of ovary forms from the cortex. The cortex contains follicles at different stages of development, corpora lutea and atretic follicles depending on the age of the women and stage of the menstrual cycle. The follicles are embedded in a stroma which is primarily comprised of collagen fibres. The central part of the ovary is called the medulla. It contains dense connective tissue, numerous veins, spiral arteries, lymphatic vessels and nerves [3].

1.1.2 Oogenesis

During embryonic development, primordial germ cells migrate to the coelomic epithelium of the gonadal ridges at the beginning of week 4 of gestation. The stage of gestation is calculated as the time since the 1st day of the woman's last menstrual period [3, 4]. Sexual differentiation occurs in weeks 6 and 7 of gestation [5]. The primordial germ cells proliferate and develop into oogonia between weeks 7 and 9 [6]. By the twentieth week of embryonic life, oogonia enter meiotic prophase and become oocytes. All germ cells then undergo meiosis in response to factors produced by the rete ovarii which are small masses of blind tubules or solid cords in the medulla of the mammalian ovary near the hilus which are homologous with the rete testis in the male [7]. Most of the oocytes are arrested at the diplotene stage of meiotic prophase I (32 μm in diameter) and are referred to as primary oocytes in primordial follicles [8]. There are many factors regulating development and differentiation of human germ cells in the fetal ovary. Immature germ cells express placental/germ-

like cell alkaline phosphatises (PLAP) and pluripotency cells which govern by OCT3/4 (Octamer3/4, a homeodomain transcription factor) expression. The gradual shift from oogonia and early oocytes to germ cells and formation of primordial follicles is accompanied with a loss of PLAP expression and activation of OCT3/4. These findings revealed that germ cells undergoing folliculogenesis were no longer proliferate. Also, expression of c-KIT, β-catenin, and E-cadherin in germ cells at all stages of development demonstrates a putative role for these factors for germ cell survival and maturation [9].

1.1.3 The ovarian reserve

Three onset of follicle atresia occur in human fetal ovaries. They are comprise of: 1) oogonia undergoing mitosis; 2) oocytes largely at the pachnytene stage (Z cells); and, 3) oocytes at diplotene stage. At 2 months post-conception, the total number of germ cells is approximately 600,000 reaching a maximum of 6,800,000 at the 5^{th} month. The population then decreases to about 1,000,000 at birth. By the 7^{th} year only about 300,000 oocytes persist [7]. The total number of follicles per ovary is obtained by estimating follicular density which is the number of structure per unit volume multiplied by the ovarian volume [10]. It was recently accepted that the primordial follicular density rapidly increases to approximately to 8,000/mm^3 at about 5 months of prenatal life and subsequently decreases to about 1,400/mm^3 8 months after birth [11]. The ultimate number of follicles is determined by the balance of oogenia proliferation, germ cell loss and productive interaction of diplotene oocytes and somatic cells. All oogonia that are not surrounded by somatic cells are expelled from the ovary [7]. The resting follicle pool forms an ovarian reserve from which follicles will be recruited for further maturation throughout reproductive life [12]. The ovarian reserve is uniquely established during the last phase of the ovarian organogenesis (definitive histogenesis) [13]. It is composed of three type of follicles: 1) primordial follicles (~35 μm in

diameter) defined as a primary oocyte surrounded by flattened (squamous) granulosa cells; 2) 'transitionary' or intermediary follicles (~38 μm in diameter) in which the primary oocyte is surrounded by a single layer of both squamous and cubidal granulosa cells; and, 3) primary follicles (~46 μm in diameter) characterized by a primary oocyte and a single layer of cubidal granulosa cells surrounded by a basement membrane [14]. Most of the follicles in the ovarian reserve are primordial and intermediary follicles [15]. Data from a recent study have confirmed that a non-renewing ovarian reserve is set in the ovaries at birth and no germline stem cells or neo-oogenesis is present in the adult human ovary [16]. However, Jonson *et al.* (2005) suggested that oocytes might be formed in the adult mouse ovary [17]. Putatively oocyte producing germ cells were identified in bone marrow and peripheral blood of adult female mice [18, 19]. Later, Bukovsky *et al.* (2007) reported the formation of germ cells in adult human ovaries. By differentiation of primitive granulosa and germ cells may occur from the bipotent mesenchymal cell precursors of the tunica albuginea in adult human ovaries [20]. Their work has challenged a central tenet of reproductive biology that there cannot be an increase in the number of primary oocytes after the ovary is fully mature.

1.1.4 Initiation of follicular growth

The mechanisms involved in the initiation of follicular growth are unknown; however, once a follicle begins to grow, growth will be continuous until the follicle meets one of two fates: ovulation or atresia [21]. Follicle growth commences with 'transition' from the primordial to primary follicle stage which is an extremely slow process [22]. There is evidence that the transition stage is gonadotropin-independent and is regulated by intra-ovarian factors [23].

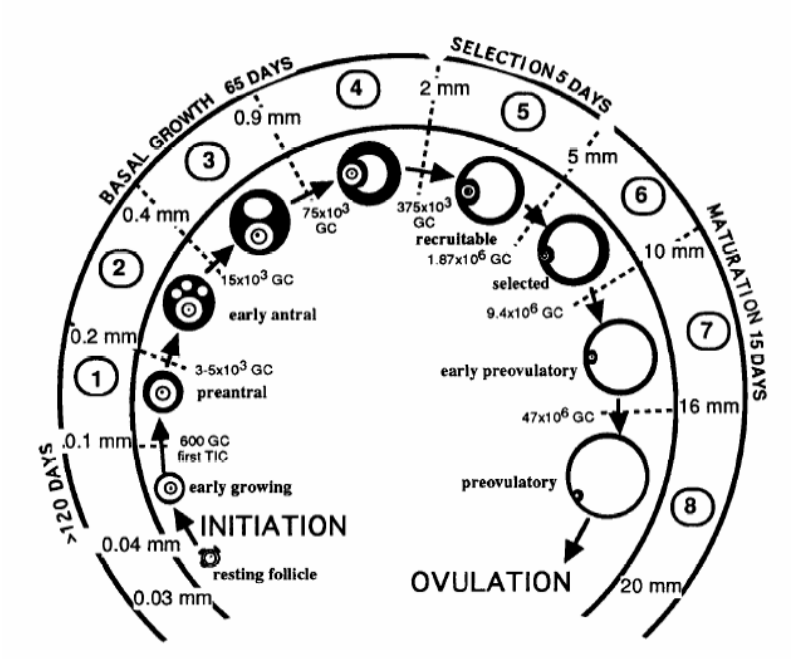

Figure 1.1: Classification of follicles in the human ovary (From Gougeon, 1996)

Haematopoietic stem cells, vascular structure, the autonomic nervous system, pre-granulosa cells, and the oocyte are known to be originators of the growth stimulating factors of primordial follicles [24]. Numerus factors have been implicated in initiating follicular growth. They include members of the transforming growth factor β super family (TGF-β), i.e., bone morphogenetic protein 15 (BMP-15) and growth differentiation factor 9 (GDF-9), oncogenes (i.e., c-myc and erb-A, C-kit), nerve growth factor (NGF), brain-derived neurotrophic factor (BDNF), fibroblast growth factor-7 (FGF-7) and neurotrophins 3 and 4 [25]. Conversely, Anti-Müllerian hormone, somatostatin, and activin A from the TGF- β family have been shown to be inhibitors of early follicular growth [26].

1.1.5 Pre-antral growth phase

Follicular growth is characterized by the increasing size of the oocyte and by proliferation of granulosa cells (GC) [27]. In the growing follicle, GC proliferation results in an oocyte embedded in several layers of cuboidal GC [28]. Meanwhile, mucopolysaccharides are secreted by the granulosa cells and condense around the oocyte to form a layer called the zona pellucida that is composed of three glycoproteins (ZP1, ZP2, and ZP3) [29]. At this stage, the follicle is termed a secondary follicle [28]. Granulosa-oocyte communication is essential for normal oocyte maturation. and gap junction proteins (connexins) are expressed at the oocyte granulosa cell junction as the primary follicle develops into a secondary follicle [30, 31]. Amino acids, glucose metabolites, and nucleotides are transferred to the growing oocyte via gap junctions and the oocyte signals the surrounding GC to support their proliferation and differentiation [32]. Similar connections also exist between adjacent granulosa cells, indicating that follicle cells can communicate throughout development [4]. The secondary follicle with a diameter of $\leq$ 120 μm migrates into the ovarian medulla [3]. When the follicle reaches the secondary stage, granulosa cells express follicle stimulating hormone (FSH), estrogen and androgen receptors [7]. As the secondary follicle enlarges, the theca interna and externa layers form from the stromal cells and can be recognized as individual cells on the basement membrane [13, 33]. The secondary follicle becomes preantral once the theca interna cells become epitheloid (fibroblast-like precursor cells) and acquire organelle characteristics of a steroid secreting cell. Preantral follicles are categorized as Class 1 follicles [14]. The theca externa is highly vascularised, therefore the secondary follicle is directly exposed to factors circulating in the blood stream that are necessary for further development [28]. It takes approximately 3 months for primary follicles to develop into Class 1 or early-antral follicles [8].

1.1.6 Antral growth phase

As follicle growth continues, Class 1 (pre-antral, 0.1-0.2mm) follicles develop into Class 2 follicles (early-antral, 0.2-0.4 mm) or tertiary follicles [4]. Follicles enter into Class 1 during the early luteal phase, 25 days later (late follicular phase of the following cycle) they develop to the tertiary follicle stage [4]. Over this period, small fluid-filled cavities, or lacunae, form between the GC which eventually aggregate and develop into a single cavity called an antrum. Simultaneously, the GC immediately surrounding the oocyte form the cumulus oophorus [28]. Two types of granulosa cells are classically described beyond this stage: those which surround the oocyte are cumulus cells (CC) and those which surround the antrum are termed mural granulosa cells (MGC). Structural and functional differences between CC and MGC have been documented. Cell replication is higher in CC compared with MGC, they have different responses to FSH, and CC secrete about six-fold higher levels of progesterone than MGC [34].

Approximately 20 days later (during late luteal phase) follicles convert into Class 3 (0.4 - 0.9 mm), and after 15 days (the late follicular phase of the subsequent cycle) pass into Class 4 (0.9 - 2 mm) [4]. Class 3 and 4 follicles respectively consist of 7.5×10^4 and 3.7×10^5 granulosa cells [14, 15]. Approximately 10 days later, in the late luteal phase, follicles enter into Class 5 (2 - 5mm) and consist of 1.9×10^6 granulosa cells. These are referred as 'selectable follicles' [15]. The conversion of a Class 1 pre-antral follicle (0.12 - 0.2 mm in diameter) into a Class 5 follicle (2 - 5 mm in diameter) has been termed 'the tonic growth phase' and occurs over the course of approximately 2 months in humans [8]. Oocyte growth is parallel to early follicular growth and the diameter of the oocyte rapidly increases from approximately 30 μm in primary follicle to 100 μm in early antral follicle. Thereafter, oocyte grows more slowly and ultimately reaches approximately 140 μm in the preovulatory follicle. It is suggested that the kit ligand system (C-Kit) induces the oocyte growth at the time of initiation of follicular growth [35].

The follicular fluid provides the avascular GC and oocyte with a characteristic endocrine microenvironment. It is comprised of free and protein-bound sex-steroid hormones, plasma and locally derived proteins, proteoglycans, and electrolytes [36]. It is well established that gonadotropins are required for antral follicular development; however, their role remains unclear in the differentiation of preantral follicles. Basal levels of gonadotropins are necessary to sustain growth and development of the follicle from approximately 2 mm diameter to Class 5. Follicles become dependent on cyclic changes of gonadotropins when they reach Class 5 and they remain dependent on them until they ovulate at the end of Class 8 stage [14, 15]. According to the "two-cell two-gonadotropin model" each gonadotropin acts as a specific individual on a separate set of ovarian follicle cell, FSH on GC and luteinizing hormone (LH) on theca cells [37]. LH stimulates ovarian theca cells to produce androgens, mainly androstendione, that are transferred to GC where they aromatized to estrogens (E_2) which are released into the follicular fluid, the intrafollicular space or the systemic circulation [15, 38]. FSH facilitates in the conversion of androgens to estrogens by stimulating the GC aromatase enzyme system, and also induces follicle antrum formation [13, 38].

1.1.7 Recruitment

Follicle development from Class 5 to Class 8 takes approximately 21 days and is termed the 'exponential growth phase' [39]. In humans, this phase includes 3 predominant events: 1) recruitment; 2) selection; and, 3) ovulation. During the exponential growth phase, a small group of early antral follicles begin to grow rapidly in the late-luteal phase. This is known as recruitment. Recruitment is followed by selection of a dominant follicle (DF) in the mid-follicular phase of the next cycle. The DF is selected for preferential growth and ovulation [14]. Throughout the life history of ovarian follicles, two distinct events are associated with recruitment. MacGee *et al.* (2000) considered these to be: 1) initial recruitment, and 2) cyclical recruitment [12].

During initial recruitment, some primordial follicles are stimulated by endocrine and paracrine factors to initiate growth whereas others remain quiescent. Initial recruitment begins after follicle formation and is continuous throughout life. The oocyte has started to grow, but full development will not be completed during initial recruitment. After initial recruitment, oocytes remain arrested in the prophase stage of meiosis. Follicles not initially recruited will remain dormant.

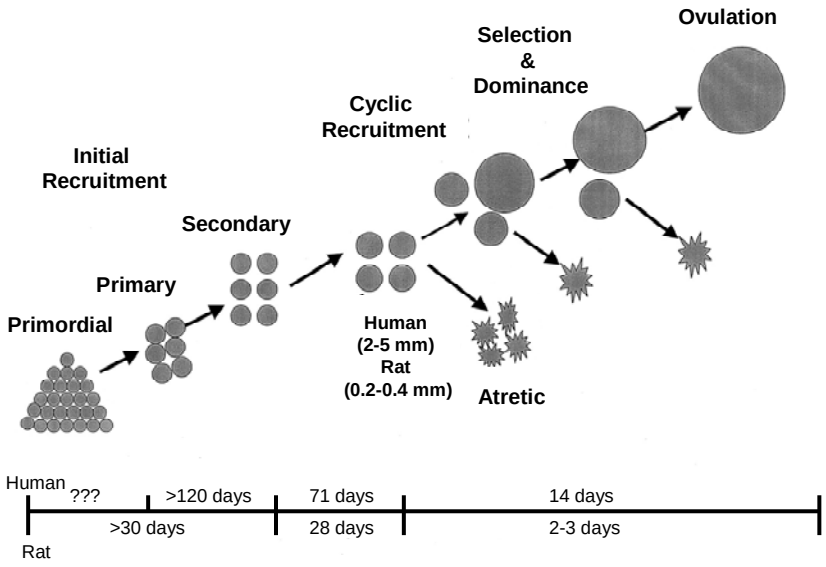

Figure 1.2: Initial and cyclic recruitment (McGee, E. A. *et al.* Endocr Rev 2000).

Cyclic recruitment begins after puberty due to increasing circulating levels of FSH. Three to 11 antral follicles of diameters from 2 to 5 mm are recruited from the ovarian follicle pool in each cycle for further growth [40]. Throughout cyclic recruitment, a limited number of follicles survive atresia and the oocytes recommence meiosis [12]. To avoid confusion, we will consider the term recruitment to mean "cyclic recruitment" in the rest of this text.

The process of follicle recruitment occurs as gonadotropin secretion rises following regression of the corpus luteum. At this time in the late-luteal phase, early antral follicles enter into the wave of developing follicles from which the preovulatory follicle will emerge. Follicle stimulating hormone (FSH) appears to impart a survival action on antral follicles. Luteal regression results in decreased progesterone, estradiol and inhibin-A allowing for an increase in FSH. Indeed, FSH levels rise around 12 days after the preceding mid-cycle LH surge slightly above (10% to 30 %) the 'threshold' needed rescuing a cohort of small antral follicles from atresia [37, 41, 42]. The duration of FSH rise is limited due to a negative feedback of E_2 and secretion of inhibin B by antral follicles and therefore the concept of the "FSH window" has been proposed [43, 44]. The number of follicles in the recruited cohort might be determined by the duration of elevated levels of FSH above threshold (window concept) rather than its magnitude [43, 45]. Recently, an important role for β anti-mullerian hormone (AMH) in the regulation of FSH sensitivity in the ovary during recruitment has been identified in humans [46]. Expression of AMH in women first occurs in GC of primary follicles but higher levels of expression are observed in granulosa cells of secondary follicles, preantral and small antral follicles ≤ 4 mm in diameter [47]. Anti-mullerian hormone ceases in follicles 8 mm in diameter and larger. It is speculated that AMH inhibits follicular recruitment in humans. The physiology of AMH inhibition may be similar to that observed in rodents [43]. Responses to increasing FSH are also modulated by nonsteroidal products of GC and/or theca interna cells such as: 1) the insulin-like growth factors (IGF); 2) epidermal growth factors (EGF); 3) fibroblast growth factors (FGF); and, 4) transforming growth factors (TGF); 5) inhibin, and others [48-51].

1.1.8 Selection

Follicle selection is the process wherein one follicle from a wave of growing follicles becomes physiologically selected for preferential growth, attains physiological dominance and continues development to ovulation [52]. Our understanding of folliculogenesis has recently been elucidated by findings that women exhibit two to three follicular waves per ovarian cycle [53]. Therefore, selection occurs 2 to 3 times during ovarian cycles. Only the wave that initiates development during the late luteal phase produces a pre-ovulatory sized follicle that subsequently ovulates [53, 54]. Estimates of follicle diameter at selection time differ. Chikazawa *et al.* (1986) examined ovaries obtained from women by surgery during the follicular and late luteal phases. They were sliced serially and then the stained slices were examined to assess the sizes, numbers and physiological status of atretic and nonatretic follicles. It was observed that estrogen secretion increased proportionally to the growth of DF equal or greater than 8 mm in diameter. A DF seems to be selected from 2 to 3 competing follicles with diameters of approximately 5 mm during the late luteal phase [55]. Gougeon (1989) believes that follicles are selected between 5.5 and 8.2 mm in diameter (Class 6) based on a higher granulosa cell mitotic index in the largest healthy follicle compared with other follicles of the cohort. This auther used the ovaries of women undergoing laparotomy for various gynecological disorders not directly related to ovarian disease [14, 49]. Macklon and Fauser (1999) Pache *et al.* (1990) observed the first appearance of the DF at mean size 9.9 ± 3.0 mm using transvaginal ultrasound examinations [56, 57]. Later, Van Dessel *et al.* (1996) obtained fluid from ovarian follicles *in vivo* during surgery from regularly cycling women with proven fertility and showed that intrafollicular estradiol concentrations rose only in follicles greater than 9 mm in diameter. A significant increase in aromatase enzyme activity occurs only in the selected DF [58]. Finally, Baerwald *et al.* (2003) demonstrated that follicle selection was manifest at approximately 10 mm in diameter based on transvaginal ultrasonographic evaluations of natural menstrual cycles

[53, 54]. The overall consensus seems to be that the selection process does not occur before follicles reach 8 mm in diameter [48].

Selected follicles enter Class 5 (4.7 ± 0.2 mm in diameter) during the late luteal phase and 5 days later enter Class 6 (5.5 to 8.2 mm in diameter) in the early to late mid-follicular phase. Dominant follicles can be distinguished from their cohorts by their larger size (6-10 mm), higher mitotic index, detectable amounts of FSH and a considerable amount of estrogen in the follicular fluid [59, 60]. Five days later, the DF reaches 10 to 16 mm in diameter and then ovulates in another 5 days [4]. During selection, the follicle gradually enlarges from 7 mm (2 to $5x10^6$ GC) during the early follicular phase to 9 mm (50 to $100x10^6$ GC) in the late follicular phase [15]. The mechanism of selection of a DF is a critical, but a poorly understood. Identification of the timing of preovulatory selection is a key component in understanding natural and peri-menopausal ovarian function, ovarian suppression for contraception, and improvement of ovarian stimulation protocols.

Ireland *et al.* (1983) showed that the binding of labelled hCG was not different between estrogen active and estrogen inactive follicles on days 3 or 5 of the estrous cycles in cattle (presumably DF and SF) [186]. Later, Evans *et al.* (1997) reported that the DF has been selected by day 2 of the first follicular wave in cattle based on their diameters and estradiol secretion *in vitro*. There was also a lack of mRNA for LH receptor in granulosa cells on days 2 or 3 of the follicular wave [187]. This result was in agreement with the finding that the acquisition of LH receptor on granulosa cells does not play a role in selecting the dominant follicle.

There is presumptive evidence that biochemical changes occur in selected follicles before it is obviously larger than other follicles of the wave [61, 62]. The recruitment process is preceded by an FSH surge and there are two significant responses of the GC to FSH: 1) the induction of aromatase; and 2) the induction of LH receptors. The aromatase activity of GC is required for androgen conversion to estradiol. The increasing levels of circulating estradiol and inhibin secreted

from GC of DF contribute to FSH's decline to basal levels through a negative feedback mechanism which is necessary to sustain the development of less mature follicles. In humans, there is a simultaneous increase of estradiol in the follicular-fluid of DF and systemic circulation [51]. High concentrations of estradiol in the follicular fluid are hallmark of dominant preovulatory follicles [61]. In addition, DF are characterized by decreased levels of inhibitory low molecular weight IGF-binding proteins (IGF-2,-4, and-5) [63]. The resultant increase in bioactive (free) IGF allows the DF to synergize with FSH enhancing follicular growth and estradiol production [64, 65]. The induction of LH receptors is responsible for further maturation of the DF during the mid-to-late follicular phase when LH concentrations begin to increase [66]. Occupancy of FSH and LH receptors result in a similar cellular responses since both receptors are coupled to a cAMP signalling system [67]. Therefore, the GC of DF respond similarly to both FSH and LH; however, at non-saturating levels of both gonadotropins the responses are additive [68]. It is speculated that LH is able to substitute for FSH in the FSH-stimulated DF and provide the maturing follicle with an additional source of gonadotropic support [69]. In an extensive series of studies, early DF has been shown to contain higher levels of mRNA for LH receptors in both theca and GC than the SF of the same cohort. Levels of mRNA for the FSH receptors in granulosa cells were similar in dominant and SF. likewise, mRNA levels for 17α-hydroxylase and aromatase which convert progestins to androgens in theca cells and androgen to estrogen in GC, respectively, are higher in newly selected DF than SF [61]. Another significant aspect of the DF compared to SF is the development of an extensive vascular plexus in the thecal layer which creates a blood supply providing preferential delivery of gonadotropin to the newly formed LH receptors [70, 71]. If a gonadotropin surge occurs the mature follicle will ovulate and in the absence of gonadotropin surge it has the same fate as the SF, atresia [69].

1.1.9 Atresia

During puberty, the ovarian reserve contains only 300,000 follicles, from which 400-500 will ovulate in the course of a normal reproductive life span [7]. Atresia literally means as "without perforation" [72]. The mechanisms engaged in regulating and controlling atresia are not fully elucidated. Since 1990, there have been extensive studies designed to determine the precise temporal and molecular processes. Our current understanding is that deprivation of survival agents and presence of "death ligands" are the first steps of atresia [72]. Pituitary hormones (FSH, LH, and GH), estrogen and locally produced growth factors promote follicular growth and suppress the apoptosis process [73, 74]. A stimulus for apoptosis is the absence of these factors [75]. Recent studies reveal that atresia is mainly cause by apoptosis of granulosa cells [76]. Potential triggers for apoptosis in the granulosa cells are death ligands and receptors, intracellular pro-and anti-apoptotic molecule, cytokines, and growth factors. Death receptors include a subfamily of the tumor necrosis factor receptor superfamily (TNFRsf) which contains a cytoplasmic death domain necessary for the activation of apoptosis [77]. TNF-α has a dual action which induces both cell death and cell proliferation through different receptors (TNFR-1 and TNFR-2 are apoptotic and anti-apoptotic respectively) [78]. At the beginning of atresia, the TNFR-1 receptor is trimerized then binds to death ligands which include the tumour necrosis factor-α (TNF-α), TNF-α receptors (TNFRs), Fas ligand (FasL), Fas (CD95, APO-1, TNFRsf6), and TNF-α-related apoptosis-inducing ligand (TRAIL), TRAIL receptors [79, 80]. The extracellular DD (death domain) of the cell death receptors have an intracellular DD by which it binds with the DD of the adaptor protein (Fas-associated death domain: FAD) [77, 78]. Thereafter, an initiator caspase (procaspase-8; FLIC) attaches to FADD through the death effectors domain, resulting in a death-inducing signalling complex, fragmentated DNA, and finally apoptosis [79]. Recently, it has been documented that the FasL protein is located in the cytoplasm of granulosa cells in healthy follicles. When GC apoptosis commences, Fas moves

from the cytoplasm to the cell membrane and initiates the process [80]. In some species, Fas is observed in the oocytes and also in cumulus cells suggesting a role in oocyte death [81].

1.1.10 Ovulation

Ovulation is a complex, inflammatory-like process wherein the fertilizable cumulus oocyte complex is expelled from a mature preovulatory follicle. It is preceded by a preovulatory rise in LH [82, 83]. In 1932, the first major report on ovulation was written by Carl Hartman. He considered ovulation as the "sine qua non" of the reproductive process and pointed out that the cyclic sexual phenomena are separated into those occurring before and after ovulation [84]. Three years later, Adsell argued that follicle rupture as a consequence of increasing intrafollicular pressure, promoted by the contraction of smooth muscle tissue in the ovarian stroma [82]. This premise was believed to be true until 1962. Since then it has been shown that ovulation occurs due to a series of biochemical, and morphological changes induced by the mid-cycle gonadotropin surge.

Prior to ovulation, there are five distinctive layers at the apex of a Grafian follicle [83]. The outermost layer is the surface epithelium. The second layer is the tunica albuginea which is the most durable part and consists of fibroblasts and collagens. The third layer is the theca externa, which is the follicle's own capsule of collagen fibres and connective tissue. The theca interna is the forth layer consisting of steroid-secreting cells and vascular tissues. It is separated from the innermost layer by a basal lamina. The innermost layer is the stratum granulosum [3]. Around the time of ovulation, the apical follicle wall becomes thinner and the deep internal wall becomes thicker. Subsequently, a conical stigma forms on the surface of the ovary as the follicle protrudes from it [85]. The stigma is the site of follicular rupture and release of the cumulus-oocyte complex (COC). The COC is the oocyte surrounded by the cumulus oophours cells. Ovulation starts with gentle expulsion of the

oocyte and antral fluid when intrafollicular hydrostatic pressure of about 20 mm Hg finally overcomes the resistance of the very thin apical tissue layers [85].

It is documented that LH induces marked increases in ovarian blood flow prior to ovulation [86]. The high concentration of intrafollicular esteradiol and androstenedione decreases with the ovulatory LH surge due to an LH induced inhibition of the thecal P450-$17_{\alpha/lyase}$ complex. At the same time, a marked increase in progesterone and 17α-OH progesterone occurs from GC which in turn terminates the LH surge by negative feedback on the hypothalamo-pituitary-ovarian axis [15, 87]. Progesterone is important in ovulation; however, its proteolytic function has not been determined. Since progesterone is the main indicator representative of luteal function, it seems that luteinisation of follicular tissue begins before follicular rupture [83].

The lutinzation process that commences before follicular rupture consists of 2 distinct but parallel events: 1) the transformation of the theca interna and stratum granulosum of the follicle wall into steroidogenically active lutein tissue, and 2) the disruption of the basement membrane between the GC and the thecal layer and vascular migration into the luteinizing granulosa layer [91]. The corpus luteum synthesizes substances essential for initiation and maintenance of pregnancy. Besides progesterone, the corpus luteum also produces estrogen, relaxin, and inhibin-related peptins [53]. If fertilization does not occur, the corpus luteum regression begins after approximately 7 days. Alternatively, if pregnancy occurs, the corpus luteum persists in the ovary until the time of the luteal-placental shift. It has been suggested that LH along with two local factors, estrogen and $PGF_2\alpha$ are responsible for the corpus luteum regression [94].

Oocyte Maturation Inhibitor (OMI) restrains oocyte maturation prior to ovulation while increased LH level during mid-cycle suppresses its action [88]. The LH threshold must be attained and be constant for about 14 to 27 hours to provoke meiosis resumption and development from the

diplotene stage to metaphase II. A second meiotic arrest occurs at the time of ovulation and meiosis will only be completed after fertilization [84, 87].

Shortly after the LH surge, attachments between the leukocytes and the endothelial cells along the post-capillaric venules are initiated due to gonadotropin-induced gene expression. This is a recognized inflammatory event. In addition to the leukocytes driving inflammatory mediators, local hydrolytic enzymes play an important role in initiation of the inflammatory cascade during ovulation. Different inflammatory agents have been studied in ovulatory tissue. Kinin, a vasodilatory agent, formation increases 10-fold during the ovulatory process in the rat ovary. In contrast, ovarian histamine and plasminogen activator factor (PAF) decrease at the same time probably due to degranulation of mast cells and histamine release. There is also activation of the arachidonate cascade [83]. Immediately after the LH surge, the GC and theca interna cells produce plasminogen activator (PA) which converts of plasminogen to plasmin in the follicular fluid. Plasmin which acts as a proteolytic enzyme catalyzes procollagenase conversion to collagenase. Collagenases break down collagen within the follicular apex [85]. Prostaglandins (PG) E and F increase in preovulatory follicles. The specific roles of prostanoids in ovulation in not fully understood; however, the PG play significant roles in inflammatory reactions [86]. It is not certain whether they serve as degradative agents or they are a response to the inflammatory-like changes in the follicle.

The mid-cycle gonadotropin peak induces the expression of numerous genes in the cumulus oocyte complex as well as in the GCs and theca cells [89]. These include prostaglandin synthase-2 (*Ptgs*2 *or Cox*2), genes associated with the cumulus oocyte complex (COC) matrix formation, hyaluronin (HA) synthase 2 (*Has*2), the HA-binding proteins, TNFα-induced orotein-6, and a vast number of other genes involved in inflammatory processes [90, 91]. Different events are observed in COC during ovulation as a consequence of specific gene expression at the time of ovulation. They include: 1) "cumulus cell expansion"; 2) altered interaction of the somatic cells with the germ cell;

and, 3) the resumption of meiosis. Cumulus cell expansion is associated with secretion of hyaluronic acid and the disruption of gap junctions between the neighbouring cumulus cells [92]. When the follicle wall finally ruptures at the apex of stigma the follicular fluid and oocyte evacuate the antral cavity. The cumulus oophorus cells remain with the ovulated oocyte and probably assist with the capture of the oocyte by the fimbriated end of the oviduct [93]. The duration of follicle evacuation appears to be associated with the stigma size and ranges from 6 seconds to 18 min [90].

1.1.11 Wave theory of folliculogenesis

Introduction of ultrasonography in the late 1980's ushered in a new understanding of ovarian follicular dynamics. Our understanding of follicular waves was first elucidated in animal models (e. g., bovine, equine, ovine). Follicular waves are described as the synchronous growth of a group of follicles from which one or more follicles are selected for further preferential growth. The majority of bovine estrous cycles are comprised of two or three such waves [95, 96]. In cows, the final wave of follicular development is ovulatory, while all preceding waves are anovulatory [97, 98]. Animals with 2 waves of follicular development exhibited an inter-ovulatory interval (IOI) of 20 days. Those with 3 waves exhibited a longer IOI (23 days) which was attributed to a longer luteal phase (i.e., longer lifespan of the CL) while the follicular phase remained unchanged [99]. The progesterone secreted by the corpus luteum in cows had a suppressive effect on LH and inhibited the ovulation of DF in major anovulatory waves which occurred in the luteal phase [100].

Ovarian follicular waves with major and minor follicular wave patterns also have been documented in the mare [94]. Major waves were defined as the growth of a cohort of follicles followed by the selection of a follicle for preferential growth (DF) and the regression of all other follicles (SF). Two types of major waves were characterized: primary and secondary. Primary waves occurred during diestrus and gave rise to an estrous ovulation. Secondary waves originated during estrus or early diestrus and gave rise to a dominant anovulatory follicle, hemorrhagic follicle or a

diestrus ovulation. Minor waves were characterized by the failure of any one follicle to become dominant [101]. In cows and mares, the emergence of each follicular wave was preceded by an increase in the circulating level of FSH [100]. The selection of DF was associated with a decrease in FSH level, acquisition of granulosa LH receptors, and rising circulating concentration of estradiol [102, 103]. Recent comparative studies in monovular farm animals (cattle, mares) and women have indicated similarities of the dynamic of follicular waves [104, 105]. These results have encouraged the use of cows and mares as the most relevant experimental models for the study of folliculogenesis in women.

In humans, morphological studies by Block (1952) initially demonstrated 2 periods of increased follicular growth during the 'sexual cycle'. The first wave, from which an ovulatory follicle developed, occurred early in the cycle under the influence of FSH. The second wave of folliculogenesis occurred in the early luteal phase. He reported that follicles that grew > 5 mm within the second wave in the mid-late luteal phase were atretic [106]. In 1986, Gougeon provided a different understanding of the folliculogenesis based on histological observations in ovaries obtained during gynecological surgery in women. He postulated a continuous entry of follicles into the growth phase [4]. The idea of continuous follicular recruitment has been termed the "Propitious Moment Theory". According to this theory a single follicle grew by chance during a hormonally-privileged period of the cycle in women [110]. Accordingly, antral follicles were recruited and grew continuously until occurrence of a gonadotropin surge that stimulated ovulation of the mature follicle [111]. A biphasic pattern of reproductively active hormones has been shown during endocrine evaluations of the human menstrual cycle. Luteinizing hormone (LH) pulse frequency rose in the early luteal phase (~20 pulses per day) and early follicular phase (~20 pulses per day),

compared to the mid-luteal phase (~ 5 pulses per day) [102]. Activin and inhibin were shown to be secreted in biphasic patterns during the cycle as well [107].

It was generally accepted that a cohort of follicles were recruited to grow in the late luteal phase of the menstrual cycle, a single follicle was selected for preferential growth the mid-follicular phase. Ovulation occurred at mid-cycle and there was limited follicle development during the luteal phase. The dynamic and physiological events of follicular wave development were not fully appreciated until the discovery and characterization of human follicular wave dynamics [12, 48, 53, 98, 108, 109].

Recent studies have characterized a wave-like pattern of human ovarian follicular development [94]. Non-invasive, high-resolution transvaginal ultrasonographic evaluations have shown that each menstrual cycle in women is compromised of two or three major or minor waves of follicular development. Major waves were defined as those in which a single follicle was selected at 10 mm of diameter to attain further growth and become the DF while the other follicles (SF) underwent atresia. In minor waves, the selection of the DF was not manifest. The DF of ovulatory major waves ovulated, whereas the anovulatory DF regressed during major waves. The final wave of the interovulatory interval (IOI) was an ovulatory major wave, whereas preceding waves were minor or major anovulatory waves [53, 112]. The emergence of both major and minor follicular waves was preceded by an increase in the circulating level of FSH. Women with two wave cycles exhibited shorter cycles than those with three waves of folliculogenesis. Therefore, during the follicular phase, the blood level of estradiol increased earlier in women with two versus three follicular waves, which attributed to earlier production of E_2 by DF cycles. Likewise, preovulatory surges of FSH, LH, and E_2 occurred earlier in women with two versus three follicular waves [53].

1.2 Ultrasonographic imaging of the ovaries

1.2.1 Overview of ultrasonographic imaging

Prior to the introduction of ultrasonography, studies of human ovarian follicles were based on autopsy and surgical specimens. The histological studies provided non-dynamic information of ovarian physiology at single points in time. They were time-consuming, invasive, and did not allow elucidation of ovarian events over time. Ultrasonography profoundly changed our ability to detect morphological changes that occur within the reproductive organs without interfering with the physiological processes of these organs. Ultrasonographic imaging provided a direct, non-invasive and atraumatic tool to observe natural changes in the ovarian follicle dynamics *in vivo* and has become an essential tool for understanding ovarian physiology as well as diagnosis of ovarian disease for clinical purposes [95, 113, 114, 115].

Transabdominal ultrasound (TA) provides an overview of the pelvic contents. Some early comparative studies showed that transvaginal ultrasonography (TV) could effectively replace TA examinations for routine ultrasonography of the female pelvis. Increased resolution, less patient discomfort, and elimination of the need for patient preparation are potential advantages of TV ultrasound over TA approaches [109, 116]. Transvaginal ultrasonography is used to observe ovarian follicular maturation and ovulation during menstrual cycles, detect early pregnancy, and assess the uterus and ovaries for anomalies such as cysts, tumours, fibroids and endometriomas. In addition, it is useful in management of infertility, ovulation induction prior to insemination, oocyte retrieval, and management of controlled ovarian hyperstimulation [115, 117].

Ultrasound instruments are comprised of a piezoelectric transducer connected to a console that contains the image adjustment controls used by the operator and the viewing screen. The transducer sends high frequency acoustic pressure waves into the body, converting electric energy

into mechanical energy to generate ultrasonic waves then receives echoes and converting the returning acoustic energy into electric energy which may be viewed. Ultrasound is defined as acoustic pressure waves that have a frequency (above 20,000 hertz) beyond the human audible range (20 and 20,000 hertz). Ultrasonographic imaging is based upon the ability of different tissue structures to reflect high frequency sound waves [115]. Acoustic pressure waves are emitted from the piezoelectric transducer and transmitted into adjacent tissues. Ultrasound waves can travel through liquids, tissues and solids, and are either reflected or scattered by tissues and tissue interfaces. The characteristics of the tissue interfaces (changes in tissue density) determine what proportion of the sound wave will be reflected or transmitted (ecogenicity). Each tissue has a characteristics signature which is reflective of acoustic impedance [118].

The reflected echoes are detected by the transducer, processed and displayed on the ultrasound unit screen, in shades of gray extending from black to white. Hyperechoic tissues (dense tissues, such as bone) reflect much of the sound waves and appear bright whereas anechoic parts of organ (fluid) do not reflect sound waves and appear black in the ultrasound images. The speed of sound waves depends upon the characteristics of the medium in which the sound wave is traveling. It increases with increasing tissue density. In soft biological tissues, the velocity of ultrasound waves is approximately 1540 m/s. In fluid, it is about 1480 m/sec, and in bone it is 3500 m/sec. Most ultrasound devices are calibrated for average velocity of sound in soft tissues or water [115, 119]. In addition to tissue density and sound waves velocity, the "gain" controls of ultrasound system adjust the optimal balance of the grey tones displayed in the images. Echoes returning to the transducer from tissues located at large distance from the transducer are weaker than those returning from nearby tissues, resulting from sound beam attenuation in the medium. Therefore the intensity of viewing screen varies at different depths of tissue. Receiver amplification can be increased by

applying the internal gain controls. Thereby, balancing echoes originating from distal reflectors and echoes originating close to the transducer [120]. Overall, near and far gains regulate the near field, and the far field brightness of the image respectively [119].

The transducer receives reflected sound waves and converts them into electrical energy. Then the scan convertor amplifies and stores the images in a binary formatted, analog-to-digital conversion. The digital scan converter memory consists of a matrix of elements, or pixels, and is typically 480 x 640 pixels in the current generation of ultrasound instruments. The echoes stored or written in the memory are displayed on a monitor. An electron beam is directed and displayed as scanning and raster lines on a monitor. The image is made up of a number of pixels, varying in grey-scale value from 0 (black) to 255 (white) [121, 122].

The ultrasonographic appearance of a tissue is referred to echotexture. Echoes can be displayed in different modes. A-mode or Amplitude shows echo signal amplitude verses reflection distance. It enables accurate transducer-to-tissue distance measurements. M- mode or motion mode is generated by sweeping a B-mode trace across the screen while the ultrasound beam is stationary. It is mostly applied in echocardiography. In B-mode, or brightness mode, the echo signals are converted to intensity-modulated dots on the screen and used in both generating M-mode and two dimensional imaging [107, 115].

The first step in interpreting ultrasound images is to obtain detailed knowledge of the relationship between tissues and echoes, and ability to differentiate between factual and artificial responses. Certain shapes and structures of tissues change the direction of sound waves which produces artifacts. If sound waves strike an interface that is smooth and wider than the beam and parallel to the transducer, a specular reflection will be generated. Non-specular reflections are produced when the sound waves strike a rough or narrow interface scattering the sound wave in

many directions. Blockage or deviation of the sound waves makes a shadow artifact. When the beam passes through a reflector-free structure, the pulse is not attenuated resulting in a column of brighter echoes beneath the structure known as an enhancement artifact. Another type of atrifact is termed reverberation in which the wave sounds bounce back and forth between two strong interfaces until the beam are exhausted by attenuation [115, 121]. However, artifacts can cause misinterpretation of normal or pathological structures, therefore knowledge and discrimination of nature and origin of the actual and artifactual echoes can decrease misinterpretation.

1.2.2 Ultrasonographic characteristics of the normal ovary

In women, normal ovaries contain follicles and/or corpora lutea throughout the reproductive age range. The ovaries are normally observed as almond-shaped organs located lateral to the uterus, above and medial to the hypogastric vessels. The size of ovary is related to the phase of follicular development and age, but normal healthy ovaries do not usually exceeded 4 x 3 x 2 cm. Their size is variable during menstrual cycle. Ovarian size also decreases as menopause approaches [123]. In ultrasonographic images, the ovary is visualized as a coarse, low-level echo pattern interrupted with anechoic (i.e., dark) areas that represent developing follicles, functional cysts or corpora lutea. Ovarian follicles are imaged as circular hypoechoic (i.e., dark) structures surrounded by a thin hyperechoic (i.e., brighter) follicle wall [124]. Follicles as small as 2 mm in diameter can be detected by ultrasound [125]. A mature preovulatory follicle generally measures 20 to 24 mm in diameter [124]. The ovarian vasculature can be easily detected using Color and Power Doppler imaging techniques [111]. The ovarian artery is a branch of the uterine artery and passes through the infundibulopelvic ligament. As ovulation approaches, vascularization of the theca cell layer increases. Therefore, thecal and granulosa cell differentiation produces a subtle double contour inside the follicle wall [124].

Ultrasonographically detectable changes associated with impending ovulation include cumulus-oophorus expansion 12 to 24 hours before ovulation, thinning of the apex of the follicle wall approximately 3 hours before ovulation and the follicle wall becoming less echoic (darker), more loosely organized and better vascularized [90, 126]. The follicle wall becomes irregular in shape [109]. Fifteen to 20 minutes before ovulation, a stigma forms at the follicular apex followed by the rupture of the wall and the rapid release of 50% of follicular fluid within the first 15 seconds. Complete evacuation of follicular fluid occurs within 6 to 18 seconds [7, 90].

The corpus luteum (CL) forms immediately after the collapse of the follicle and extrusion of the egg and follicular fluid. Ultrasound characteristics of the corpus luteum are highly variable and involve significant macroscopic changes. The CL usually appears as a hypoechoic structure with an irregular wall and may contain some internal echoes corresponding to haemorrhages. Four to eight days after ovulation, it appears as an echoic area approximately 15 mm in diameter. The CL tissue area and vascularity reach maximal levels 6-7 days after ovulation. Haemorrhage within the corpus lutem has been observed in 60% of women and appears as a solid or complex mass on ultrasonography. There is no correlation between the CL size and structure and progesterone level during luteal phase [127]. Some investigators have classified the CL into four groups by assessment the relative hypoechogenicity or hyperechogenicity and the maximum thickness of the wall [128]. The luteal regression occurs 6-7 days after ovulation. The CL degenerates into an amorphous hyaline mass held together by strands of connective tissue referred to as the corpus albicans (CA). The end product CA is a hyperechoic mass of scar tissue that eventually regresses completely over the course of the next few menstrual cycles [129].

Failure of ovulation may is rise to 1 of 3 distinct types ovarian structures: 1) anovulatory follicular cysts; 2) luteinized unruptured follicles (LUF); and, 3) hemorrhagic anovulatory follicles

(HAF) [128]. Anovulatory follicles are characterized by a thin highly echoic (i.e., bright), clearly demarcated follicular wall of uniform thickness with an echotexture that is distinctive of a cohesive tissue layer. The increased gray-scale values of the follicular wall may be associated with decreased vascularity. Echoic structures protruding into the follicular antrum and floating freely in the follicular fluid may be observed [128]. The COC and stigma are not usually visible [126]. These types of follicles generally exceed normal ovulatory diameter (i.e., >25 mm) remain static for one to several days and then regress without apparent luteinization [130]. Luteinized unruptured follicles (LUF) attain ovulatory diameter with thick follicular walls and hazy indistinct borders at the antrum/wall interfaces. The walls have similar echotexture to luteinized tissue. There is occasionally visual evidence of occyte is trapped within the LUF. Luteinized unruptured follicles typically regress after a time course similar to the CL. Hemorrhagic anovulatory follicles are identified by haemorrhage into the antral cavity and the formation of fibrin network within the antrum [130]. All of these types of ovulation failure have been reported in healthy women and are associated with infertility [125].

1.2.3 Computer-assisted image analysis

The human eye can perceive smooth transitions in shades of gray, but can only distinguish among 18 to 20 shades of gray, therefore, most of the gray-scale information within an ultrasound image is inaccessible to the human eye [124]. Recently, new techniques have been developed to evaluate ultrasound image attributes. Computer-assisted image analysis techniques have been used to quantify echotextural characteristics within the image by using a series of processing steps and complex computer algorithms [131]. The validation of this technique has been verified through correlation of ultrasound image attributes with histological attributes in animal models. It is important to avoid placing sampling lines on image artifacts (i.e., enhanced through-transmission,

shadowing, specular echoes, refraction, and beam width artifacts). These artifacts may falsely increase or decrease image attribute values resulting in inaccurate interpretation of the physiologic status of the ovarian structure. For multiple examinations of images of the same structure over time, consistency in equipment (scanner and transducer) and machine settings (near field, far field, and overall gain) is essential [132-135].

Three image attributes are quantified during ultrasound image analysis of ovarian follicles. They are: 1) numerical pixel value (NPV) defined as the mean pixel gray-scale value of the sampled pixels, which is an average value of all pixels (black=0, white=255) within the area of interest; 2) pixel heterogeneity (PH) defined as the degree of deviation from the mean (standard deviation) of pixels values of the sampled area; and, 3) the region selected volume (RSV) defined as mean gray-scale values within the selected region in 2 dimensions, length and width (GSV/mm^2). Application of spot metering, linear and time-series analyses, and regional surface analyses allow us to extract numerical data and enhance our visual interpretation of the ultrasonographic image [131, 136].

1.2.4 Spot metering

The simplest quantitative method for analysing ultrasound images is to select one or more small circular areas of interest. Then the computer software determines the precise gray-scale value of the pixels within the sample area and provides image attributes such as NPV, PH. This technique is applied to compare different areas within the same follicle or the same area of the follicle at different times. For instance, different portions of the follicle wall or corpus luteum may be analyzed to evaluate characteristics associated with follicular growth and regression, impending ovulation, atresia and luteal development and regression [111, 131]. Results are generated in the form of numerical values which are representative of morphological and histological characteristics of the follicle tissue at different stages of development.

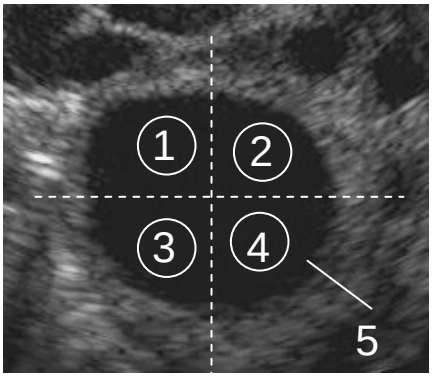

Figure 1.3: Computer-assisted image analysis of the ovarian follicle ultrasound. Spot analysis of the antrum was performed to measure the mean numerical pixel values and pixel heterogeneity by placing small circles at four different locations (1, 2, 3, 4) over the follicle antrum. Line analysis of the follicle wall was performed by drawing a line at 4 o'clock position (5).

1.2.5 Linear and time series analysis

In the linear analysis approach, a computer-generated line (one or more pixels wide) is drawn across a specific region of the follicle or luteal structure of biological interest. The intensity of each pixel within the line are displayed on a two dimensional graph which compares distance versus pixel value. This technique is used to evaluate changes in the wall of a single follicle or different follicles over time. The computer software determines the precise gray-scale value of the pixels along the line and provides image attributes such as NPV, PH, and RSV. To provide information of changes over time, many lines at different locations of the follicle wall and antrum can be concatenated to obtain a single image. This is termed the time series technique. In the next step, a shading algorithm is applied to show detailed analysis of the surface contours of the follicular walls and fluid. The resultant three-dimensional graph displays follicle diameter, pixel intensity and time. By using time

series analyses in combination with other methods, the follicular wall and antrum can be assessed visually as the follicle progresses through different stages of growth and regression [111, 131].

1.2.6 Region analysis

Region analysis is the most promising technique for visual evaluation of the physiological status of a follicle. This technique involves overlaying a pixel-by-pixel mesh onto a selected region of the follicle to produce a three-dimensional image. The graph compares the follicle diameter (length and width), and pixel intensity. A computer-generated skin can be placed over the mesh framework to provide a topographical image. Shading algorithms and color can be added to the image to enhance visual perception and allow comparison of different portions within images of different follicles or images of the same follicle over time. Region analysis may develop into a clinical tool useful tool to instant assessment of ultrasound image attributes associated with the health and viability of the follicle. By applying the region analysis technique, DF can be inspected for echotextural changes indicative of physiological status. Therefore, biologically important times can be identified and employed to evaluate the effects of infertility therapies or contraceptive regimens to increase their effectiveness [111, 131].

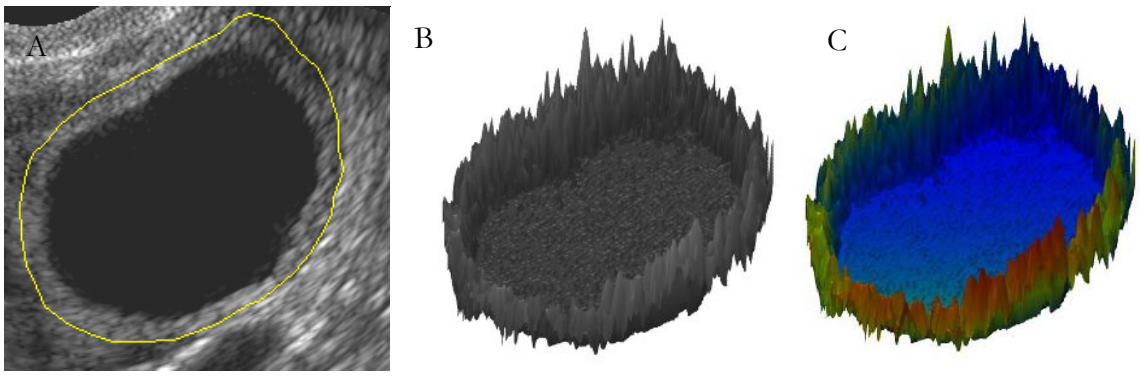

Figure 1.4: Regional analysis of a preovulatory follicle. An image of the follicle is shown with follicle wall identified by the yellow line (A). Computer generated "skin" stretched over the selected area of the follicle (B). Height-shaded color algorithm added to enhance visual appreciation (C).

1.3 Ovarian follicular development during oral contraceptive use

1.3.1 Characteristics of oral contraceptives

The development of oral contraception in 1960 radically changed the contraceptive choices for women. Enovid™, which contained synthetic estrogen (150 μg mestranol) and synthetic progestin (9.85 mg norethynodrel) was initially introduced as a menstrual regulator [128, 137]. In 1960, the Food and Drug Administration approved Enovid™ as an oral contraceptive. Today, OC (oral contraceptives) are the most commonly used, reversible type of contraceptive in the world [129, 138]. Combined OC contain an orally-active progestin and estrogen. The currently used OC combine ≤35 μg Ethinyl estradiol (EE) with a synthetic progestin [139]. Supra-physiologic levels of estrogen and progestin provide negative feedback on the hypothalamo-pituitary axis [140]. Reductions in endogenous GnRH, FSH and LH suppress ovarian follicular development, preventing ovulation and subsequent conception. The progestin component of OC directly affects ovarian function with inhibition of the LH surge and subsequent ovulation [141]. In addition, progestin decreases the permeability of the cervical mucus and endometrial receptivity for embryo implantation, and decreases tubal and uterine motility causing a delay in gamete transport [142]. The

exact mechanism of action of the estrogen component has not yet known. In primates, estrogens have been shown to inhibit the growth of pre-antral and medium-sized antral follicles through inhibition of FSH secretion [143, 144]. Estrogen is also required to provide socially acceptable bleeding patterns in women during regular OC use [129]. The most recent OC formulations contain EE doses as low as 15 μg. In addition, use of 3rd and 4th generation progestins (i.e., levonorgestrel, deosgestrel, gestodene, and norgestimate) has resulted in more effective OC regimens [129].

Oral contraceptives are generally categorized into monophasic and triphasic formulations, based on their hormonal content. Monophasic OC contain the same amount of EE and progestin hormones in each pill, while triphasic OC have varying amounts of either EE, progestin, or both throughout the cycle [139]. Triphasic OC were designed to mimic the rising and falling of estrogen and progesterone during the natural cycle [146]. Conventional OC administration consists of a 28 day cycle comprised of 21 daily active pills followed by a 7-day hormone free interval (HFI) to mimic the physiological event of natural menstrual cyclicity [147]. Currently, continuous OC dosing scheme is used in which women take OC continuously for months at a time and discontinue for a withdrawal bleed only a few times a year [148]. Progestin-only OC are also used as contraceptives in special cases such as during lactation; however, they are less efficient in preventing pregnancy than to combine OC [149].

In most studies, the efficacy rate of OC is reported as failure rate during 1 year of use. The expected efficacy rate is < 2%, but the actual rate is reportedly < 5% [150, 151]. The Pearl Index is the standard way for reporting the effectiveness of a birth control method and is defined as the number of pregnancies per 100 women-years of treatment [141, 144, 150, 152]. Ovarian follicular development is not completely inhibited in OC users, and the degree of ovarian activity depends on the type and dose of steroid in the OC, the administration regimen, and user compliance [152].

Adverse reactions to OC are considered to be estrogen, progesterone, or androgen-related effects. They include nausea, fluid retention, headaches, breast tenderness, breakthrough bleeding, spotting, hypertension, fatigue, depression, oily hair and skin, hirsutism, increased appetite, weight gain, and acne [153, 154]. A small increase in risk of breast cancer has reported. Incidences of myocardial infarction and cerebrovascular disease are slightly higher in OC users who smoke compare to the normal population [155, 156]. Oral contraceptives also offer many non-contraceptive benefits. These include improvement of dysmenorrhoea, increasing bone mineral density, prevention of iron deficiency anaemia, lower risk of ovarian and breast cyst formation, and decrease the risk of endometrial, ovarian, and colorectal cancers [146, 157].

1.3.2 Follicular development during oral contraceptive use

Follicular development to ≥ 10 mm in diameter and "escape" ovulation have been observed in OC users [158, 159]. During natural menstrual cycles DF become physiologically selected for preferential growth over its cohort at a diameter of 10 mm and ultimately ovulate [53]. Most of DF that develop during OC use fail to ovulate, and regress by inhibition of the LH surge or the inability of the follicle to respond to LH due to the effects of progesterone or sensitivity of LH receptors [148, 150-152, 160, 161]. However, there are reports of ovulation and pregnancies during OC use [60, 162, 163]. The high incidence of DF development during conventional OC use suggests that the current OC dosing schemes does not completely suppress follicular development [164, 165]. Follicles which develop to pre-ovulatory diameter during OC use have similar ultrasound image attributes and are indistinguishable from comparable natural-cycle follicles [151, 160]. These similarities can be interpreted to mean that follicles which develop during OC use have similar physiologic status to natural cycle follicles; therefore, ovulations can occur resulting in pregnancy and OC failure. During OC use, the degree of pituitary-ovarian suppression is related to the dose of

EE, rather than the dose and type of progestin [157, 159, 166, 167]. The maximum diameter of detected follicles and number of follicles observed was greater in women taking low EE dose (i.e., 20 μg) compared to moderate EE dose OC regimens (i.e., 30-35 μg) [168, 169]. Also 20 versus 30 μg EE formulations have been associated with greater serum FSH and LH levels [161].

1.3.3 Follicular development during the hormone free interval

Conventional OC regimens were introduced in the 1960s. The dosing scheme provided a 7 day HFI designed to induce a withdrawal bleeding each 28-day cycle and decreased exposure to exogenous hormones. Several years later, numerous studies have reported DF development during the HFI, many of which continued development to pre-ovulatory follicle status. This was particularly evident with low EE formulations [151, 166, 170, 171]. Approximately 85% of DF development is initiated during HFI and follicles > 10 mm have been ultrasonographically detected in this period [151, 152, 162, 172]. The HFI allows pituitary-ovarian activity to recover to levels observed during the early follicular phase of the natural menstrual cycle. Thus, FSH and estradiol levels at the end of the HFI increase and reach the levels which observed during the natural cycle [160, 173]. Initiation of the OC following the HFI causes a decrease in FSH regardless of the presence of a DF [154]. If no DF developed during the HFI, folliculogenesis is suppressed. If a DF is present during the HFI, follicle growth continued despite initiation of OC and declining of FSH concentrations due to the decreased dependence of DF on gonadotropins [42, 148]. It has been reported that shortening the HFI from 7 days to 3 or 4 days or replacing some hormone-free days with administration of unopposed EE suppresses follicular development better than conventional dosing schemes [167, 171, 172, 174, 175]. A new OC regimen, in which the last 5 days of the 7days HFI replaced with pills containing 10 μg EE reduces follicular growth compared to the conventional

OC dosing scheme [171, 172]. These findings are interpreted to mean that omitting or even shortening the HFI increase contraceptive efficacy by decreasing the risk of DF development.

1.3.4 Return to fertility following discontinuation of oral contraceptives

Oral contraceptives are the only reversible contraception that inhibits ovulation by suppressing follicular development and ovulation [138]. Since most OC users are young women who have not started their families yet, it is essential to determine if OC have residual effects on ovarian function following discontinuation. It is apparent that women who discontinue OC commonly experience a two to three month delay in conception, but their infertility is transient [170, 176]. However, a study conducted in Malaysian women reported no difference between conception rates of previous OC users and previous users of non-hormonal contraception. Approximately 39%-56% of all previous OC users conceive within three months of discontinuation [166, 167, 169]. It has been reported that miscarriage rate is higher for the first 3 months following OC cessation [170, 177]. Furthermore, 90-99% conception rates were observed within 2 years after discontinuation of OC. It appears that conception rates return to normal expected values within two years following discontinuing of OC [166, 174, 175, 178]. The delay in fertility following OC use may be due to continued hypothalamic suppression for a short period of time following OC discontinuation. Anovulation, or dysfunctional ovulation following discontinuation of OC, may account for the delay in fertility; however, approximately 98% of women ovulate within three months following discontinuation of OC [166, 178]. The concentration of EE can affect the median time to conception, for example OC with EE doses ≥50 μg increase the median time to conception following discontinuation of OC by one month compared to OC containing < 50 μg EE [170]. Since OC containing ≥50 μg EE are no longer prescribed commonly, this factor is likely not responsible for the delay in fertility. A woman's parity, previous cycle irregularity, age, and

behavioural factors (the timing and frequency of intercourse) can affect the delay in fertility following discontinuation of OC [166, 170, 179, 180]. Therefore, the delay in fertility is due to a combination of both biological and behavioural factors. Further research is needed to determine the exact mechanisms of action responsible for the delay in fertility following discontinuation of OC.

1.3.5 Summary

Recently, oral contraceptives have undergone significant changes. These changes have focused on maintaining contraceptive efficacy and reducing adverse effects. They include progressive reduction of the ethinyl estradiol (EE) dose, development of new progestins, phasing the level of hormonal treatment, and extending the duration of hormonal exposure. It appears that reducing the estrogen dose to minimize adverse effects may cause lower follicular suppression effects, particularly during the HFI. It is currently unknown why some follicles ovulate during OC use while others regress. It has been well established that following OC discontinuation a two to three month lag in fertility occur compared to non-hormonal contraceptives. At this time there are no acceptable hypotheses to explain the delay in fertility following discontinuation of OC. A better understanding of the exact effects of OC on the reproductive organs would likely assist in the explanation of the delay in fertility following discontinuation of OC. Studies are required to provide insight into the mechanisms responsible for ovarian and uterine suppression during OC use.

Computer-assisted quantitative echotexture analysis of ultrasound images accurately reflected the functional and endocrine characteristics of dominant and subordinate follicles at specific stages of development and regression. Based on findings in animal studies, computer-assisted image analysis can be developed as a safe and non-invasive technology to evaluate human ovaries.

Chapter 2

2. OBJECTIVES AND HYPOTHESES

The objectives of the studies contained in this thesis were to:

1) Determine if, and when, human preovulatory (dominant) follicles may be prospectively identified from others in their cohort in vivo using computerized image enhancement and analysis;
2) Evaluate differences in image attributes of DF and SF1 of major anovulatory waves;
3) Elucidate differences in image characteristics of ovulatory and anovulatory DF of the same cycle;
4) Compare ultrasonographic image attributes of ovulatory DF of natural cycles with those that developed following OC discontinuation; and,
5) Evaluate ultrasonographic image attributes of DF and SF1 of the first cycle following discontinuation of conventional and continuous oral contraceptive regimens.

The corresponding research hypotheses were tested:

1) Image attributes of the ovulatory DF would differ quantitatively from those of atretic (subordinate) follicles in the same cohort;
2) Image attributes of anovulatory DF quantitatively would differ from SF1 in the same cohort;
3) Image characteristics of the ovulatory DF differ from anovulatory DF in the same cycle;
4) Ultrasonographic image attributes will differ between DF of natural cycles and DF of the first cycle following OC discontinuation; and,
5) Ultrasonographic image attributes of dominant and SF1 will differ between the first cycles following discontinuation of continuous versus conventional OC regimens.

Chapter 3

3. ULTRASONOGRAPHIC IMAGE ANALYSIS OF OVARIAN FOLLICLES DURING THE HUMAN MENSTRUAL CYCLE

3.1 Abstract

Background: Morphologic characteristics obtained by ultrasonography are not easily quantitated by the human eye. Computer-assisted image analysis overcomes subjective human evaluation of ultrasonographic images. The objectives of this study were to test the hypotheses that ultrasonographic image analyses would allow: 1) prospective identification of the follicle destined to become the ovulatory follicle from others in its cohort; 2) there are differences in image attributes of dominant and 1st subordinate follicles of the same cohort from ovulatory and anovulatory major waves; and 3) there are differences between ovulatory and anovulatory dominant follicles of major waves. Identification of the timing of preovulatory selection is a key component in understanding natural ovarian function, ovarian suppression for contraception, and improvement of ovarian superstimulation protocols.

Methods: Daily ultrasonographic images obtained from healthy women of reproductive age (range 18-40 years) recorded in a previous study [53] were analyzed to determine timing of dominant follicle selection. Follicular walls and antra of dominant and 1st subordinate follicles (n=30) from major ovulatory waves (experiment 1), as well as dominant (n=8) and 1st subordinate follicles of major anovulatory waves (experiment 2) were analyzed using custom designed software (SYNERGYNE 2©, Saskatoon, SK, Canada). Differences in image attributes between 1st subordinate and dominant follicles were compared using repeated measure ANOVA (PROC MIXED).

Results: Physiologically-selected dominant follicles were retrospectively identified by the difference in their diameters 7 days before ovulation ($p<0.0001$). In experiment 1, image attributes of the follicle antrum and wall in major ovulatory waves exhibited higher numerical pixel value (NPV; $p<0.0001$) and pixel heterogeneity (PH; $p<0.0001$) in 1st subordinate compared to dominant follicles, started 9 days before ovulation. In experiment 2, image attributes of anovulatory dominant follicles demonstrated higher NPV ($p=0.0208$) and PH ($p=0.0046$) in the antrum and higher NPV ($p=0.0002$) and PH ($p=0.0033$) in the wall compared to ovulatory dominant follicles, which was detected approximately 6 days after wave emergence and continued until the day of ovulation.

Conclusion: Our results supported the hypothesis that dominant follicles may be prospectively identified from the follicular cohort using computer-assisted analyses of ultrasonographic images. Furthermore, image analyses can be used to differentiate anovulatory versus ovulatory dominant follicles.

3.2 Introduction

The introduction of ultrasonography in the 1980's provided an unprecedented opportunity to visualize the inner workings of the reproductive system. Non-invasive imaging-based techniques have made it possible to monitor reproductive organs sequentially in living animals and humans, and it remains the only *in vivo* method for directly assessing ovarian function [108]. However, as a research and diagnostic tool, ovarian ultrasonography is limited due to: 1) inter-observer variability; 2) the need for serial evaluations to elucidate ovarian status [133, 134]. Recent advances in ultrasonographic techniques and development of computer-assisted image analysis tools have overcome some of the subjectivity of image assessment. Image analysis has been used to characterize several quantitative indicators of physiological function of ovarian structures in domestic animal models and humans [108, 131, 133, 180].

Practical and ethical limitations prohibit detailed study of the hormonal microenvironment and physiologic status of follicles in humans. However, the bovine model has been useful for understanding human folliculogenesis since there are similarities in the size, morphology, physiology, and pathology of the ovaries in cows and women [95, 97, 103, 108, 133, 135]. Women and mares also share similarities in the development of minor and major follicular waves during the ovarian cycles. Therefore, comparative studies with the equine model have enhanced our understanding of folliculogenesis [53, 54, 95, 103, 181-184].

The use of computer-assisted analysis of ovarian follicles has been validated *in vitro* in the bovine model by Singh *et al.* (1998) [133]. The physiologic status and phase specific changes in image echotexture analysis of follicles and steroid hormone content of follicular fluid were characterized. Tom *et al.* (1998) quantified pixel values of follicles *in vivo* [135]. Significant, temporal changes were found in the ultrasound image echotexture of the follicle wall and antrum during the bovine estrous cycles which were associated with developmental phase. These findings were in agreement with histological changes of ovulatory and atretic follicles determined by histology and endocrine studies [133, 229].

Selection of the dominant follicle (DF) in cattle becomes manifest when the largest follicle is 8.5 mm, 22.5 mm in mares, and 10 mm in women [15, 54]. In heifers, administration of FSH for 2 days before the time of selection of DF delayed the time of DF divergence from SF [230]. However, there is biochemical evidence that selection of DF may occur prior to morphological selection (divergence in diameter). Rivera *et al.* (2003) examined a group of follicles in cattle before divergence of the DF and 1st subordinate follicle (SF1) based on when the follicles were 7 mm in diameter or less. An increase in proteolytic activity in IGFBP-4/-5 (PAPP-A) and in estradiol elaboration occurred prior to DF

selection. It was suggested that the increased PAPP-A degraded IGFBP-4 and -5, freeing more IGF to act synergistically with FSH and increase estradiol production in the future DF [185].

Early histological studies of human ovaries obtained surgically documented that estrogen secretion increases in proportion to the growth of DF ≥8 mm in diameter [49]. Gougeon (1989) reported that follicles are selected at 5 to 8 mm in diameter, based on a higher granulosa cell mitotic index in the largest healthy follicle compared with other follicles of the cohort [14]. Macklon and Fauser (1999) and Pache *et al.* (1990) reported the first appearance of the DF at mean size 10 ± 3 mm. Van Dessel *et al.* (1996) showed that increased aromatase enzyme activity occurs only in selected DF, with intrafollicular estradiol concentrations rising only in follicles greater than 9 mm in diameter [51, 56, 57].

Current work in our laboratory has focused on elucidating human ovarian physiology during the menstrual cycle. Recently, Baerwald *et al.* (2003) identified wave-like patterns of follicular growth and development in human ovaries during the menstrual cycle. Sixty eight percent of women exhibited 2 waves and 32% exhibited 3 waves of follicular development during an ovarian cycle. The final wave of each cycle resulted in ovulation of a dominant follicle. All preceding waves were either minor or major anovulatory waves [53]. Major waves were those in which a single DF was selected to grow larger than all other SF of the cohort. Minor waves are defined as those that selection of DF was not manifest. Follicle selection is characterised by a divergence in the growth profiles of DF and SF1 when the DF is 2 mm larger than SF1 in diameter [53, 188].

Physiologic selection of DF remains one of the great mysteries in reproductive biology. It has been recently demonstrated that in approximately 30% of women there may be 2 or 3 times during the cycle when selection of a DF is manifest [53, 188]. That is, DF selection may occur 1 or 2 times during the cycle before the ultimate selection of the ovulatory follicle, depending on whether

the individual woman has 2 or 3 major waves of follicle development [1]. Accordingly, we wished to determine if the selected follicles exhibited image attributes reflective of their physiologic status. Our rationale was that all DF would exhibit similar attributes during the early phases of their development. Approximately 23% of ovarian stimulations as a treatment for anovulation fail due to inadequate ovarian response [189]. Evidently, better control of ovarian response is necessary which might be influenced by the status of the DF at the time stimulatory treatment is initiated. Rapid non-invasive assessment of the physiological status of individual follicles represents a tremendous advance in the diagnosis and management of many aspects of fertility, infertility and evaluation of different therapeutic inventions.

The primary objective of the present study was to determine if and when the human preovulatory (dominant) follicle may be prospectively identified from others in its cohort during the ovulatory wave *in vivo* using computerized image enhancement and analysis. We hypothesized that image attributes of the DF would differ from the SF1 of the same cohort. Secondary objectives were to evaluate differences in image attributes of DF and SF1 of anovulatory major waves and to assess differences in image attributes of ovulatory DF compared to anovulatory DF of the same cycle. We hypothesised that image attributes of anovulatory DF would differ from SF1 and that the ovulatory DF would differ from anovulatory DF.

3.3 Materials and methods

The study was a retrospective analysis of ultrasound images obtained in a previous study designed to characterize ovarian follicular wave dynamics during natural cycles. Participants in the original study included 50 healthy women of reproductive age (mean $\pm$ SD = 28.0 $\pm$ 6.9 years, range = 19 - 43 years). High-resolution ATL Ultramark 5 - 9 HDI and HDI 5000 ultrasound machines with 5-9 MHz multi-frequency convex array transducers (Advanced Technologies Laboratories;

Bothell, WA, USA) were used to acquire images. The study protocols for the original and current studies were approved by the University of Saskatchewan Biomedical Research Ethics Board [53, 190].

In the original study, follicular development in each ovary was monitored by daily transvaginal ultrasonography for one IOI (inter-ovulatory interval). An IOI was defined as the interval from one ovulation to the following ovulation. Ovulation was defined as the disappearance of the largest follicle ($\geq$15 mm) that had been identified by ultrasonography and the subsequent visualization of a corpus luteum [53]. Wave emergence was defined as the day on which the largest follicle of the wave was first identified at 4 to 5 mm.

The location and diameter of individually-identified follicles ($\geq$ 4 mm) and corpora lutea were recorded each day. Images were recorded digitally and transferred to a customized database during the ultrasound examinations. The dominant follicle was defined as the largest follicle of the wave and the SF1 was defined as the second largest follicle of the same wave. Major waves were defined as waves in which one follicle grew to ≥10 mm and grew larger than the next largest follicle by ≥ 2 mm. Minor waves were defined as those in which the largest follicle developed to < 10 mm and did not exceed other follicles of the wave by ≥2 mm. Physiologic selection was defined as the first day of divergence in the diameter of the DF and SF1 in their follicle growth profiles. Ovulatory major waves were those in which the DF ovulated, while in anovulatory major waves the fate of the DF was atresia [188]. Daily images of DF and SF1 of each ovulatory major wave were identified retrospectively from day of ovulation to the day of wave emergence at 4 -5 mm. Images selected for analysis were obtained at the largest cross-sectional diameter with the fewest image artifacts. All image analyses were performed by the same individual (ER).

Image attributes of DF and SF1 were analyzed using customized software optimized for ultrasonography (SYNERGYNE 2©, Saskatoon, SK, Canada). Three different techniques were applied: 1) spot analysis; 2) line analysis; and, 3) region analysis. All were designed to quantify gray-scale values of selected areas of an image [131]. Three quantitative image attributes were evaluated: 1) numerical pixel value (NPV), defined as the mean gray-scale value of the sampled pixels; 2) pixel heterogeneity (PH), defined as the standard deviation of the gray-scale values of the sampled pixels; and, 3) the region selected volume (RSV) defined as sum of the brightness of all of the pixels within the selected area (GSV/mm^2) [108].

In spot analyses, the follicle antrum was divided into 4 quadrants and pixel values from each region were measured by a computer-generated circle (15 pixels in diameter). Follicle wall pixel values were obtained by placing 4 small circles, each measuring 2 pixels in diameter, on the wall of each follicle. Spots were placed at the 2, 4, 8, and 10 o'clock positions to minimize specular reflection artifacts. Antral and wall NPV and PH were obtained as an average of the 4 measurements. For all analyses, images were normalized using the maximum and minimum pixel values from the gray-scale bar generated by the ultrasound instrument [133]. Line analysis was used to measure the NPV and PH values of pixels along a line placed across a specified section of the follicle wall. A 2-dimensional graph of the numerical pixel values was produced that depicted the intensity of the echoes located along the line. Four lines were drawn from the antrum-wall interface to the stroma. The antrum-wall interface was defined as the last pixel along the line after which a sequential rise in gray-scale occurred [131]. The second sudden rise in grey-scale values along the line was representative of stroma interface. The 4 lines were located at the 2, 4, 8, and 10 o'clock positions of the follicle wall to avoid enhanced through-transmission, refraction and shadowing artifacts. NPV and PH of each follicle wall were reported by averaging the values for 4 lines for each

image. The values for the lines comprising the mean differed slightly in length based on follicle wall thicknesses at each of the locations.

Region analyses involved overlaying a computer-generated pixel-by-pixel mesh onto a selected area to generate a 3-dimensional framework representing pixel values. A computer-generated surface was then placed over the framework to produce a topographical image. Color shading was applied to enhance visual appreciation. The antrum-wall interface was used to outline the internal border of the follicle wall. The visually detectable margin between follicle wall and peripheral stroma was used to outline the identify border of the follicle wall. This technique enhanced rapid visual assessment of ultrasonographic attributes associated with follicle viability and atresia and made the numeric data easier to visualize [111]. The area selected for region analyses were used to measure NPV, PH and RSV for the entire follicle and follicle wall. In current study, first the whole follicle was analyzed and then follicle walls were isolated for evaluation.

Experiment 1: Daily sequential images of the individually-identified DF and SF1 were used for the analyses. Images of DF (n=30) and SF1 (n=30) were analyzed and data were centralized to the day of ovulation.

Experiment 2: Images of individual DF (n=8) and SF1 (n=8) of major anovulatory waves and DF (n=8) of ovulatory waves were evaluated. Only 8 of the 30 women (26%) in the previous study exhibited major anovulatory waves. Data were centralized to the day of wave emergence.

Image attributes were compared using repeated measures analysis of variance (PROC MIXED, SAS, Version 9) for main effects of follicle type, day, and follicle by day interaction. Significance was set at $p< 0.05$. Results are expressed as the mean ± SEM.

3.4 Results

3.4.1 Experiment 1

3.4.1.1 Dominant follicles versus first subordinate follicles of ovulatory major waves

Mean diameter profiles of the DF and SF1 in major ovulatory waves are presented (Figure 3.1, A). The mean diameter of DF was 21.1 ± 1.1 mm on Day –1 (Day 0 = day of ovulation). On the day of divergence, the DF was 10.4 ± 0.3 mm and the SF1 was 8.3 ± 0.3 mm in major ovulatory waves, as previously documented [188]. The DF became larger ($p<0.0001$) than the SF1 7 days before ovulation.

Spot analysis of follicle antrum and wall: Evaluations of NPV and PH of the antral fluid images by spot analysis are shown (Figure 3.1: B, C). Numerical pixel values were higher in SF1 than DF ($p<0.0001$). Differences were detected from day -9 to day 0 (i.e., 9 days before ovulation to day of ovulation; $p=0.0013$). Heterogeneity of the follicle fluid was higher in SF1 than DF ($p<0.0001$). Pixel heterogeneity of SF1 antra increased as the follicle regressed, whereas antral heterogeneity of DF decreased as the interval to ovulation decreased. Follicle by day interaction was attributed to a greater decrease in NPV ($p=0.0061$) and PH ($p<0.0001$) as the interval to ovulation decreased (greater in which follicle?). Spot analysis of the follicle wall demonstrated higher NPV in SF1 compared to DF ($p=0.0002$). The follicle by day interaction was not different ($p=0.6045$). Pixel heterogeneity was similar between SF1 and DF ($p=0.1829$).

Line analysis of follicle wall: Numerical pixel values for the follicle wall were higher ($p<0.0001$) in SF1 compared to DF and NPV of DF progressively decreased as the DF neared ovulation. This difference began 10 days before ovulation and continued until the day of ovulation ($p=0.0274$). Pixel heterogeneity of the follicle wall was higher in SF1 compared to DF, ($p<0.0001$; Figure 3.1, D).

Differences between PH of follicle walls were first detected 9 days before ovulation (P=0.0214; Figure 3.1, E).

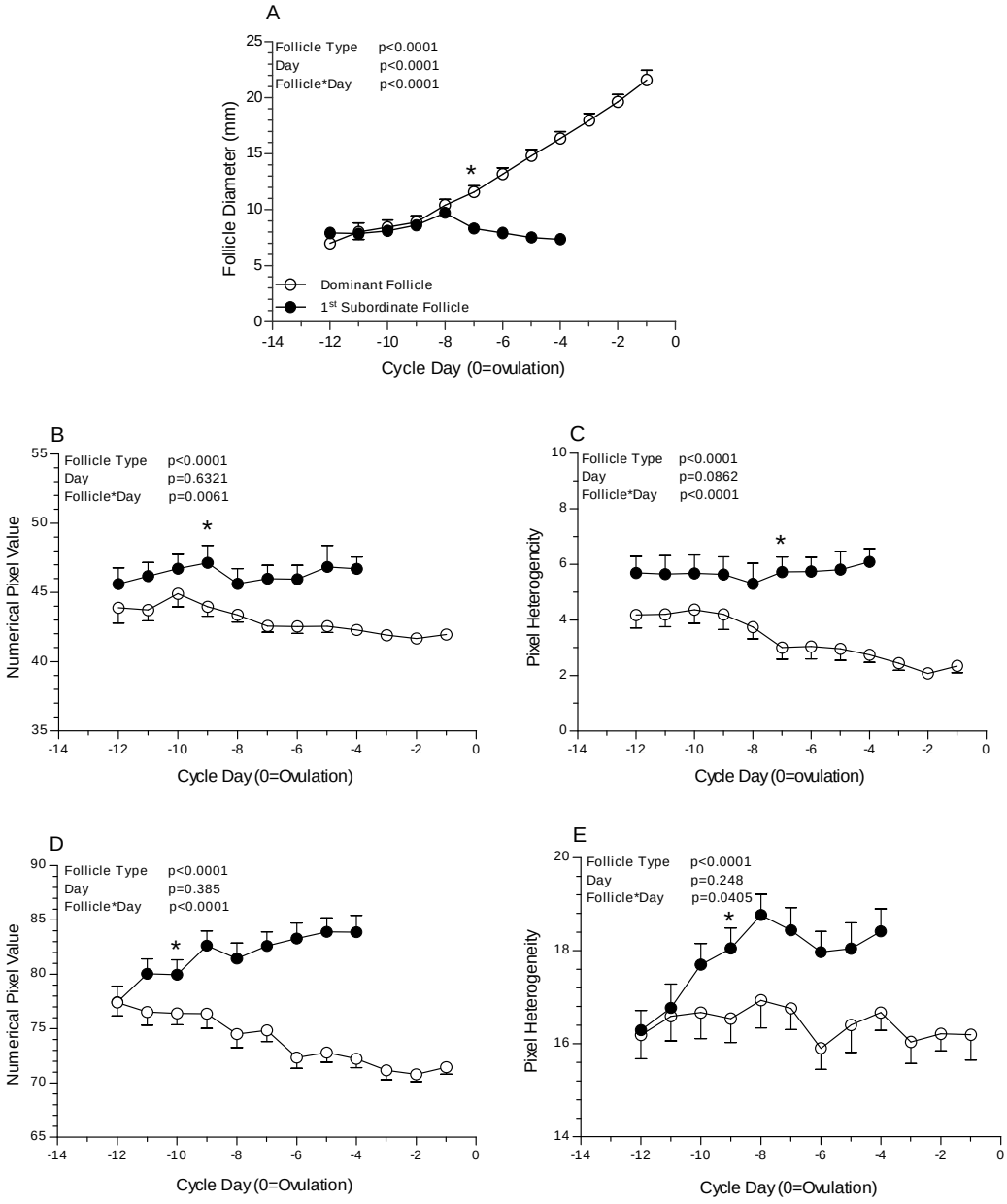

Figure 3.1: Mean follicle diameter (A), NPV (B), PH (C) of the antrum obtained by spot analysis, and NPV (D), PH (E) of the wall obtained by line analysis of dominant (○; n=30) and 1st subordinate (●; n=30) follicles of ovulatory waves (*=first day of significant difference). Data are represented as the mean ± standard error.

Region analysis of follicles: Numerical pixel values were greater in SF1 compared to the DF ($p=0.0003$). Interactions ($p=0.3717$) between follicle type and day were not observed. There were no differences in PH ($p=0.1043$) between DF and SF1 (Figure 3.2, A, C, E). Volume of the selected region (RSV) was greater ($p<0.0001$) in DF than SF1 beginning 8 days before ovulation ($p<0.001$).

Region analysis of the follicle wall: Numerical pixel values of the follicle wall were greater in DF compared to SF1 ($p=0.001$) beginning on day -6 ($p=0.0009$). Pixel heterogeneity exhibited a similar pattern with higher values ($p=0.0182$) in DF starting 6 days before ovulation ($p=0.01$; Figure 3.2, B, D, F). DF showed higher RSV ($p<0.0001$) compared to SF1 beginning 8 days before ovulation ($p<0.001$).

Three-dimensional color images representing the whole follicle and follicle wall obtained by the regional analysis tool were examined visually for qualitative differences between DF and SF1 (Figures 3.3, 3.4). Apparent differences observed were: 1) a less defined and irregular follicular-wall in SF1; 2) a sharply defined wall with a distinct boundary from the antrum of the DF; 3) a "rough" and heterogeneous antrum in SF1; and, 4) a smooth and homogenous antrum in DF.

Follicle region analysis: Follicle wall region analysis:

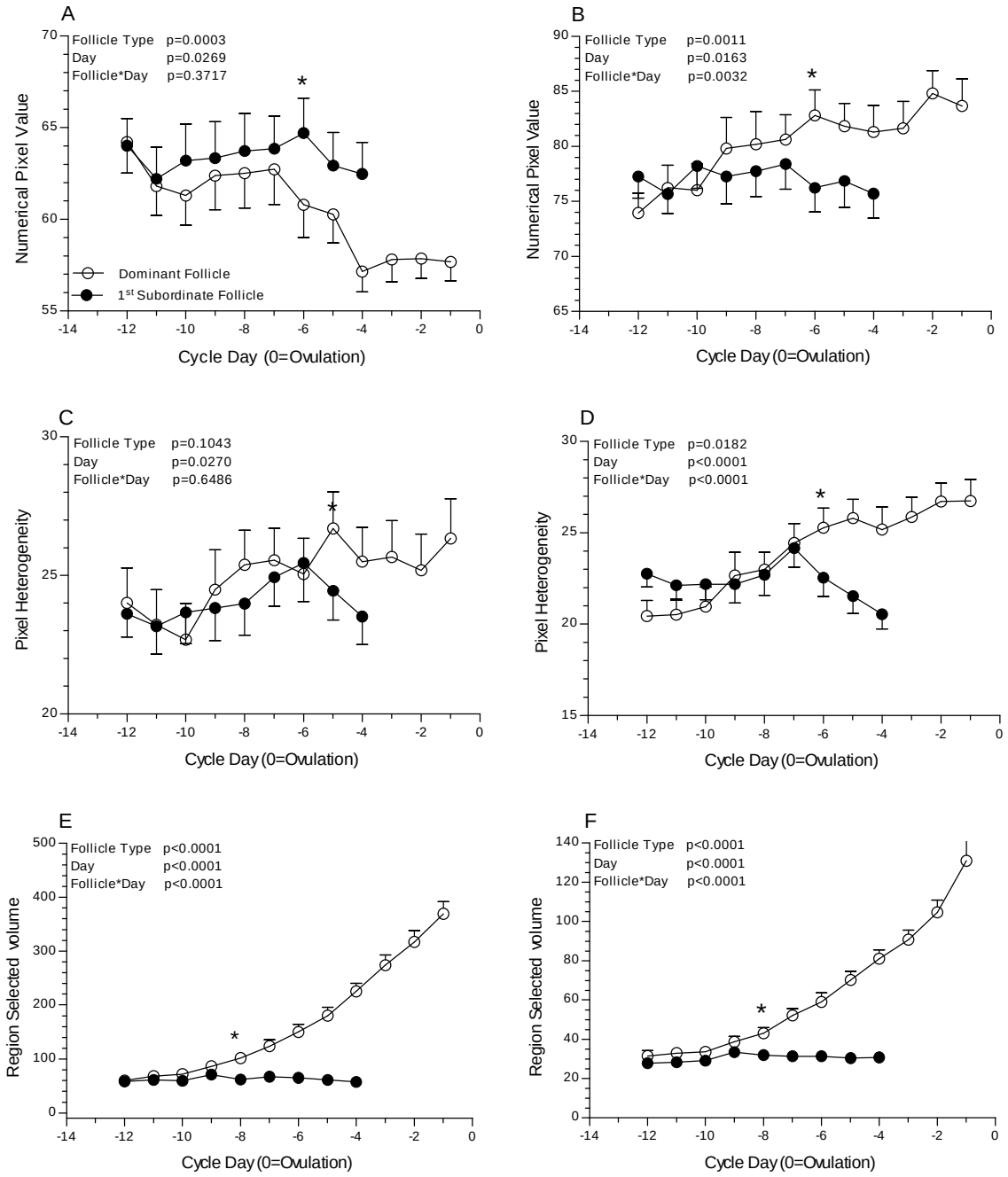

Figure 3.2: NPV (A, B), PH (C, D), and RSV (E, F) obtained by region analysis of dominant (○; n=30) and 1st subordinate (●; n=30) follicles of major ovulatory waves (*=first day of significant difference). Region analyses for the entire follicle (A, C, E) and follicle wall (B, D, F) are shown. Data are represented as the mean ± standard error.

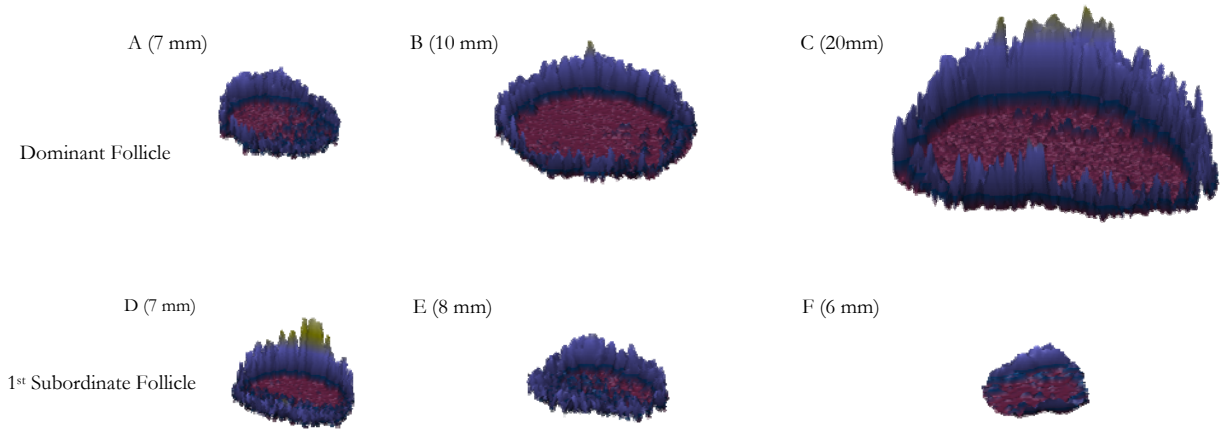

Figure 3.3: Three dimensional images of dominant (A, B, C) and 1st subordinate follicles (D, E, F) from ovulatory waves (Experiment 1) generated by the region analysis at 10 (A, D) and 8 (B, E) days before ovulation, and 1 day (C, F) before atresia. X and Y axes represent the length and width dimension of the original images. The vertical axis represents the quantitative pixel values.

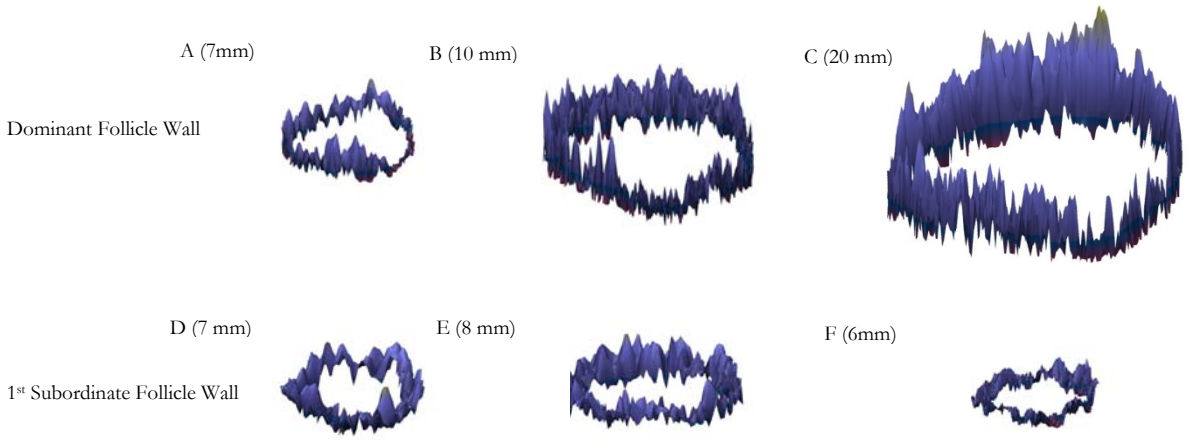

Figure 3.4: Three dimensional images of dominant (A, B, C) and 1st subordinate follicles (D, E, F) wall from ovulatory waves (Experiment 1) generated by the region analysis at 10 (A, D) and 8 (B, E) days before ovulation, and 1 day (C, F) before the follicles become atretic. X and Y axes represent the length and width dimension of the original images. The vertical axis represents the quantitative pixel values.

3.4.2 Experiment 2

3.4.2.1 Dominant follicles versus 1st subordinate follicles of anovulatory major waves

Spot analysis of follicle antrum: The SF1 antrum exhibited higher NPV ($p<0.0094$) compared to the DF in the anovulatory major waves (Figure 3.5, A). Antral PH was higher ($p=0.0049$; Figure 3.5, B) in the SF1 than the anovulatory DF. There were no differences between anovulatory DF and SF1 antral NPV ($p=0.5710$) and PH ($p=0.7383$) 1 day before they were no longer detected during the final regression phase. Both types of follicles exhibited similar attributes 1 day before they became atretic.

Line analysis of follicle wall: The follicle wall exhibited higher NPV in SF1 compared to the DF ($p<0.0001$) of anovulatory major waves (Figure 3.5, C). There was no interaction between follicle and day ($p=0.1561$). Pixel heterogeneity was the same in anovulatory DF and SF1 ($p=0.7791$). The attributes of the follicle wall from anovulatory DF and SF1 were similar 1 day before their disappearance (NPV and PH, $p=0.7450$ $p=0.8398$, respectively).

Three-dimensional color images of anovulatory DF and SF1 representing the whole follicle obtained by the regional analysis tool were examined visually. The images demonstrated: 1) a sharply defined wall with a distinct boundary from a homogeneous antrum of the DF 6 days after wave emergence; 2) a thick and less defined follicular wall and "rough" and heterogeneous antrum in anovulatory DF and SF1 one day before ovulation (Figure 3.6).

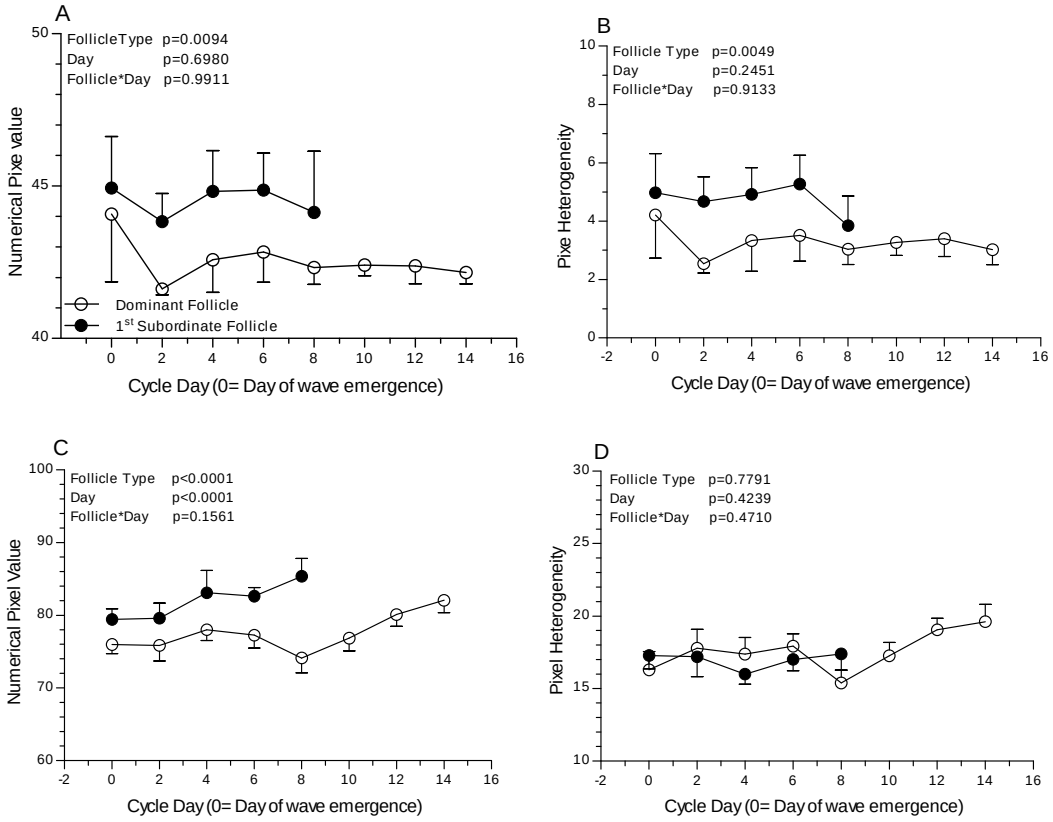

Figure 3.5: NPV (A) and PH (B) of the antrum obtained by spot analysis, and NPV (D) and PH (E) of the wall obtained by line analysis of dominant (○; n=8) and 1st subordinate (●; n=8) follicles of anovulatory waves. Data are represented as the mean ± standard error.

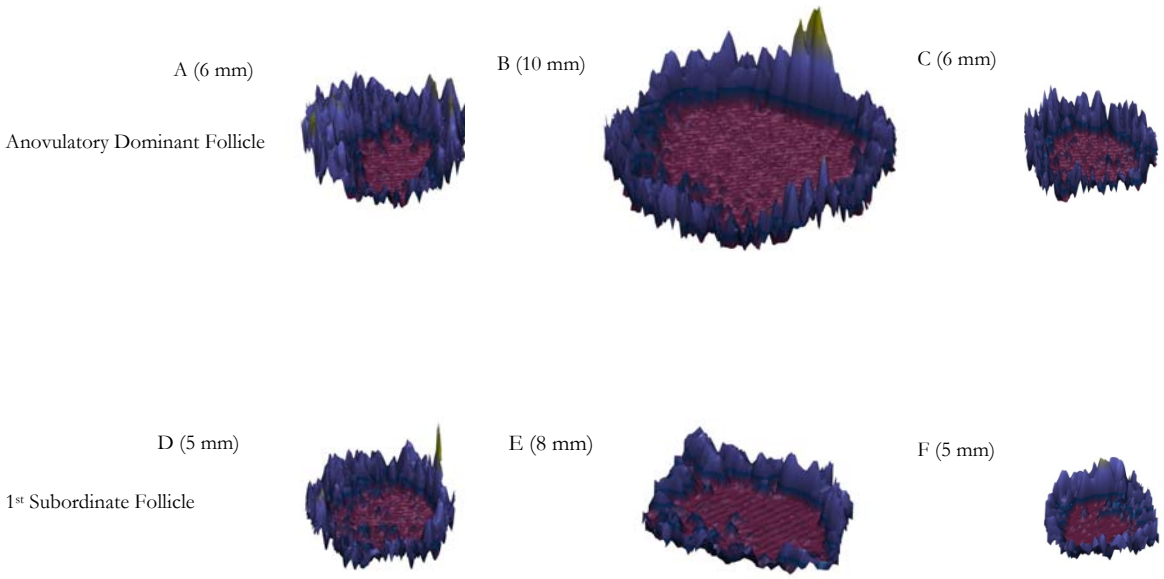

Figure 3.6: Three dimensional images of dominant (A, B, C) and 1st subordinate follicles from anovulatory waves (Experiment 2) using the region analysis at 1 (A, D) and 6 (B, E) day after wave emergence, and 1 day before they become atretic (C, F). X and Y axes are in the length and width dimension of the original images. The vertical axis represents the quantitative pixel values.

3.4.2.2 Ovulatory dominant follicles versus anovulatory dominant follicles of major waves

The diameter of ovulatory DF was greater than anovulatory DF from 5 days ($p=0.0063$) after wave emergence until the end of the wave (Figure 3.7, A). Numerical pixel values of the antra of anovulatory DF were higher than those of ovulatory DF ($p<0.0208$; Figure 7, B). Pixel heterogeneity of the antrum was higher ($p<0.0046$; Figure 3.7, C) in anovulatory versus ovulatory DF beginning 6 days ($p=0.0241$) after wave emergence and continuing until they could no longer be identified. Changes in antral PH over time were affected by the follicle type ($p=0.0346$). Higher NPV were observed in anovulatory follicle walls beginning 6 days ($p=0.0011$) after wave emergence ($p<0.0002$; Figure 3.7, D) and higher PH were observed in the follicle wall of anovulatory DF compared to ovulatory follicles ($p<0.0033$; Figure 3.7, E).

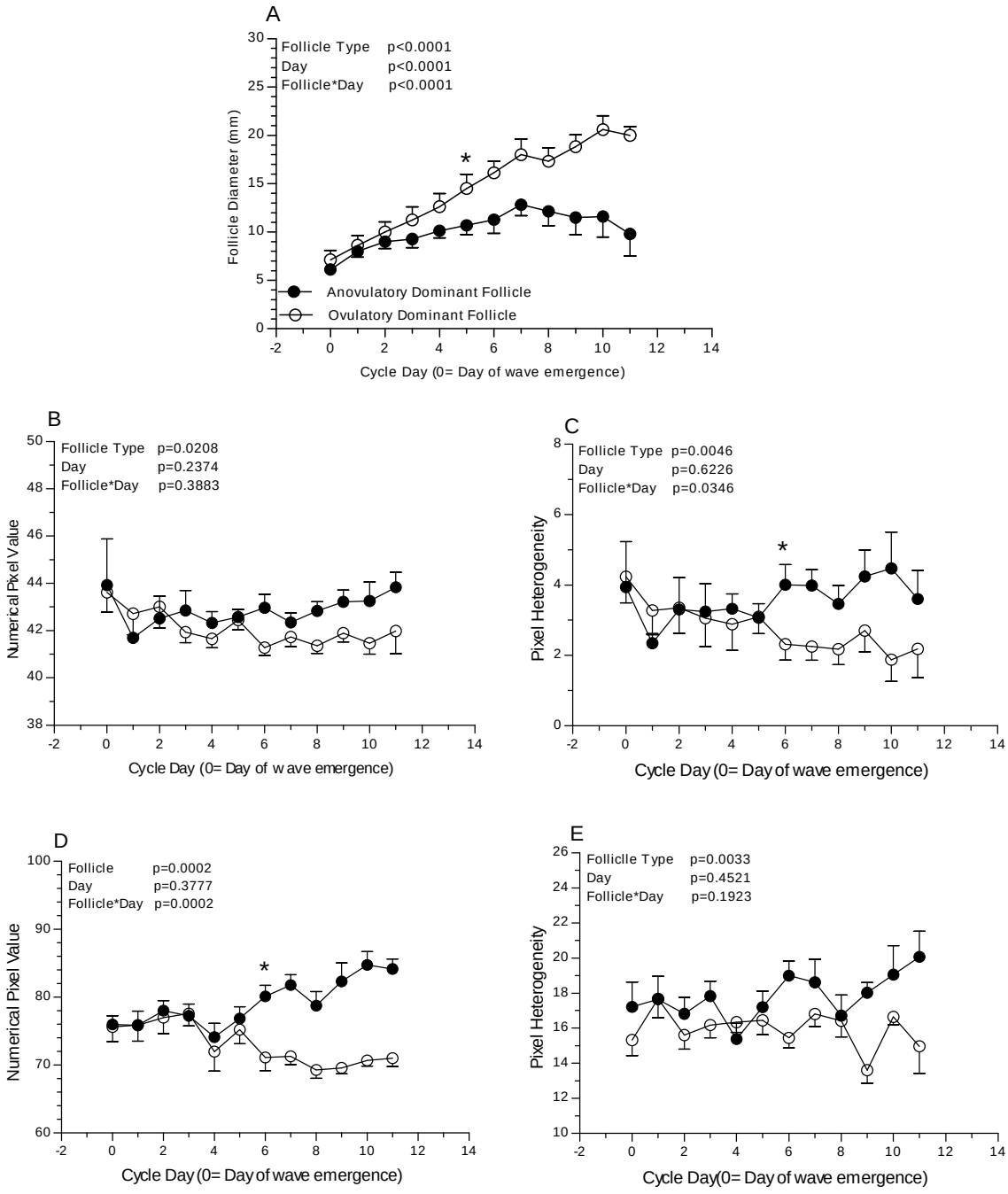

Figure 3.7: Mean follicle diameter (A), NPV (B), PH (C) of the antrum obtained by spot analysis, and NPV (D), PH (E) of the wall obtained by line analysis of ovulatory dominant (○; n=8) and anovulatory dominant (●; n=8) follicles (*=first day of significant difference). Data are represented as the mean ± standard error.

3.5 Discussion

Our results supported the hypotheses that quantitative echotextural differences exist between ultrasonographic images of the DF and SF1 of major ovulatory and anovulatory waves during the human menstrual cycle. Differences in image attributes can be detected prior to the time that selection is manifest by divergence in follicular diameter.

Our retrospective examination of follicle diameter profiles revealed that physiologic selection of a dominant follicle occurred 8 days before ovulation. Divergence was manifest when DF and SF1 were approximately 10 and 8 mm in diameter, respectively; however, image attributes of the walls and antra were greater in SF1 and were first detected 2 days before divergence in their diameters. It appears that morphological differences were present before the DF was visually identified by its larger diameter. Our results in humans were in close agreement with results from previous studies in animal models in that the ovulatory follicle wall was thicker and had lower grey-scale values than observed in atretic follicles [104, 133].

Our results for follicle wall spot analyses were not well correlated with the physiological status of follicles. Similar to antrum, spot analysis of the wall exhibited higher NPV in the SF1 than the DF; however, there was no interaction effect between follicle type and day and no difference in wall PH. The ambiguous nature of the different findings between follicle walls and antra could be interpreted to mean that sampling small areas within the follicle wall were not applicable to image attributes of the follicle wall. However, Tom *et al. (*1998) reported meaningful changes in echotextural characteristics of bovine DF walls that were reflective of status of the DF using spot analysis of wall. The reason for this discrepancy remains unresolved [135].

Region analyses of the whole follicle (wall and antrum together) showed a greater NPV in SF1 compared to DF 6 days before ovulation unlike the results of spot and line analysis. Follicular

fluid and cellular components of follicle wall have different tissue properties and their characteristics differ during the course of follicular development in DF or SF. Therefore, it can be postulated that the effects of adding 2 different echotextures, antrum and wall, is not an optimal way to compare the attributes of DF and SF1. Region analysis of the follicle wall has also revealed a lower NPV in SF1 compared to DF which was not in agreement with results of spot and line analysis of follicles. It may be that the greater size of DF wall than SF1 wall compensates for the higher wall NPV and PH of SF1 compared to DF. We interpreted these inconsistencies to mean that region analysis were not an appropriate method to evaluate quantitative differences between DF and SF1.

In domestic animals and humans, morphological changes indicative of atresia appeared to be initiated in the granulosa layers as cells were sloughed into the antrum. Conversely, preovulatory follicles possessed the thickest wall, lowest cell density of granulosa and thecal layers, and highest vascularity. This is consistent with our findings from image analysis. Ultrasound image attributes of bovine follicles have been observed to be highly correlated with endocrine profiles and morphometric characteristics of follicles. In 1998, Singh *et al.* reported higher NPH and PH in SF1 compared to DF in bovine models. In addition, follicular fluid of ovulatory follicles appeared uniform while the fluid of anovulatory follicles was "rough" and heterogeneous [133]. The differences could be attributed to the changes in fluid viscosity and semi-solid components in the fluid, which would more apparent in the antra of anovulatory follicles. According to histological findings in human atretic follicles the antrum is invaded by fibroblasts. It would be logical to assume that shedding of granulosa cells into follicular fluid during atresia would be expected to cause a more heterogeneous appearance of the antrum compared to antra of non-atretic or ovulatory follicles. Therefore, it was concluded that changes in NPV, PH, and other values reflected histomorphologic changes.

Our hypothesis that image characteristics of anovulatory DF would differ quantitatively from SF1 of the same cohort and from ovulatory DF of the same cycle was supported. Higher values were observed in the SF1 compared to the DF anovulatory waves. Time did influence image attributes, but DF and SF1 were influenced in the same way. Quantitative values of anovulatory DF walls and antra increased 3 days before the follicles were no longer identifiable (become atretic) and reached the same values of the SF1 one day before they regressed. Anovulatory DF showed higher NPV and PH compared to ovulatory DF. These findings demonstrated that for the first few days of anovulatory waves, DF and SF1 have the same image attributes, DF diverge from the cohort in the middle of the wave (6 days after wave emergence) and acquire DF characteristics, but acquired characteristics of atresia at the end of the wave. These findings were consistent with our observations of DF and SF1 of ovulatory waves, except for the fate of DF which is atresia. Although ovulatory and anovulatory DF were physiologically selected and attained dominance, they exhibited different image characteristics throughout their lifespans. Continued investigations are needed to assess the physiologic status and ovulatory potential of DF of anovulatory waves.

The study of ovarian follicular dynamics using ultrasonographic image analysis tools is a relatively new research area with profound clinical relevance. Understanding the precise timing of morphological changes indicative of physiological status such as selection, ovulation, and atresia is expected to help improve stimulation protocols and help to reduce the overall amount of pharmaceutical intervention as the protocol could be tailored to the ovarian response of individual patient. Incorporating image analysis tools within the ultrasound instrument could easily provide a more efficient technique to evaluate ovarian physiology and manage clinical observations in vivo.

Conclusion

Quantitative analyses of DF and SF1 in human ovulatory follicle waves reflect their physiologic status and are in agreement with animal studies. Values for the antrum and wall were noticeably low in preovulatory DF, presumably due to a smooth and clear antrum fluid and higher vascularity of the wall. In addition, echotextural attributes of SF1 appeared to reflect histological changes associated with atresia, such as shedding of the granulosa cells into the antrum. Our results revealed that quantitative echotextural changes occurred before the time of divergence of DF from the cohort. The anovulatory DF demonstrates different attributes compared to the SF1 regardless of their identical ultimate destiny which is atresia. Dominant follicles of ovulatory and anovulatory waves were exhibited different echotextural attributes. Ovulatory DF exhibited lower values compared to anovulatory DF. Thus, the ultrasound image attributes of follicles can be used as a non-invasive indicator of follicle viability and health.

3.6 References

1. Baerwald AR, Adams GP, Pierson RA. A new model for ovarian follicular development during the human menstrual cycle. Fertil Steril 2003; 80: 116-122.

2. Pierson RA., Adams GP. Computer-assisted image analysis, diagnostic ultrasonography and ovulation induction: Strange Bedfellows. Theriogenology 1995; 43: 105-112.

3. Singh J, Pierson RA, Adams GP. Ultrasound image attributes of bovine ovarian follicles and endocrine and functional correlates. J Reprod Fertil 1998; 112: 19-29.

4. Tom JW, Pierson RA, Adams GP. Quantitative echotexture analysis of bovine corpora lutea. Theriogenology 1998; 49: 1345-1352.

5. Duggavathi R, Bartlewski PM, Pierson RA, Rawlings NC. Luteogenesis in cyclic ewes: ecohotextural, histological, and functional correlates. Biol Reprod 2003; 69: 634-639.

6. Singh J, Adams GP, Pierson RA. Promise of new imaging technologies for assessing ovarian function. Anim Reprod Sci 2003; 78: 371-399.

7. Vassena R, Adams GP, Mapletoft RJ, Pierson RA, Singh J. Ultrasound image characteristics of ovarian follicles in relation to oocyte competence and follicular status in cattle. Anim Reprod Sci 2003; 76: 25-41.

8. Tom JW, Pierson RA, Adams GP. Quantitative echotexture analysis of bovine ovarian follicles. Theriogenology 1998; 50: 339-346.

9. Adams GP, Jaiswal R, Singh J, Malhi P. Progress in understanding ovarian follicular dynamics in cattle. Theriogenology 2008; 69: 72-80.

10. Adams GP, Matteri RL, Ginther OJ. Effect of progesterone on ovarian follicles, emergence of follicular waves and circulating follicle-stimulating hormone in heifers. J Reprod Fertil 1992; 96: 627-640.

11. Adams GP, Pierson RA. Bovine model for study of ovarian follicular dynamics in humans. Theriogenology 1995; 43: 113-120.

12. Adams GP. Comparative patterns of follicle development and selection in ruminants. J Reprod Fertil Suppl 1999; 54: 17-32.

13. Adams GP, Matteri RL, Kastelic JP, Ko JC, Ginther OJ. Association between surges of follicle-stimulating hormone and the emergence of follicular waves in heifers. J Reprod Fertil 1992; 94: 177-188.

14. Ginther OJ, Beg MA, Bergfelt DR, Donadeu FX, Kot K. Follicle selection in monovular species. Biol Reprod 2001; 65: 638-647.

15. Ginther OJ, Gastal EL, Gastal MO, Bergfelt DR, Baerwald AR, Pierson RA. Comparative study of the dynamics of follicular waves in mares and women. Biol Reprod 2004; 71: 1195-1201.

16. Pierson RA, Ginther OJ. Ultrasonic evaluation of the corpus luteum of the mare. Theriogenology 1985; 23: 795-806.

17. Gougeon A. Regulation of ovarian follicular development in primates: Facts and hypotheses. Endocr Rev 1996; 17: 121-155.

18. Rivera GM, Fortune JE. Proteolysis of insulin-like growth factor binding proteins -4 and -5 in bovine follicular fluid: Implications for ovarian follicular selection and dominance. Endocrinology 2003; 144: 2977-2987.

19. Ireland JJ, Roche JF. Development of nonovulatory antral follicles in heifers: Changes in steroids in follicular fluid and receptors for gonadotropins. Endocrinology 1983; 112: 150-156.

20. Evans AC, Fortune JE. Selection of the dominant follicle in cattle occurs in the absence of differences in the expression of messenger ribonucleic acid for gonadotropin receptors. Endocrinology 1997; 138: 2963-2971.

21. Gougeon A, Lefevre B. Evolution of the diameters of the largest healthy and atretic follicles during the human menstrual cycle. J Reprod Fertil 1983; 69.

22. Gougeon A. Some aspects of the dynamics of ovarian follicular growth in the human. Acta Eur Fertil 1989; 20: 185-192.

23. Macklon NS, Fauser BC. Aspects of ovarian follicle development throughout life. Horm Res 1999; 52: 161-170.

24. Pache TD, Wladimiroff JW, De Jong FH, Hop WC, Fauser BC. Growth patterns of nondominant ovarian follicles during the normal menstrual cycle. Fertil Steril 1990; 54: 638-642.

25. Van Dessel HJ, Schipper I, Pache TD, van Geldorp H, de Jong FH, Fauser BC. Normal human follicle development: An evaluation of correlations with oestradiol, androstenedione and progesterone levels in individual follicles. Clin Endocrinol (Oxford) 1996; 44: 191-198.

26. Baerwald AR, Adams GP, Pierson RA. Characterization of ovarian follicular wave dynamics in women. Biol Reprod 2003; 69: 1023-1031.

27. Mashiach S, Dor J, Goldenberg M. Protocols for induction of ovulation: The concept of programmed cycles. In: Jones HW, Schrader C (eds), In Vitro Fertilization and Other Assisted Reproduction. Ann NY Acad Sci 1988; 541: 37-45.

28. Birtch RL, Baerwald AR, Olatunbosun OA, Pierson RA. Ultrasound image attributes of human ovarian dominant follicles during natural and oral contraceptive cycles. Reprod Biol Endocrinol 2005; 3: 12.

29. Martinuk S, Chizen D, Pierson R. Ultrasonographic morphology of the human preovulatory follicle wall prior to ovulation. Clin Anat 1992; 5: 339-352.

30. Singh J, Adams GP. Histomorphometry of dominant and subordinate bovine ovarian follicles. Anat Rec 2000; 257: 58-70.

31. Adams GP, Kot K, Smith CA, Ginther OJ. Selection of a dominant follicle and suppression of follicular growth in heifers. Anim Reprod Sci 1993; 30: 259-271.

Chapter 4

4. ULTRASOUND IMAGE ATTRIBUTES OF HUMAN OVARIAN FOLLICLES FOLLOWING DISCONTINUATION OF CONVENTIONAL AND CONTINUOUS ORAL CONTRACEPTION

4.1 Abstract

Objective: To test the hypotheses that: 1) dominant follicles of natural cycles would quantitavely differ from those that developed following OC discontinuation; and, 2) image attributes of dominant (DF) compared to 1st subordinate (SF1) follicles would differ following conventional and continuous OC regimens.

Methods: Ultrasonographic images obtained from healthy women of reproductive age recorded in previous studies were analyzed to determine differences in image attributes of ovulatory DF developed during natural menstrual and 1st cycle following OC discontinuation. The images were also analyzed to evaluate changes related to selection of the DF from its cohort in the first wave following OC discontinuation. Dominant (n=24) and 1st subordinate (n=24) follicles from the first wave following OC discontinuation, and DF of natural major ovulatory waves (n=24) were compared in a retrospective study. Ultrasonographic images of the follicular walls and antra were analyzed with 2 different techniques (spot and line analyses) using custom designed software (SYNERGYNE 2©, Saskatoon, SK, Canada). Numerical pixel values (NPV) and pixel heterogeneity (PH) of the wall and antrum were quantified. Differences in image attributes between DF and SF1 were assessed by general linear models repeated measure ANOVA. Statistical tests were set at the 95% significance level.

Results: Higher NPV ($p<0.0001$) and PH were observed in the antrum ($p=0.002$) and NPV ($p<0.0001$) in the wall of DF which developed following OC discontinuation compared to those of

natural cycles. No differences were observed in NPV and PH of DF that developed following discontinuation of conventional versus continuous OC regimens. Nor were there differences among image attributes of the SF1 developed following discontinuation of either OC regimen. Higher NPV and PH were observed in the antrum ($p<0.0001$ and $p<0.0001$, retrospectively) and wall ($p<0.0001$ and $p<0.0001$, retrospectively) of SF1 compared to DF following OC use regardless of their regimen.

Conclusion: Differences between image attributes of DF that developed following OC termination and DF of natural cycles were detected; thereby supporting our primary hypothesis. No differences were observed in image attributes of DF versus SF1 that developed following discontinuation of conventional versus continuous OC regimens. Thus, our secondary hypothesis was not supported. Computer-assisted image analyses may be useful for predicting physiologic status of follicles and may improve our understanding of factors responsible for the fertility delay or increased miscarriage rate following OC discontinuation.

4.2 Introduction

The biochemical structures of the reproductively active steroid hormones were determined in the 1930's [191]. Subsequently, it was learned that high doses of estrogens or progesterone could inhibit ovulation [192]. In 1960's, the U.S. Food and Drug Administration (FDA) approved the use of Enovid™ 10 mg (9.85 mg norethynodrel and 150 μg mestranol) for menstrual disorders and later as the first oral contraceptive (OC). All currently marketed OCs combine ≤35 μg ethinyl estradiol (EE) with a synthetic progestin [191, 193]. Several generations of combined OC utilizing orally active EE and several different progestins have been used by millions of women worldwide. Oral contraception is one of the most effective, tolerable and reversible methods of contraception [139, 145, 150, 161, 194-197].

Combined OC are designed to prevent folliculogenesis and ovulation. Estrogens have been shown to inhibit the growth of both preantral and medium-sized antral follicles in primates [198]. Concurrently, the progestin component acts to reduce LH pulsatility and amplitude of the preovulatory LH surge, thicken cervical mucus, decrease tubal mobility, and inhibit endometrial development [197]. The conventional OC administration scheme was designed to mimic natural menstrual cycles, permitting approximately 4 days of menses every 28 days. A 7-day pill free interval is required to allow 4 days of menstrual bleeding. Therefore, the conventional dosing regimen is comprised of 21 hormonally active pills, followed by a 7-day hormone free interval (HFI) [199].

It has recently become clear that conventional dosing schemes do not completely suppress folliculogenesis and ovulation [151, 152, 154]. There are reports that ovulation does occur during OC use, but most DF regress or form anovulatory cysts [151, 200]. Follicular development during the HFI was attributed to quick recovery of the hypothalamic-pituitary-ovarian axis leading to elevated levels of FSH [14, 20, 34, 55, 201, 202]. During the HFI, FSH rises above the threshold required for initiation of a new follicle wave [151, 164, 171, 203]. Consequently, follicles may continue to develop and produce estradiol, even when OC use is reinitiated following the HFI [151, 196, 201]. The dominant follicles which develop during OC administration show ultrasonographic characteristics similar to those of comparable natural-cycle follicles [149, 190]. It has therefore been suggested that follicles which develop during OC administration exhibit physiologic status similar to those that develop during natural cycles.

New dosing methods have recently been developed to suppress monthly menses with continuous administration of OC for 3, 6 or 12 months followed by a 7-day HFI. Loudon *et al.* (1977) reported that women accepted suppression of monthly menstruation using 3 months of continuous OC [204]. Shortening or removing the HFI has been shown to increase OC efficacy

[149, 162-164]. Killick *et al.* (1998) reported that the addition of 5 days of 10 mcg EE during the traditional 7-day HFI more effectively suppressed ovarian follicular activity than conventional regimens [150]. Schlaff *et al.* (2004) compared women on 3 different regimens and demonstrated that continuous OC use provided better follicular suppression compared to the conventional dosing scheme with a 7-day HFI or with 5 days of low-dose estrogen added to the usual HFI [163]. Birtch *et al.* (2006) recently demonstrated that a continuous OC regimen more effectively prevented follicle development, dominant follicle selection, and breakthrough ovulation [171].

Reversibility of contraceptive methods is of interest to many OC users since most are young women who have not started their families. It has been suggested that OC users may experience a slight delay in regaining fertility compared with those who have not used contraception or were previous users of non-hormonal contraceptive methods [170, 173, 174, 177, 205-207]. Ovarian suppression continues following OC cessation, which decreases the conception rate. The length of ovarian suppression following OC withdrawal varies among women. However, OC do not permanently affect fertility in previous users [166, 170, 173]. Parity, previous menstrual disorders, the concentration of EE in the OC, duration of OC use, behavioural factors, and age are all important factors that can affect the delay in fertility following OC discontinuation [166, 170, 174, 205]. It has been shown in our laboratory that the selection of DF took 3 days longer, dominance was manifest 2 days later, and it took approximately 5 days longer for follicles to ovulate once OC were discontinued compared to natural cycle follicles [171]. The occurrence of miscarriage also is reportedly higher in the first 3 months following OC cessation [169, 176].

Ultrasound image echotexture reflects the histological structure of the tissue [208]. Each digitally acquired image is composed of thousands of discrete picture elements, or pixels, in 1 to 256 shades of gray from black to white [208]. The human eye can discriminate a limited number of shades of gray, which reduces the precision of tissue characterization. To overcome limitations of

visual assessments of ultrasonographic images, a computer-assisted image analysis technique was developed in our laboratory to allow quantification of ultrasound images [108, 131, 133, 136].

The objectives of the present study were to evaluate ultrasonographic image attributes of DF that developed following OC discontinuation with those of natural cycles and to compare DF and SF1 of the first cycle following discontinuation in conventional and continuous OC regimens. We hypothesized that ultrasonographic image attributes would differ between DF of natural cycles and DF of the first cycle following OC discontinuation. We further hypothesized that image attributes of DF versus SF1 would differ during the first cycle following discontinuation of continuous versus conventional OC regimens.

4.3 Materials and methods

This study was a retrospective and observational. The images were obtained in 2 previous studies designed to: 1) characterize ovarian follicular dynamics during and after continuous versus conventional dosing schemes of OC; and, 2) characterize ovarian follicular wave dynamics during natural cycles [53, 190]. Participants were healthy women of reproductive age (24.5 ± 0.02 years, mean ± SEM). The study protocols were approved by the University of Saskatchewan Biomedical Ethics Review Board.

In both studies, ovulation was defined as the disappearance of a follicle ≥15 mm in diameter detected ultrasonographically the previous day followed by the subsequent visualization of a corpus luteum [92, 121]. Selection was defined as the first day the DF exceeded the diameter of the SF1 by > 2 mm [53]. High-resolution ATL Ultramark HDI 5000 ultrasound machine with 5 - 9 MHz multi-frequency convex array transducers (Advanced Technologies Laboratories; Bothell, WA, USA) were used to acquire follicular data in both studies [188, 190]. Follicle growth rates (mm/day) were determined over time in both studies by: [maximum follicle diameter – minimum follicle

diameter]/number of days of growth. This experiment consisted of 3 study groups. In the first group, sequential images of DF (n=12) and SF1 (n=12) from the first cycle after conventional OC regimen discontinuation were evaluated. The second group consisted of DF (n=12) and SF1 (n=12) images from the first cycle following discontinuation of continuous OC dosing regimen. The third group was comprised of sequential images of DF (n=24) from 30 individuals during the menstrual cycle study. Women whose data sets analyzed randomly were selected from the complete set of data from original studies.

Natural cycle study

Participants were healthy women (n = 30) of reproductive age (mean $\pm$ SEM= natural cycles 28.0 $\pm$ 6.9 years). Each woman's ovaries were imaged daily for 1 complete IOI (inter-ovulatory interval). An IOI was defined as the interval from one ovulation to the following ovulation [53].

Oral contraceptive study

Women (n = 36) received one of 2 monophasic OC formulations in either a continuous or conventional dosing scheme for 3 sequential 28-day dosing cycles [171]. In all groups, OC were initiated on the first day of menses during cycle 1. The conventional regimen consisted of 21 days of hormonally active pills followed by a 7-day hormone free interval (HFI). The continuous regimen consisted of 28 daily active pills with no HFI. The 4 study groups were: 1) 30 μg EE /150 μg levonogestrel (LNG) (21 days and 7 day HFI; n=8); 2) 30 μg EE/150 μg LNG (28 days; n=9); 3) 35 μg EE/250 μg norgestimate (NGM; 21 days and 7 day HFI; n=8); and, 4) 35 μg EE /250 μg NGM (28 days; n=11).

Women did not take OC during the fourth and final cycle of the study. Cycle 4 day 1 was defined as the first day following discontinuation of OC. Ultrasound examinations for cycle 4 began

on the second day of the cycle and were continued every second day. Daily ultrasound examinations were initiated when a follicle reached ≥16 mm in diameter and continued until the physiologic fate of the follicle was determined (ovulation or atresia).

Image analysis

Image attributes of follicles were analyzed using a graphics workstation equipped with customized software optimized for ultrasonography (SYNERGYNE 2©, Saskatoon, SK, Canada). Spot analysis and line analysis techniques were applied as described by Pierson *et al.* (1995) and Rezaei *et al.* (2009) [108, 136]. Numerical image attributes of the wall and antrum were quantified by using spot, line, and region analysis techniques. Numerical pixel value (NPV) was defined as the mean pixel gray-scale value of the sampled pixels, and pixel heterogeneity (PH) was defined as the standard deviation of the mean gray-scale values of the sampled pixels [108, 131, 133, 136].

In spot analyses, the follicle antrum was divided into 4 quadrants and pixel values from each region were measured by 4 computer generated spots approximately 15 pixels in diameter. Antral NPV and PH were obtained as an average of the 4 measurements. Line analysis was used to measure the NPV and PH values of pixels located along a 1 pixel wide line which was placed across the follicle wall. Mean pixel value and pixel heterogeneity of each follicle wall were obtained by averaging the values for 4 lines per image. Region analyses involved selection of the area of interest using a one-pixel-wide line to outline the external and internal follicular wall with the fewest image artifacts. Then a computer-generated pixel by pixel mesh was overlaid onto the area to generate a 3-dimensional framework representing processed pixel values. A computer-generated surface was placed over the framework to produce a topographical image. Color shading was applied to make subtle differences in the surface contours more visible [108, 131, 133, 136].

Image attributes of both experiments were compared using repeated measures analysis of variance (PROC MIXED, SAS/STAT, Version 9) for main effects of follicle type, day, and follicle by day interaction. Significance was set at $p< 0.05$. Results are expressed as the mean ± SEM.

4.4 Results

4.4.1 Ultrasound image characteristics during continuous and conventional OC regimens

Data for all endpoints were analyzed initially to examine differences between the continuous versus conventional dosing schemes. No differences were observed in: 1) antral and wall NPV of DF ($p=0.1453$, and $p=0.4876$, respectively); 2) antral and wall NPV of SF1 ($p=0.5848$, and $p=0.2261$, respectively); 3) antral and wall PH of DF ($p=0.1813$, $p=0.0502$, respectively); 4) antral and wall PH of SF1 ($p=0.2865$, and $p=0.7671$, respectively) in follicles developed following discontinuation of conventional and continuous dosing schemes using spot analysis of the follicle antrum and line analysis of follicle wall. Consequently, data obtained from the first cycle following discontinuation of conventional and continuous OC regimens were combined.

4.4.2 Ultrasound image characteristics of dominant follicles of natural cycles versus the first cycle following OC discontinuation

Image attributes of DF from natural cycles were compared to those of the first cycle following OC discontinuation. There were no differences between diameter profiles of DF that developed following OC discontinuation and DF of natural cycles through their developmental stages ($p=0.3563$); although, their growth rates were different ($p=0.0019$; 1.4 mm/day and 1.2 mm/day in natural cycles and OC cycles, respectively) (Figure 4.1: A).

No differences were observed by visual assessments of ultrasound images of dominant follicles from either group; although, numerical values obtained by the region analysis technique

were higher in DF that developed following OC compared to those of natural cycles (NPV $p<0.0001$; SD $p<0.0001$; Figure 4.2). Dominant follicles that developed following OC discontinuation had a higher NPV ($p<0.0001$) and PH ($p<0.0022$) in antral fluid compared to DF of natural cycles (Figure 4.1: B & C). Higher NPV ($p<0.0001$) were also detected in the walls of DF following OC termination compared to DF of natural cycle (Figure 4.1: D). There were no differences in wall PH ($p=0.1533$) between DF that developed following OC termination compared to DF from natural cycles.

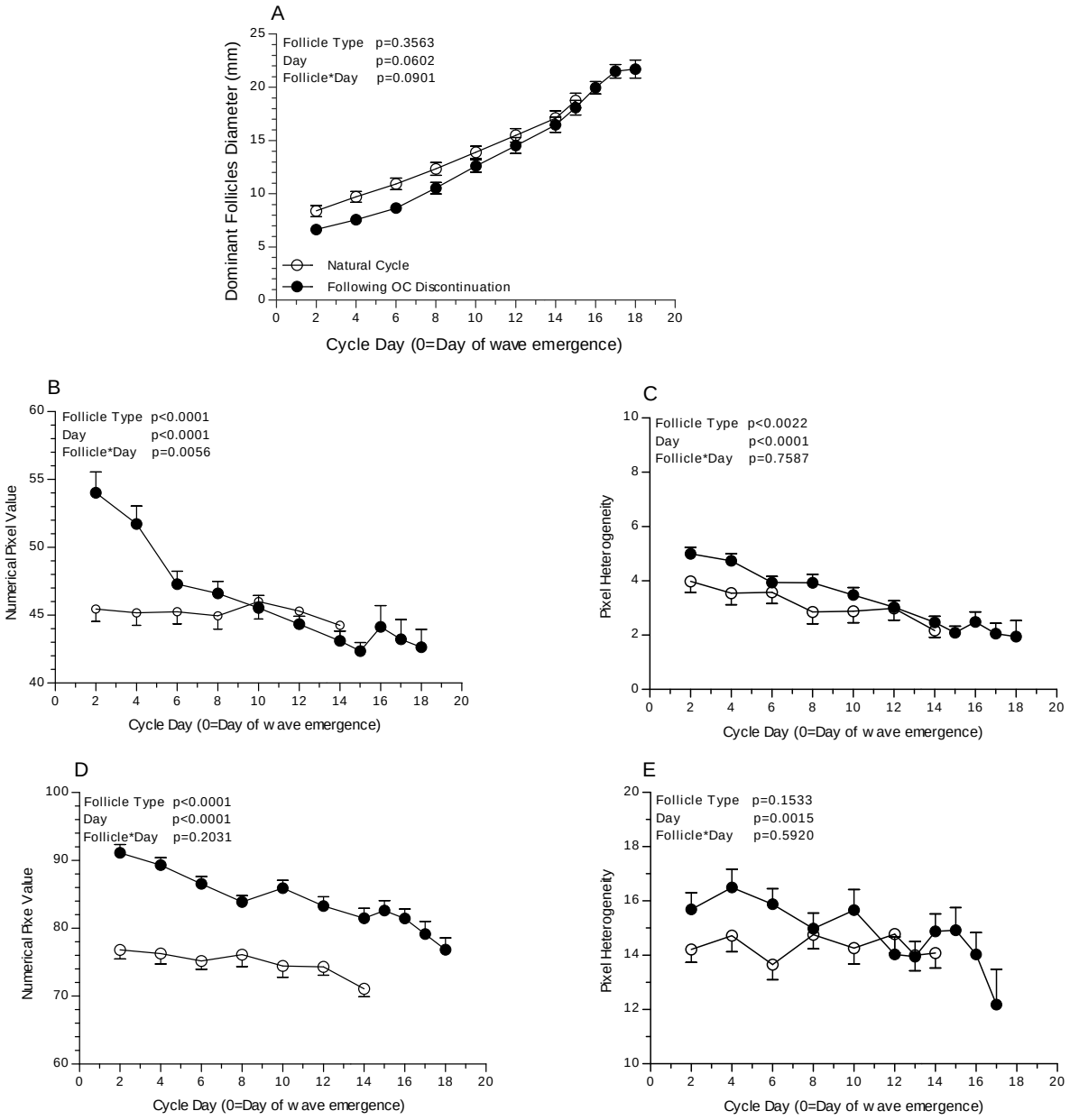

Figure 4.1: Mean follicle diameter (A), NPV (B) and PH (C) of the antrum obtained by spot analysis, and NPV (D), PH (E) of the wall obtained by line analysis of the dominant follicle that developed following OC discontinuation (●; n=24) and the dominant follicle of the natural cycle (○; n=24). Data points are represented as the mean ± standard error.

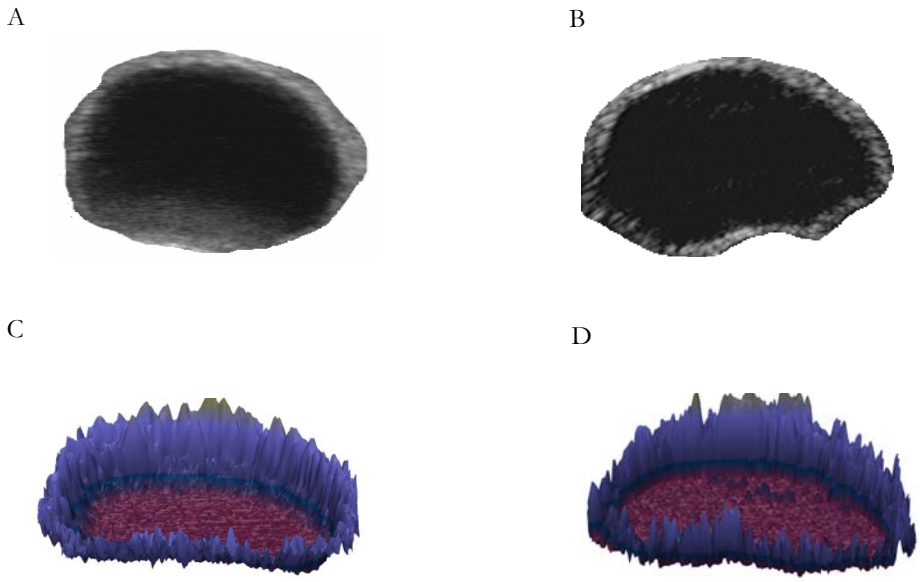

Figure 4.2: Ultrasonographic images and visual assessment (region analyses) of preovulatory dominant follicles using the region analysis. Dominant follicle of the first cycle following OC discontinuation (A, C) and ovulatory dominant follicle of natural cycle (B, D) are shown. Both dominant follicles share the same visual ultrasonographic characteristics and show a sharply defined wall with a distinct boundary from the smooth and homogenous follicular fluid and antrum. C, D represents 3-dimentional images generated using region analysis technique. Images are tilted forward 25° to enhance appreciation of the 3-dimensional aspects of the image.

4.4.3 Ultrasound image characteristics of dominant follicles compared to 1st subordinate following OC discontinuation

Twenty two of the 24 women evaluated (91.7%) grew a single preovulatory follicle and ovulated in the first cycle following OC discontinuation. The remaining 2 women formed hemorrhagic anovulatory follicles (HAF) and were excluded from analyses. The growth profiles of dominant and SF1 following OC cessation are presented (Figure 4.3: A). Physiological selection of the DF (as identified by its divergence in diameter from the SF1) occurred approximately 12 days after wave emergence following OC discontinuation ($p<0.0001$).

Spot analysis of follicle antrum: Numerical pixel values were higher in SF1 than DF ($p<0.0001$; Figure 4.3: B) which was first manifest 6 days after wave emergence. Pixel heterogeneity values (PH) were greater ($p<0.0001$; Figure 4.3: C) in the follicular fluid of SF1 compared to DF. The differences between antral PH were first observed ($p<0.0001$) 6 days after wave emergence and remained higher until the day of ovulation. Day effects for NPV ($p<0.0031$) and PH ($p=0.0500$) were significant indicating that time influenced the pixel values. Follicle by day interactions for NPV ($p<0.0001$) and PH ($p<0.0001$) were significant indicating that changes in antral NPV and PH over time were affected by the follicle type.

Line analysis of follicle wall: Numerical pixel values for the follicle wall were higher in SF1 ($p<0.0001$) compared to DF (Figure 4.3: D) starting 6 days ($P=0.0005$) after wave emergence and continuing until the day of ovulation. Follicle wall NPV progressively decreased as the DF approached the day of ovulation. There was a day effect of NPV ($p=0.0105$) indicating that time influenced wall NPV. Follicle wall PH (Figure 4.3: E) was higher in SF1 compared to DF ($p<0.0001$). Differences between PH of follicle walls were first detected 8 days ($P=0.0205$) after wave emergence and continued until the day of ovulation. The follicle by day interactions for NPV ($p<0.0001$) and PH ($p<0.0001$) indicated that the changes in NPV and PH over time were influenced by follicle type.

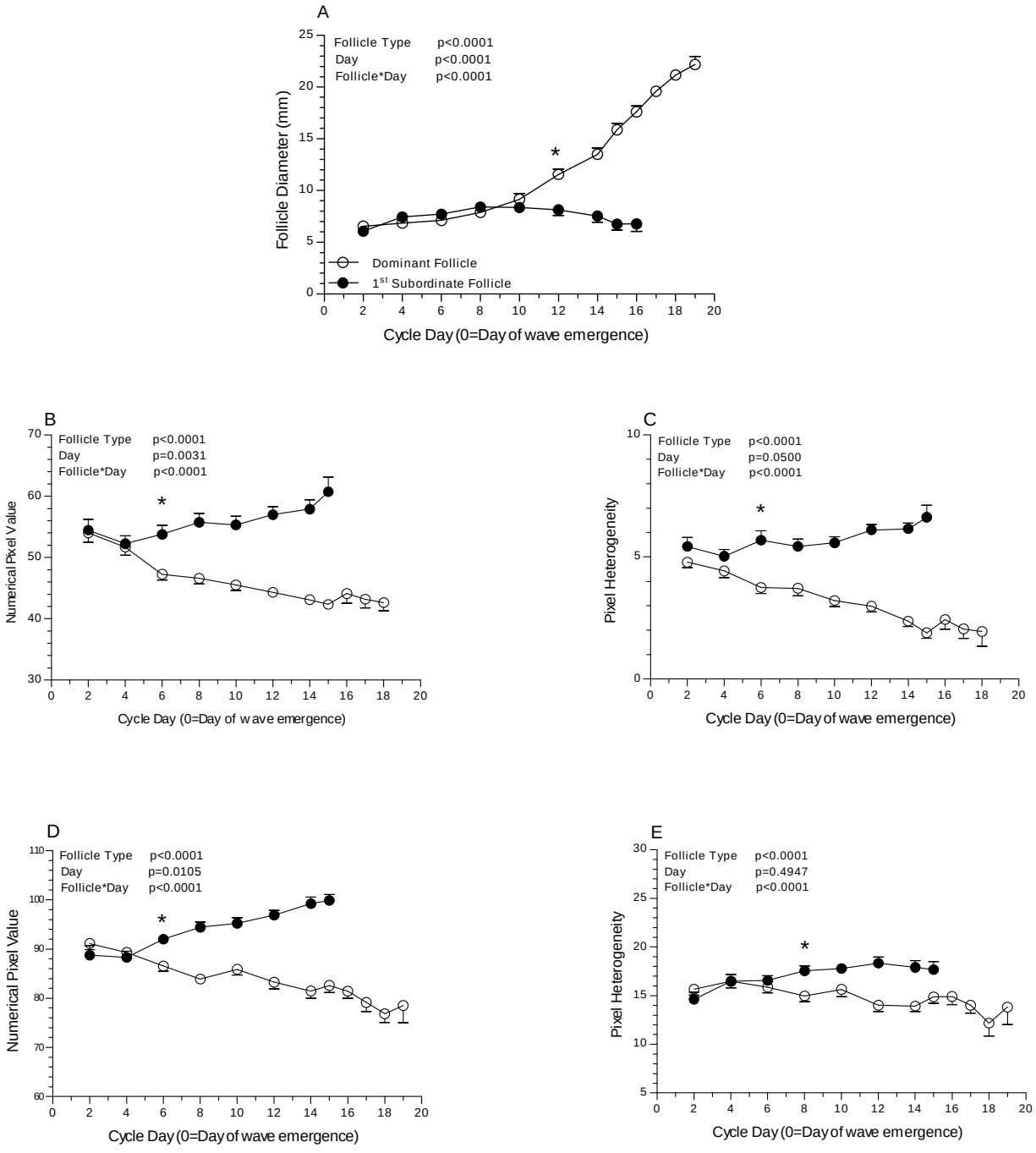

Figure 4.3: Mean follicle diameter (A), NPV (B), PH (C) of the antrum obtained by spot analysis, and NPV (D), PH (E) of the wall obtained by line analysis of the dominant (○; n=24) and 1st subordinate (●; n=24) follicles in the 1st wave following OC discontinuation (*=first day of significant difference). Data points are represented as the mean ± standard error.

4.5 Discussion

There were significant differences between ultrasonographic image attributes of ovulatory DF of natural cycles and those that developed following OC discontinuation. Image attributes of DF were similar following discontinuation of continuous and conventional OC regimens. Image attributes of SF1 also were similar. Therefore, the primary hypothesis that ultrasonographic image attributes would differ between DF of natural cycles and DF of the first cycle following OC discontinuation was supported. The secondary hypothesis that image attributes of DF versus SF1 would differ during the first cycle following discontinuation of continuous versus conventional OC regimens was not supported. These results were interpreted that exposure to exogenous steroid hormones in OC may affect follicular status, albeit in the same way regardless of dosing schemes.

A short and temporary impairment of fertility have been reported in women who discontinued OC compared with women who stopped using non-hormonal methods of contraception [37-39]. There have also been concerns about association between duration, dosage, and schemes (conventional and continuous) of OC use and impaired fertility [37]. In the present study, DF that developed after OC termination showed higher values compared to DF developed during natural cycles. These findings were interpreted to mean that the OC-induced suppressive effects on the hypothalamo-hypophyseal axis continued after OC cessation may affect the follicle's health.

Follicular wave length, interval from wave emergence to divergence of DF, and interval from selection to ovulation were greater following OC compared to these from women in natural cycles in previous study from our laboratory [171]. The follicles that develop during natural cycles are recruited and begin to grow during the late luteal phase [209]. The longer intervals to selection, dominance and ovulation in follicles following OC discontinuation may be due to residual

suppressive effects of exogenous steroids on hypothalamus-hypophyseal axis resulting in a delay in follicular recruitment compared to natural cycles [171]. It is also possible that OC synchronize follicular wave development such that follicles are at an earlier stage of development and take longer to attain selection, dominance and ovulation than in natural cycles [190].

Visual assessments of ultrasonographic images of DF developed during natural cycles and those of the 1st cycle fowling OC cessation were similar. The three-dimensional images created by region analysis technique were visually identical. However, their values obtained by region analysis differed. This apparent discrepancy was interpreted to mean that there are subtle image characteristics which cannot be detected by visual evaluation alone.

The findings in the present experiment are in a good agreement with results from a previous study in our laboratory in which the image attributes of DF versus SF1 of natural cycle were characterized. Following OC discontinuation, follicular antra and walls exhibited greater NPV and PH in SF1 compared to DF and greater values also were observed in SF1 compared to DF during natural cycles [136]. Similar patterns of follicular development were observed in both the OC and natural cycle studies; however, the changes in NPV and PH occurred at different times with higher values in DF which developed following OC cessation compared to those of natural cycles. The SF1 exhibited higher values than DF in either cycle. Taken together, the findings of current study and previous histological studies that the DF developed following OC cessation exhibit: 1) thicker walls and had lower gray-scale values indicating a lower intensity seen with ultrasonography; 2) higher blood flow; and, 3) a lesser amount of collagen tissues, compared to SF1 as they approach to ovulation [104, 108, 133]. We interpreted these findings to mean that physiologic selection is a dynamic process that is initiated well before the time that DF can be detected by its larger diameter from other follicles in the cohort.

It is logical that the histomorphological changes which occur as follicles develop to fulfill their biological function are characterized in the attributes displayed in ultrasonographic images. During follicular regression, granulosa cells from the follicle wall are detached and released into the antral fluid resulting accumulation of cellular debris within the antral cavity [101]. We observed that the SF1 of natural cycles and those of the cycle following OC termination demonstrated heterogeneous antral fluid as they start to become atretic consistent with the histological observations.

Conclusion

In summary, 3 months of conventional or continuous OC use was associated with quantitative echotextural changes within the wall and antrum of the DF that developed in the 1st wave after OC cessation. Quantitative image echotextural changes reflecting selection occurred at approximately the same time in natural cycles and following OC discontinuation; however, the values of DF developed following OC were higher than those of natural cycles. While interesting, the differences observed cannot completely explain the 3 month lag in fertility after OC termination. Further research should be performed to evaluate endocrine, histological, and imaging changes in follicles and oocyte viability assessment following OC discontinuation. This approach may improve our understanding of factors responsible for the fertility delay or increased miscarriage rate following OC discontinuation.

4.6 References

1. Goldzieher JW, Rudel HW. How the oral contraceptive came to be developed. JAMA 1974; 230: 421-425.

2. Shampo MA. The Pill: Its History and Development (The 40th Anniversary). J Pelvic Surg 2001; 7: 196-198.

3. Calderoni ME, Coupey SM. Combined hormonal contraception. Adolesc Med Clin 2005; 16: 517-537.

4. Wilkie J. Combined oral contraceptives in the new millennium what pharmacists should know. In: Canadian Pharmacist Association; 2007.

5. Sullivan H, Furniss H, Spona J, Elstein M. Effect of 21-day and 24-day oral contraceptive regimens containing gestodene (60 microg) and ethinyl estradiol (15 microg) on ovarian activity. Fertil and Steril 1999; 72: 115-120.

6. Mishell DR. Oral contraception: Past, present, and future perspectives. Inter J Fertil 1992; 37: 7-18.

7. Derman R. Oral contraceptives, assessment of benefits. J Reprod Med 1986; 31: 879-886.

8. Pierson RA, Archer DF, Moreau M, Shangold GA, Fisher AC, Creasy GW. Ortho Evra/Evra versus oral contraceptives: Follicular development and ovulation in normal cycles and after an intentional dosing error. Fertil Steril 2003; 80: 34-42.

9. Killick S, Fitzgerald C, Davis A. Ovarian activity in women taking an oral contraceptive containing 20 micrograms Ethinyl Estradiol and 150 micrograms Desogestrel: Effects of low estrogen doses during the hormone-free interval. Am J Obstet Gynecol 1998; 179: 18-24.

10. Frye CA. An overview of oral contraceptives: Mechanism of action and clinical use. Neurology 2006; 66: S29-36.

11. Marlin J, Koering, Dougias R, Danforth, Gary D Hodgen. Early folliculogenesis in primate ovaries: testing the role of estrogen. Biol Reprod 1991; 45: 890-897.

12. Wiegratz I, Kuhl H. Long-cycle treatment with oral contraceptives. Drugs 2004; 64: 2447-2462.

13. Baerwald AR, Olatunbosun OA, Pierson RA. Ovarian follicular development is initiated during the hormone-free interval of oral contraceptive use. Contraception 2004; 70: 371-377.

14. Emans SJ, Grace E, Woods ER, Smith DE, Klein K, Merola J. Adolescents' compliance with the use of oral contraceptives. JAMA 1987; 257: 3377-3381.

15. Polaneczky M, Slap G, Forke C, Rappaport A, Sondheimer S. The use of levonorgestrel implants (Norplant) for contraception in adolescent mothers. N Engl J Med 1994; 331: 1201-1206.

16. Fu H, Darroch JE, Haas T, Ranjit N. Contraceptive failure rates: New estimates from the 1995 National Survey of Family Growth. Fam Plann Perspect 1999; 31: 56-63.

17. Baerwald AR, Pierson RA. Ovarian follicular development during the use of oral contraception: a review. J Obstet Gynaecol Can 2004; 26: 19-24.

18. Bukovsky A, Caudle MR, Svetlikova M, Upadhyaya NB. Origin of germ cells and formation of new primary follicles in adult human ovaries. Reprod Biol Endocrinol 2004; 2: 20.

19. Chikazawa K, Araki S, Tamada T. Morphological and endocrinological studies on follicular development during the human menstrual cycle. J Clin Endocrinol Metab 1986; 62: 305-313.

20. Gougeon A. Some aspects of the dynamics of ovarian follicular growth in the human. Acta Eur Fertil 1989; 20: 185-192.

21. Khamsi F, Roberge S. Granulosa cells of the cumulus oophorus are different from mural granulosa cells in their response to gonadotrophins and IGF-I. J Endocrinol 2001; 170: 565-573.

22. Brian L, Cohen M.B. Further studies on pituitary and ovarian function in women receiving hormonal. Contraception 1981; 24 (2): 159-172.

23. Birtch RL, Olatunbosun OA, Pierson RA. Ovarian follicular dynamics during conventional vs. continuous oral contraceptive use. Contraception 2006; 73: 235-243.

24. Cohen BL, Katz M. Pituitary and ovarian function in women receiving hormonal contraception. Contraception 1979; 20: 475-487.

25. Spona J, Elstein M, Feichtinger W, Sullivan H, Ludicke F, Muller U, Dusterberg B. Shorter pill-free interval in combined oral contraceptives decreases follicular development. Contraception 1996; 54: 71-77.

26. Birtch RL, Baerwald AR, Olatunbosun OA, Pierson RA. Ultrasound image attributes of human ovarian dominant follicles during natural and oral contraceptive cycles. Reprod Biol Endocrinol 2005; 3: 12.

27. Killick S, Eyong, E., Elstein, M. Ovarian follicular development in oral contraceptive cycles. Fertil Steril 1987; 48: 409-413.

28. Loudon N, Foxwell M, Potts D, Guild A, Short R. Acceptability of an Oral Contraceptive that Reduces the Frequency of Menstruation: The Tri-Cyclic Pill Regimen. Br Med J 1977; 2: 487-490.

29. Schlaff WD, Lynch AM, Hughes HD, Cedars MI, Smith DL. Manipulation of the pill-free interval in oral contraceptive pill users: The effect on follicular suppression. Am J Obstet Gynecol 2004; 190: 943-951.

30. Van Heusden AM, Coelingh Bennink HJ, Fauser BC. FSH and ovarian response: Spontaneous recovery of pituitary-ovarian activity during the pill-free period vs. exogenous recombinant fsh during high-dose combined oral contraceptives. Clin Endocrinol (Oxford) 2002; 56: 509-517.

31. Fraser IS, Weisberg E. Fertility following discontinuation of different methods of fertility control. Contraception 1982; 26: 389-415.

32. Harlap S, Baras M. Conception-waits in fertile women after stopping oral contraceptives. Int J Fertil 1984; 29: 73-80.

33. Linn S, Schoenbaum SC, Monson RR, Rosner B, Ryan KJ. Delay in conception for former 'pill' users. JAMA 1982; 247: 629-632.

34. Wolfers D. Letter: The probability of conception after discontinuance of oral contraception: A note on "Oral contraception, coital frequency, and the time required to conceive". Soc Biol 1970; 17: 57-59.

35. Hassan MA, Killick SR. Is previous use of hormonal contraception associated with a detrimental effect on subsequent fecundity? Hum Reprod 2004; 19: 344–351.

36. Chasan-Taber L, Willett WC, Stampfer MJ, Spiegelman D, Rosner BA, Hunter DJ. Oral contraceptives and ovulatory causes of delayed fertility. Am J Epidemiol 1997; 146: 258-265.

37. Vessey MP, Wright NH, McPherson K, P W. Fertility after stopping different methods of contraception. Br Med J 1978; 1: 265-267.

38. Pardthaisong T, Gray R H, Gaspard U, Lambotte R, Spira A. The return of fertility following discontinuation of oral contraceptives in Thailand. Fertil Steril 1981; 35: 532-534.

39. Ford JH, MacCormac L. Pregnancy and lifestyle study: The long-term use of the contraceptive pill and the risk of age-related miscarriage. Hum Reprod 1995; 10: 1397-1402.

40. Garcia-Enguidanos A, Martinez D, Calle ME, Luna S, Valero de Bernabe J, Dominguez-Rojas V. Long-term use of oral contraceptives increases the risk of miscarriage. Fertil Steril 2005; 83: 1864-1866.

41. Ginther OJ. Waves and Echoes. In: Ginther OJ (ed.) Ultrasound imaging and animal reproduction: Fundamentals: Cross plains : Equiservices Publishing; 1995: 27-34.

42. Pierson RA. Computer-assisted image analysis, diagnostic ultrasonography and ovulation induction: Strange Bedfellows. Theriogenology 1995; 43: 105-112.

43. Rezaei E, Baelward AR, Pierson R A. Ultrasonographic image analysis of ovarian follicles during the human menstrual cycle. Reprod Biol Endo 2009; Submitted.

44. Singh J, Adams GP, Pierson RA. Promise of new imaging technologies for assessing ovarian function. Anim Reprod Sci 2003; 78: 371-399.

45. Singh J, Pierson RA, Adams GP. Ultrasound image attributes of bovine ovarian follicles and endocrine and functional correlates. J Reprod Fertil 1998; 112: 19-29.

46. Baerwald AR, Adams GP, Pierson RA. A new model for ovarian follicular development during the human menstrual cycle. Fertil Steril 2003; 80: 116-122.

47. Hanna MD, Chizen DR, Pierson RA. Characteristics of follicular evacuation during human ovulation. Ultrasound Obstet Gynecol 1994; 4: 488-493.

48. Pierson RA, Chizen D. Transvaginal Ultrasonographic assessment of normal and aberrant ovulation. In: Jaffe R, Pierson R, Abramowicz J (eds.), Imaging in infertility and reproductive endocrinology: Philadelphia: JB Lippincott Company; 1994: 129-144.

49. Baerwald AR, Adams GP, Pierson RA. Characterization of ovarian follicular wave dynamics in women. Biol Reprod 2003; 69: 1023-1031.

50. Erickson G, Yen S. New data on follicle cells in polycystic ovaries: A proposed mechanism for the genesis of cystic follicles. Seminars Reproductive Endocrinology 1984; 2: 231-234.

51. Martinuk S, Chizen D, Pierson R. Ultrasonographic morphology of the human preovulatory follicle wall prior to ovulation. Clin Anat 1992; 5: 339-352.

52. Gougeon A. Qualitative changes in medium and large antral follicles in the human ovary during the menstrual cycle. Annals Biol Anim Bioch Biophys 1979; 19: 1464–1468.

Chapter 5

5. GENERAL DISCUSSION

The studies presented in this thesis were designed to evaluate ultrasound image attributes of dominant and 1st subordinate ovarian follicles during human menstrual cycles using computer-assisted echotexture analysis. The biologically important periods studied were major ovulatory and major anovulatory follicular waves (Chapter 3) during natural menstrual cycles and the first major ovulatory waves following oral contraceptive discontinuation (Chapter 4). Our results have provided rationale for further development of image analysis techniques as a research and clinical diagnostic tool.

5.1 Ultrasound image analysis: A novel approach to understanding ovarian follicle physiology

Our understanding of ovarian physiology has increased dramatically since the introduction of ultrasonography as a research and diagnostic tool. However, evaluating the physiological status of follicles at a single ultrasound examination and elucidating the mechanism and timing of physiologic selection have remained elusive. Serial ultrasound examinations are necessary to determine individual follicular growth or regression and to understand where a given follicle is in its life cycle. Similarly, scrutiny of ultrasound images has been limited to visual evaluation of follicles and the tissue characteristics associated with the state of the follicle's viability or atresia which cannot be readily quantitated by the human eye.

In 1996, immunohistochemical labelling was used to estimate quantitative characteristics of follicular structure in Mishan gilts. The rates of granulosa and thecal cell proliferation were estimated *in vitro* by using a thymidine analogue that is incorporated into newly synthesized DNA [210]. Since the *in vitro* technique was time consuming and impractical in human studies, a method for

determining a follicle's physiologic *in vivo* status remains, therefore, highly desirable. In an early study in our labarotory, an automated computer-based method of segmentation has been applied to ultrasound images to help in detecting changes in follicles during development [211, 212]. Image segmentation is defined as the division of an image into homogeneous regions. Homogeneity can be defined in terms of intensity, color, reflectivity, and texture. The tissues represented in an ultrasound image have different textures which can be differentiated using a segmentation algorithm to partition the image [213]. Region growing, watershed, and multi-resolution texture analysis are three different segmentation methods that have been used to evaluate changes in follicles during development. Their disadvantages were over-segmentation, sensitivity to noise, time requirements, and poor detection of thin structures, such as the opposed walls of adjacent follicles [214-216].

The ultimate goal of applying imaging techniques to ovarian biology is to develop a non-invasive tool or method to determine the physiologic status of ovarian follicles on the basis a single ultrasound examination. Recently, a novel computer-assisted quantitative echotexture analysis was developed which offers a highly sensitive method which makes ultrasound images more readily appreciable. This technique allows rapid quantitation of minute variations in the images and has the potential to assess physiologic status of individual follicles (i.e., dominant versus subordinate, regressing versus growing) [108, 131] .

There are endocrinologic differences between dominant and subordinate follicles in the cattle [133]. It was demonstrated that estrogen active follicles were healthy, potentially ovulatory follicles while estrogen inactive follicles were atretic [37, 186]. The estrogen active follicles were larger than the estrogen inactive follicles and had characteristics of preovulatory follicles such as: 1) high antral concentrations of estradiol; 2) low antral concentrations of progesterone and androgens; 3) greater number of granulosa cells; and, 4) capacity of follicle cells to bind to LH. Estrogen

inactive follicles were morphologically similar to atretic follicles and exhibited: 1) low antral concentrations of estradiol; 2) high antral concentration of progesterone and androgens; and, 3) lower numbers of granulosa cells [37, 186, 217]. These types of endocrine evaluations of follicles are expensive to perform, require removal of the follicle from its *in vivo* environment and are neither practical nor ethical in clinical settings.

Computer-assisted echotexture analysis was first validated *in vitro* using bovine ovaries by Singh *et al.* (1998) [132, 133]. Pixel values of the follicle wall and antrum decreased in dominant follicles (DF) as they developed. In contrast, the pixel values in the walls of SF1 increased progressively. In addition, higher NPV were observed in the walls and antra of SF compared to DF. Significant correlations were observed between the pixel heterogeneity of the follicle antrum with intrafollicular 17β-estradiol and 17β-estradiol to progestrone ratio. Regressing follicles contained significantly higher concentrations of progesterone. The ratio of 17β-estradiol to progesterone was influenced by remarkable changes in 17β-estradiol concentration in the follicular fluid. Early-static phase dominant follicles of the first follicular wave produced less 17β-estradiol compared to the growing dominant follicles while growing dominant follicle, and preovulatory follicles produced markedly more 17β-estradiol than all other follicle types. Pixel heterogeneity (PH) of follicle wall and antrum increased during the late-static and regression phases. Therefore, as follicles regressed, the concentration of 17β-estradiol in the follicular fluid decreased and numerical values of the antra increased [132, 133].

In vivo, the growing phase of DF was characterized by decreasing antral heterogeneity [135]. The static phase was marked by a drop in wall NPV and increasing antral PH. During regression, atretic follicles were characterized by high NPV of the follicle wall and a heterogeneous antrum.

These findings were in perfect agreement with histological assessments of preovulatory and atretic follicles [133, 135]. Quantitative echotexture analysis of ultrasound images reflected the functional and endocrine characteristics of DF and SF at specific stages of development and regression.

Practical and ethical limitations prohibit the *in vivo* assessment of the hormonal microenvironment and physiologic status of follicle in humans. The only *in vivo* method we are really able to use for assessing the physiologic status of follicles remains the application of imaging techniques. Since there are similarities in morphology, physiological changes, and pathology of the ovaries in cows and women, the bovine model has been highly developed as a means for helping us to understand human folliculogenesis [97, 181, 218]. Based on our findings in animal studies, we believe that computer-assisted image analysis can be developed as a safe, effective, and non-invasive technology to evaluate human ovaries. Similarly the biological information gleaned from bovine studies is expected to migrate seamlessly to image interpretation in women.

Histomorphological studies in rhesus monkeys, sheep, cattle, and humans have revealed that the walls of dominant (preovulatory) follicles consistently have the thickest theca interna and the greatest degree of vascularity. An extensive vascular plexus in the thecal layer of preovulatory follicles provides preferential delivery of gonadotropins [70, 78]. The blood is hypoechoeic and would therefore decrease NPV because the relative proportion of blood flow to the surrounding tissues influences echotexture. In bovine studies, the walls of preovulatory follicles exhibited the greatest vascularity and the lowest pixel values and observation were consistent with those from previous histomorphological studies [70, 132]. The low pixel values observed in the preovulatory follicle wall were attributed to increased blood flow and corresponding interstitial edema.

Conversely, blood flow to SF decreases during the regression phase (or atresia) which would be expected to result in higher pixel values.

Time-related changes were observed in image attributes of the antrum and wall of dominant (DF) and first subordinate follicles (SF1) human ovarian follicles in the studies comprising this thesis. Growing DF were characterized by decreasing values in the follicle walls, whereas regressing follicles were characterized by increasing values of the wall and heterogeneity of the antrum. A significant histological characteristic of follicular regression is sloughing of granulosa cells from the follicle wall into the antral fluid. This degenerative process results in decreased numbers of granulosa cell layers comprising the stratum granulosum and accumulation of cellular debris within the antrum. Cellular debris was interpreted to be responsible for the heterogeneous pixel values observed in follicular fluid. Higher NPV and PH in antrum of SF compared to DF are attributed to greater Raleigh scatter from the granulosa cell debris [71, 208, 219, 220].

In addition to the precise quantitative results obtained by computer-assisted image analysis, we were able to visualize the numerical pixel information contained within images using a three dimensional region analysis and visualization technique. Images created by this method demonstrated that preovulatory DF had thick and sharp walls with smooth and homogenous follicular fluid. In contrast, SF1 had dull and irregular walls with heterogeneous antral fluid. It was clear in all studies that alterations in follicle image attributes were based on different functional and histomorphological changes in the follicles through their life cycle.

5. 2 Ultrasound image analysis and selection of a dominant follicle

Selection of a DF for preferential development and ovulation is arguably the most important event in ovarian physiology. While selection occurs during both ovulatory and anovulatory major

waves, ovulation has been observed only in the ovulatory major wave. It has been suggested that granulosa cells of DF acquire LH receptors (LHr) and increase their aromatization of androgen to estradiol 17β in response to LH as well as FSH [15, 221]. This level of investigation is not yet available with visualization technology and the exact mechanisms underlying physiological selection of the DF remain to be determined. In cows, the DF already has much higher concentrations of estradiol in follicular fluid by the time of physiological selection as manifest by divergence in diameter (approximately 3 times higher), and its granulosa cells produce more estradiol *in vitro* compared to the granulosa cells from SF [54, 217, 222, 223]. An *in vivo* study in women demonstrated that estradiol increases in the follicular-fluid when the DF was first identified by its larger diameter [43, 51].

The wave phenomenon of folliculogenesis was first elucidated in animal models and has been especially well studied in the domestic animal species (bovine, ovine, equine). Bovine estrous cycles are comprised of 2 or 3 major waves (in which selection of DF occurs) per cycle and equine estrous cycles have 1 or 2 minor (in which selection of DF does not occur) or major follicle waves and a major ovulatory follicular wave [53, 89, 95, 96, 224]. It has now been well established that women develop 2 to 3 minor and major follicular waves during each menstrual cycle by studying the day-to-day changes in the diameter profiles of individual ovarian follicles using ultrasonography [53, 59, 188]. The gonadotropins and ovarian steroids are ultimately responsible for regulating all of the events of folliculogenesis. In women and domestic animals, waves of follicular development are associated with changes in the reproductive hormones (estradiol, progesterone, FSH, and LH) during the menstrual cycle. Specifically, in women and domestic animals, all minor and major follicular waves were preceded by a rise in circulating concentrations of FSH [183, 188].

The mechanisms of DF selection have been difficult to determine. In bovine, divergence of DF began when the largest follicle of the wave reached approximately 8.5 mm in diameter, about 2.5 days after follicle wave emergence at approximately 4 mm. It appeared that biochemical selection of DF occurred prior to morphological selection, as evidenced by divergence in diameter between DF and SF1 follicles [59]. Rivera *et al.* (2003) examined a group of follicles in cattle before divergence in follicular size. An increase in proteolytic activity in IGFBP-4/-5 (PAPP-A) and in estradiol was demonstrated prior to morphologic selection in the DF. It was suggested that the increased PAPP-A degrades IGFBP-4 and -5, freeing more IGF to act synergistically with FSH and thus increase estradiol production in the future DF [185]. These findings have demonstrated that the follicular microenvironment changes within the pre-selected DF. It can thus be speculated that the biochemical changes cause minute histomorphologhical changes which are not detectable by visual appreciation alone, but may one day be made visible with targeted image enhancement and analysis algorithms.

In the follicular phase of the human menstrual cycle, the DF can be identified from its cohort by larger size (10 mm), higher mitotic index, and a considerable amount of estrogen in the follicular fluid [50, 60]. The growth and divergence in follicle diameters must now be defined by serial ultrasound examinations. The largest challenge to understanding when selection really occurs is that repeated measurements of the size and shape of follicles over several days are required to determine the physiological status of follicles. Based on retrospective evaluations of DF and SF1 growth (diameter) profiles obtained in a previous study, physiological selection was defined by the day of divergence in diameters that occurred approximately 7 days before ovulation, when DF and SF1 were 10 mm and 8 mm in diameter, respectively [53]. However, based on the image analysis studies comprising this thesis, selection was manifest 9 days prior to ovulation. Echotextural differences between the antra and walls of DF and SF1 were detected approximately 2 days before

the divergence in their diameters. We interpreted these results to mean that the quantitative echotextural changes reflective of histomorphological changes and perhaps biochemical changes within the follicle wall and antrum commence earlier than the time when DF are visually identified as different from others in their cohort by virtue of larger size.

Image characteristics of anovulatory DF also differed quantitatively from SF1 of the same cohort. Attributes of the wall and antrum of the SF1 were higher compared to DF of anovulatory major waves. These observations were expected from the results of studying ovulatory wave follicles. It also reiterates and supports the notion that physiologic selection of DF occurs more than once per ovarian cycle. Interestingly, image characteristics of anovulatory DF antra and walls increased 3 days before the follicles were no longer detectable and reached the same values exhibited by the SF1 one day before they disappeared. These findings can be interpreted to mean that while DF and SF1 of anovulatory waves have different attributes at the end of their life span they both acquired the same atretic characteristics.

Anovulatory and ovulatory DF revealed different image attributes in their follicle walls and antra. Higher values (NPV and PH) were observed in anovulatory DF compared to ovulatory DF which started approximately 6 to 7 days after wave emergence. This time period was comparable to the day that selection was detected by image analysis in major ovulatory waves. Moreover, the first difference in growth profile (difference in diameters) of ovulatory and anovulatory DF was observed approximately 6 to 7 days after wave emergence. This result was interpreted to mean that 6 to 7 days after wave emergence, morphological changes began in the selected follicles. That is, 6 days after wave emergence, anovulatory DF exhibited the histomorphologic characteristics of atretic follicles. It can be concluded that the image attributes of anovulatory DF were situated somewhere between characteristics of ovulatory DF and SF1. Therefore, up to some critical point, post-selection

anovulatory DF may have the capacity to develop into an ovulatory follicle, or will become atretic, depending on the endocrine environment. It is interesting to speculate that their fate may be ultimately determined by the circulating hormonal milieu or other signalling mechanisms.

Identifying the time during the menstrual cycle when physiological selection is manifest will have a great impact in fertility treatment protocols as well as contraceptive regimens. From a fertility enhancement point of view, selection is the physiologic event which must be promoted to induce the synchronous development of a cohort of follicles each of which contains a competent oocyte. Applying stimulatory drugs prior to the time of selection would be expected to improve the ovarian response, increase the quality of oocytes and therefore increase probability of fertilization and conception in assisted reproductive technology programs. In addition, we expect that the total dose of FSH required to achieve multiple follicle development could be dramatically reduced for the assisted reproduction technologies. From a contraception point of view, selection is the physiologic event which must be suppressed to prevent ovulation. If no follicle is physiologically selected to gain ovulatory capability, then ovulation and conception cannot occur. Our work here is expected to play a significant role in the development of safer and more effective contraception.

5. 3 Follicular development following oral contraceptive discontinuation

Since oral contraceptives were introduced in 1950's, they have become the most popular reversible contraception method [129]. Approximately 100 million women across the world use OC as a safe, effective, practical, and reversible method of contraception [225]. The numbers of women desiring contraception and the numbers of women who require the use of assisted reproductive technologies to complete their families are increasing [226]. Oral contraceptives have been traditionally administered in dosing schemes that mimic monthly menstruation. The conventional dosing regimen consists of 21 daily active pills followed by a seven day hormone-free interval (HFI).

The only benefit of the HFI is to increase user acceptability by allowing the physiologic event of menses [211]. However, Loudon *et al.* (1977) reported that three months of continuous OC use followed by a HFI thus allowing 4 menstrual periods per year was well accepted by women [204]. Since then, the efficacy, acceptability, and physiologic effects of continuous OC dosing schemes lasting 3, 6, and 12 months on follicular and endometrial development have been examined in detail [163, 227].

Hormonal contraception is the only form of contraception that is designed to suppress folliculogenesis and ovulation and a large proportion of OC users are young women who have not started their families or wish better control over the spacing of their pregnancies. Therefore, reversibility and an easy return to fertility is essential. A review of the literature indicated that there is a delay in the return to fertility, but not a permanent impairment to conception in women who have used OC [228]. According to the literature, a 2 to 3 month delay in conception following discontinuation of OC is common and approximately half of all women (39%-56%) conceive within three months after stopping OC compared to 2/3 (54%-65%) for previous users of intrauterine devices, condoms, diaphragms and "other" contraceptive methods [166, 171]. The incidence of miscarriage also is reportedly higher in women who do conceive in the first 3 cycles following OC discontinuation [169, 176].

It is suggested that FSH increased during the HFI due to loss of endocrine suppression of hypothalamo-pituitary axis. That is, follicular growth is initiated in the HFI. Development of physiologically selected DF has been observed during OC use and a proportion of these follicles continue preferential development to pre-ovulatory size [149, 151, 164, 196]. It has been reported that more than 85% of DF development is initiated during the HFI and ovulation of up to 50% of pre-ovulatory sized follicles may ovulate depending on the OC formulation [176, 196]. Increasing

the duration of active hormone administration to 24 days and shortening the HFI to 4 days with combined oral contraceptives resulted in greater suppression of ovarian activity compared with the conventional 21/7 regimen [213]. Further, ultrasonographic evaluations of follicle development during continuous and conventional OC use have revealed that continuous OC dosing schemes provide more complete ovarian suppression than conventional dosing. Birtch *et al.* (2006) observed that the number of follicles decreased slightly in continuous regimen as the duration of OC use increased and suggested that recruitment of fewer follicles into the growing pool occurred due to increased hypothalamo-hypophyseal-ovarian axis suppression with each subsequent cycle of OC administration [171]. Follicles that develop during OC cycles have different image attributes than follicles developing during natural cycles. In a previous study in our laboratory, higher value image attributes were observed in follicles which developed during OC cycles compared to follicles of natural cycles [53, 171]. We interpreted these findings to mean that follicle viability may be affected in previous OC users.

Few attempts have been made to understand the physiologic mechanisms underlying the delay in fertility following OC discontinuation or the reasons for increased miscarriage rates when conception occurs immediately following OC discontinuation. Ethical boundaries in human experiments have limited such studies to imaging the ovaries or systemic hormonal evaluations. Our approach was to use computer-assisted image analysis techniques to evaluate ultrasound image attributes of the follicular development that occurred following discontinuation of both continuous and conventional dosing schemes (Chapter 4). The images can be obtained using non-invasive techniques and can therefore be created at any time during a study protocol; however, we are unable to confirm the findings using histological or other invasive techniques.

In our present study (Chapter 4), we hypothesized that ovulatory DF which developed following OC discontinuation may have different "health" status that would be reflected in their ultrasound image attributes when compared to DF of natural cycles. The rationale was based on previous findings and a detailed literature review [190]. Our work demonstrated that the image attributes of DF and SF1 of the first cycle following OC discontinuation in both conventional and continuous dosing schemes were identical. That is, the OC dosing scheme did not affect image attributes differently. Higher image values were observed in antrum and wall of SF1 compared to DF of the first cycle following OC discontinuation irrespective of the OC regimen, which was in agreement with the results of the first experiment (Chapter 3). We found that values describing image attributes increased in SF1 compared to DF approximately 6 days after wave emergence in both natural and OC studies.

Quantitative differences were detected between DF and SF1 in natural cycles (Chapter 3) and the cycle following OC cessation (Chapter 4) on approximately the same day after wave emergence. In addition, higher pixel values were observed in DF of the cycle following OC compared to those of natural cycles. We interpreted these observations to mean that following OC, suppression of the hypothalamo-hypophyseal axis causes a minor delay in follicular development such that follicles take longer to be selected and ovulate. Based on image characteristics of DF of the first cycle following OC use, it can be postulated that DF health may be compromised by exposure of the follicle to the OC during its early developmental stages. Since folliculogenesis is a dynamic process, the ovarian pool is subjected to the influence of OC hormones for the duration of OC use. It can be suggested that initial growth and development of primordial to Class 5 follicles within the ovarian medulla might be affected by different endocrine environment of the ovary during OC use. In natural cycles, follicular recruitment occurs on the first day of menses or one day before. The

longer interval to selection, dominance and ovulation in follicles following OC discontinuation may be due to recruitment after the comparable time point of natural cycles. After OC discontinuation, abnormal progesterone concentrations were observed in 40% of women following the first ovulation. Thus, reduced fertility following OC cessation may be due to luteal dysfunction [190]. Changes in image attributes of DF of natural cycles and following OC cessation demonstrate that the same trends and physiological events occur in the same sequence. The only difference is the length of each phase, wave emergence to selection or selection to ovulation, which takes longer in cycles following OC use than natural cycles. These results could not explain the 3 month delay in fertility after OC termination, but they do help us to understand the functional differences in the "health" of follicles that develop after OC use.

Oocyte quality in addition to follicle structure and morphology is another important aspect of the return to fertility in previous OC users. Vassena *et al.* (2003) utilized image analysis techniques to assess follicle image attributes associated with oocyte competence in DF and SF in the bovine model. It was demonstrated that ultrasound image attributes of SF were correlated to oocyte competence. Higher NPV and PH were observed in the peri-follicular stroma of follicles containing competent oocytes compared to follicles containing incompetent oocytes [229]. Since there are ethical limitations in human oocyte studies, imaging techniques in concert with laboratory evaluations of the probability of fertilization *in vitro* and conception following embryo transfer remain the safest and most practical method for evaluation of oocyte quality and viability. The sensitivity of image analyses is not yet sufficient to provide information about the health and viability of the oocyte; however, it demonstrates promise as a non-invasive tool to assist in the evaluation of oocyte competence. Improvements in imaging technology will enhance oocyte evaluations by facilitating direct visualization. A combination of ultrasound, endocrine, histology,

and image analysis studies are necessary to evaluate all follicle components regarding the delay in fertility in previous OC users.

A better understanding of the physiologic mechanisms underlying ovarian physiology increases our knowledge about how different hormones, factors, and proteins can alter reproductive function. These findings allow us to develop more acceptable and efficacious contraceptive techniques based on a woman's individual physiologic needs, and more practical ovarian stimulation protocols to obtain oocytes for use in the assisted reproductive technologies to improve pregnancy rates during infertility treatment. Taken all together, the results reported in this thesis demonstrate that selection of DF is detectable earlier than the time of its divergence from its cohort using computer-assisted image analysis techniques. Quantitative differences between ultrasound images of ovulatory and anovulatory DF were evident. Ovulatory DF had the lowest value quantitative image attributes and the SF1 demonstrated the highest quantitative image values. Values describing image characteristics can be indicators of follicle's viability and health which can then be the basis for further improvement of image analysis techniques to provide a safe and immediate diagnostic tool.

DF of natural cycles and those that developed following OC discontinuation differed in their quantitative and qualitative image attributes. At least some aspects of the observed delay in fertility following OC use could potentially be attributed to a decrease in the follicles physiologic status associated with exposure to and possible residual effects of the exogenous steroids used in current OC.

Computer-assisted image analysis of ultrasound images shows excellent promise to be developed into a strong diagnostic, prognostic, and research tool in the evaluation of ovarian physiology and pathology. There is tremendous potential for developing echotexture analyses

techniques to diagnose biologically important times such as selection and ovulation of DF, and to characterize abnormal follicles (i.e., follicular cysts, luteinized unovulated follicles).

5.4 Overall conclusions

Taken together, by using computerized image enhancement and analysis algorithms, there was support for the hypotheses that:

1) The follicle physiologically selected to ovulate can be identified prospectively from others in its cohort;

2) There are differences between ovulatory and anovulatory DF of major waves; and,

3) DF of natural cycles quantitatively differs from those that develop following OC discontinuation.

The following hypotheses were not supported:

1) There are no differences in image attributes of dominant and SF1 of the anovulatory major waves; and,

2) The ultrasonographic image attributes of dominant and SF1 may differ between the first cycles following discontinuation of continuous and conventional OC regimens.

Chapter 6

6. GENERAL REFERENCES

1. Ankum WM. Reinier De Graaf (1641–1673) and the Fallopian tube. Hum Reprod Update 1996; 12: 365-369.

2. Ruestow EG. De Graaf, Regnier. In: Encyclopedia of Life Sciences: John Wiley & Sons, Ltd; 2001: 1038.

3. Standring S. The Ovary. In:Gray's Anatomy. Henry Gray, Susan Standring, Harold Ellis, Barry K.B. Berkovitz (eds.). New York Elsevier Churchill Livingstone; 2005: 1321-1326.

4. Gougeon A. Dynamics of human follicular growth: Morphologic, dynamics, and functional aspects. In: Comperhencive endorinology: The Ovary. Adashi E, Leung P (eds.). San Diego, California; 2004; 25-43.

5. Falin LI. The development of genital glands and the origin of germ cells in human embryogenesis. Acta Anat (Basel) 1969; 72: 195-232.

6. Gondos B. Development of the reproductive organs. Ann Clin Lab Sci 1985; 15: 363-373.

7. Baker TG. A quantitative and cytological study of germ cells in human ovaries. Proc Royal Soc Lond B Biol Sci 1963; 158: 417-433.

8. Adashi EY. The ovarian follicle: Life cycle of a pelvic clock. In: Adashi EY, Rock JA, Rosenwaks A (eds.), Reproductive endocrinology, surgery, and technology, Vol. 1. Philadelphia: Lippincott-Raven Publishers; 1996: 212-229

9. Stoop H, Honecker F, Cools M, de Krijger R, Bokemeyer C, Looijenga LH. Differentiation and development of human female germ cells during prenatal gonadogenesis: An immunohistochemical study. Hum Reprod 2005; 20: 1466-1476.

10. Qu J, Godin PA, Nisolle M, Donnez J. Distribution and epidermal growth factor receptor expression of primordial follicles in human ovarian tissue before and after cryopreservation. Hum Reprod 2000; 15: 302-310.

11. Forabosco A, Sforza C. Establishment of ovarian reserve: A quantitative morphometric study of the developing human ovary. Fertil Steril 2007.

12. McGee EA, Hsueh AJ. Initial and cyclic recruitment of ovarian follicles. Endocr Rev 2000; 21: 200-214.

13. Hirshfield AN. Development of follicles in the mammalian ovary. Int Rev Cytol 1991; 124: 43-101.

14. Gougeon A. Some aspects of the dynamics of ovarian follicular growth in the human. Acta Eur Fertil 1989; 20: 185-192.

15. Gougeon A. Regulation of ovarian follicular development in primates: Facts and hypotheses. Endocr Rev 1996; 17: 121-155.

16. Liu Y, Wu C, Lyu Q, Yang D, Albertini DF, Keefe DL, Liu L. Germline stem cells and neo-oogenesis in the adult human ovary. Dev Biol 2007; 306: 112-120.

17. Johnson J, Skaznik-Wikiel M, Lee HJ, Niikura Y, Tilly JC, Tilly JL. Setting the record straight on data supporting postnatal oogenesis in female mammals. Cell Cycle 2005; 4: 1471-1477.

18. Bukovsky A, Ayala ME, Dominguez R, Svetlikova M, Selleck-White R. Bone marrow derived cells and alternative pathways of oogenesis in adult rodents. Cell Cycle 2007; 6: 2306-2309.

19. Johnson J, Bagley J, Skaznik-Wikiel M. Oocyte generation in adult mammalian ovaries by putative germ cells in bone marrow and peripheral blood. Cell 2005; 122: 303-315.

20. Bukovsky A, Caudle MR, Svetlikova M, Upadhyaya NB. Origin of germ cells and formation of new primary follicles in adult human ovaries. Reprod Biol Endocrinol 2004; 2: 20.

21. Fortune JE. Ovarian follicular growth and development in mammals. Biol Reprod 1994; 50: 225-232.

22. Gougeon A, Chainy GB. Morphometric studies of small follicles in ovaries of women at different ages. J Reprod Fertil 1987; 81: 433-442.

23. Eppig JJ. Oocyte control of ovarian follicular development and function in mammals. Reproduction 2001; 122: 829-838.

24. Li S, Maruo T, Ladines-Llave CA, Kondo H, Mochizuki M. Stage-limited expression of myc oncoprotein in the human ovary during follicular growth, regression and atresia. Endocr J 1994; 41: 83-92.

25. Ojeda SR, Romero C, Tapia V, Dissen GA. Neurotrophic and cell-cell dependent control of early follicular development. Mol Cell Endocrinol 2000; 163: 67-71.

26. Mizunuma H, Liu X, Andoh K. Activin from secondary follicles causes small preantral follicles to remain dormant at the resting stage. Endocrinology 1999; 140: 37-42.

27. Salha O, Abusheikha N, Sharma V. Dynamics of human follicular growth and in-vitro oocyte maturation. Hum Reprod Update 1998; 4: 816-832.

28. Bradley J, Van Voorhis. Follicular Develpment. In: Knobil E, Neill J (eds.), Encyclopedia of Reproduction, vol. 2. San Deigo: Academic Press; 1998: 376-389.

29. Roy SK. Regulation of ovarian follicular development: a review of microscopic studies. Microsc Res Technique 1994; 27: 83-96.

30. Tsafriri A. Follicular development: Impact on oocyte quality. In: Fauser BCJM (ed.) FSH Action and Intraovarian regulation, vol. 6. New York: Parthenon Press; 1997: 83-105.

31. Simon AM, Goodenough DA, Li E, Paul DL. Female infertility in mice lacking connexin 37. Nature 1997; 385: 525-529.

32. Dong J AD, Nishimori K, Kumar TR, Lu N, Matzuk MM. Growth differentiation factor-9 is required during early ovarian folliculogenesis. Nature 1996; 383: 531-535.

33. Lundy T, Smith P, O'Connell A, Hudson NL, McNatty KP. Populations of granulosa cells in small follicles of the sheep ovary. J Reprod Fertil 1999; 115: 251-262.

34. Khamsi F, Roberge S. Granulosa cells of the cumulus oophorus are different from mural granulosa cells in their response to gonadotrophins and IGF-I. J Endocrinol 2001; 170: 565-573.

35. Gougeon A. Dynamics of human follicular growth: Morphologic, dynamics, and functional aspects. In: Comperhencive endorinology: The Ovary. Adashi E, Leung P (eds.). San Diego, California; 2004; 25-43.

36. Okamura H, Okuda Y, Kanzaki H, Takenaka A, Morimoto K, Nishimura T. [Ultrastructural observation of the ovulatory changes in the capillary of the human follicular apex (author's translation)]. Acta Obstet Gynaecol Jpn 1981; 33: 215-221.

37. Hillier SG, Whitelaw PF, Smyth CD. Follicular oestrogen synthesis: The 'two-cell, two-gonadotrophin' model revisited. Mol Cell Endocrinol 1994; 100: 51-54.

38. Dorrington JH, Armstrong DT. Effects of FSH on gonadal functions. Recent Prog Horm Res 1979; 35: 301-342.

39. Voorhis BJV. Follicular Develpment. In: Knobil E. NJ (ed.) In: Encyclopedia of Reproduction, vol. 2. San Deigo: Academic Press; 1998: 376-389.

40. Pache TD, Wladimiroff JW, de Jong FH, Hop WC, Fauser BC. Growth patterns of nondominant ovarian follicles during the normal menstrual cycle. Fertil Steril 1990; 54: 638-642.

41. De Kretser, Hedger DM, Loveland MP, Phillips KL. Inhibins, activins and follistatin in reproduction. Hum Reprod Update 2002; 8: 529-541.

42. Okamura H, Okuda Y, Kanzaki H, Takenaka A, Morimoto K, Nishimura T. Ultrastructural observation of the ovulatory changes in the capillary of the human follicular apex (author's translation). Acta Obstet Gynaeco Japan 1981; 33: 215-221.

43. Fauser BC, Van Heusden AM. Manipulation of human ovarian function: Physiological concepts and clinical consequences. Endocr Rev 1997; 18: 71-106.

44. Baird DT. A model for follicular selection and ovulation: Lessons from superovulation. J Steroid Biochem 1987; 27: 15-23.

45. Macklon NS, Fauser BC. Follicle development during the normal menstrual cycle. Maturitas 1998; 30: 181-188.

46. Weenen C, Laven JS, Von Bergh AR. Anti-Mullerian hormone expression pattern in the human ovary: Potential implications for initial and cyclic follicle recruitment. Mol Hum Reprod 2004; 10: 77-83.

47. Kevenaar ME, Themmen AP, Laven JS. Anti-Mullerian hormone and anti-Mullerian hormone type II receptor polymorphisms are associated with follicular phase estradiol levels in normo-ovulatory women. Hum Reprod 2007; 22: 1547-1554.

48. Cataldo NA, Giudice LC. Insulin-like growth factor binding protein profiles in human ovarian follicular fluid correlate with follicular unctional status. J Clin End Metab 1992; 74: 821–829.

49. Gougeon A, Lefevre B. Evolution of the diameters of the largest healthy and atretic follicles during the human menstrual cycle. J Reprod Fertil 1983; 69.

50. Schwartz J, Creinin M, Pymar H, Reid L. Predicting risk of ovulation in new start oral contraceptive users. Obstet Gynecol 2002; 99(2): 177-182

51. Van Dessel HJ, Schipper I, Pache TD, van Geldorp H, de Jong FH, Fauser BC. Normal human follicle development: An evaluation of correlations with oestradiol, androstenedione and progesterone levels in individual follicles. Clin Endocrinol (Oxford) 1996; 44: 191-198.

52. Ginther OJ, Beg MA, Bergfelt DR, Donadeu FX, Kot K. Follicle selection in monovular species. Biol Reprod 2001; 65: 638-647.

53. Baerwald AR, Adams GP, Pierson RA. A new model for ovarian follicular development during the human menstrual cycle. Fertil Steril 2003; 80: 116-122.

54. Ginther OJ, Beg MA, Bergfelt DR, Donadeu FX, Kot K. Follicle selection in monovular species. Biol Reprod 2001; 65: 638-647.

55. Chikazawa K, Araki S, Tamada T. Morphological and endocrinological studies on follicular development during the human menstrual cycle. J Clin Endocrinol Metab 1986; 62: 305-313.

56. Macklon NS, Fauser BC. Aspects of ovarian follicle development throughout life. Horm Res 1999; 52: 161-170.

57. Pache TD, Wladimiroff JW, De Jong FH, Hop WC, Fauser BC. Growth patterns of nondominant ovarian follicles during the normal menstrual cycle. Fertil Steril 1990; 54: 638-642.

58. van Dessel HJ, Schipper I, Pache TD, van Geldorp H, de Jong FH, Fauser BC. Normal human follicle development: An evaluation of correlations with oestradiol, androstenedione and progesterone levels in individual follicles. Clin Endocrinol (Oxf) 1996; 44: 191-198.

59. Fortune JE, Rivera GM, Yang MY. Follicular development: The role of the follicular microenvironment in selection of the dominant follicle. Anim Reprod Sci 2004; 82: 109-126.

60. Van der Does J, Exalto N, Dieben T, H. B. Ovarian activity suppression by two different low-dose triphasic oral contraceptives. Contraception 1995; 52: 357-361.

61. Erickson G, Danforth D. Ovarian control of follicle development. Am J Obstet Gynecol 1995; 2: 736-747.

62. Spicer LJ, Echternkamp SE. The ovarian insulin and insulin-like growth factor system with emphasis on domestic animals. Domest Anim Endocrinol 1995; 12: 223-245.

63. Kolena J, Channing CP. Stimulatory effects of LH, FSH and prostaglandins upon cyclic 3',5'-AMP levels in porcine granulosa cells. Endocrinology 1972; 90: 1543-1550.

64. Zeleznik A KC. Ovarian responses in macaques to pulsatile infusion of follicle stimulating hormone and luteinizing hormone: Increased sensitivity of the maturing follicle to FSH. Endocrinology 1986; 119: 2025-2032.

65. Willis DS WH, Mason HD, Galea R, Brincat M, Franks S J Clin. Premature response to luteinizing hormone of granulosa cells from anovulatory women with polycystic ovary syndrome: Relevance to mechanism of anovulation. J Clin Endocrinol Metab 1998; 83: 3984-3991.

66. O'Shea JD, Hay MF, Cran DG. Ultrastructural changes in the theca interna during follicular atresia in sheep. J Reprod Fertil 1978; 54: 183-187.

67. Zeleznik A, Schuler H, Reichert L. Gonadotropin-binding sites in the Rhesus monkey ovary: Role of the vasculature in the selective distribution of human chorionic gonadotropin to the preovulatory follicle. Endocrinology 1981; 109: 356-362.

68. Findlay JK, Drummond AE, Dyson ML, Baillie AJ, Robertson DM, Ethier JF. Recruitment and development of the follicle; the roles of the transforming growth factor-beta superfamily. Mol Cell Endocrinol 2002; 191: 35-43.

69. Eisenhauer KM, Chun X, Billig H, Hsueh AJ. Growth hormone suppression of apoptosis in preovulatory rat follicles and partial neutralization by insulin-like growth factor binding protein. Biol Reprod 1995; 53: 13-20.

70. Jonathan L, Tilly, James K. Apoptosis in ovarian development, function, and failure. In: The Ovary, 2nd ed. San Diego: Elsevier; 2004: 321-367.

71. Carsonr S, Clarke I J, Burger H G. Estradiol, testosterone, and androstenedione in ovine follicular fluid during growth and atresia of ovarian follicles. Biol Reprod 1981; 24: 105-113.

72. Boone DL, Carnegie JA, Rippstein PU, Tsang BK. Induction of apoptosis in equine chorionic gonadotropin (eCG)-primed rat ovaries by anti-eCG antibody. Biol Reprod 1997; 57: 420-427.

73. Faddy MJ, Gosden RG. A mathematical model of follicle dynamics in the human ovary. Hum Reprod 1995; 10: 770-775.

74. Hakuno N, Koji T, Yano T, Kobayashi N. Fas/APO-1/CD95 system as a mediator of granulosa cell apoptosis in ovarian follicle atresia. Endocrinology 1996; 137: 1938-1948.

75. Ashkenazi A, Dixit VM. Death receptors: Signaling and modulation. Science 1998; 281: 1305-1308.

76. Wallach D VE, Malinin NL, Goltsev YV, Kovalenko AV, Boldin MP. Tumor necrosis factor receptor and Fas signaling mechanisms. Annu Rev Immunol 1999; 17: 331-367.

78. Tilly JL, Kowalski KI, Johnson AL, Hsueh AJ. Involvement of apoptosis in ovarian follicular atresia and postovulatory regression. Endocrinology 1991; 129: 2799-2801.

79. Kaipia A, Hsueh AJ. Regulation of ovarian follicue atresia. Annu Rev Physiol 1997; 59: 349-363.

80. Naoko I, Akihisa M, Fuko MM, Katsuhiro F, Noboru M. Expression and localization of Fas ligand and Fas during atresia in porcine ovarian follicles. J Reprod Dev 2006; 52: 723-730.

81. Nakayama M, Manabe N, Nishihara S, Miyamoto H. Species-specific differences in apoptotic cell localization in granulosa and theca interna cells during follicular atresia in porcine and bovine ovaries. J Reprod Dev 2000; 46: 147-156.

82. Asdell SA. Mechanism of Ovulation. In: Zuckerman S (ed.), The Ovary. London: Academic Press; 1962: 435-449.

83. Espey L. Ovulation. In: Knobil E, Neil JD (eds.), Encyclopedia of Reproduction, vol. 3. San Diego: Academic Press; 1999: 605-614.

84. Tsafriri A CS. Ovulation. In: Adashi EY, Rosenwaks A (eds), In: Reproductive Endocrinology, Surgery, and Technology vol. 1: Philadelphia: Lippincott-Raven 1996: 235-250.

85. Zelinski-Wooten MB, Hutchison JS, Chandrasekher YA, Wolf DP, Stouffer RL. Administration of human luteinizing hormone (hLH) to macaques after follicular

development: Further titration of LH surge requirements for ovulatory changes in primate follicles. J Clin Endocrinol Metab 1992; 75: 502-507.

86. Davies P, Maclntyre E. Prostaglandins and inflammation. In: Gallin JI, Goldstein IM, Snyderman R (eds.), Inflammation: Basic principles and clinical correlates. New York: Raven Press 1992: 123-138.

87. Hodgen GD. Neuroendocrinology of the normal menstrual cycle. J Reprod Med 1989; 34: 68-75.

88. Martin M. Matzuk, Kathleen H. Burns, Maria M. Viveiros, Eppig JJ. Intercellular communication in the mammalian ovary: Oocytes carry the conversation. Science 2002; 296: 2178-2180.

89. Chen L WS, Hendrix EM, Russell PT, Cannon M, Larsen WJ. Hyaluronic acid synthesis and gap junction endocytosis are necessary for normal expansion of the cumulus mass. Mol Reprod Dev 1990; 26: 236-247.

90. Hanna MD, Chizen DR, Pierson RA. Characteristics of follicular evacuation during human ovulation. Ultrasound Obstet Gynecol 1994; 4: 488-493.

91. Koos R. Potential relevance of angiogenic factors to ovarian physiology. Semin Reprod Endocrinol 1989; 7: 918-922.

92. Bryant-Greenwood. The human relaxins: consensus and dissent. Mol Cell Endocrinol 1991; 79: 125-132.

93. Ellinwood WE, Norman RL, Spies HG. Changing frequency of pulsatile luteinizing hormone and progesterone secretion during the luteal phase of the menstrual cycle of rhesus monkeys. Biol Reprod 1984; 31: 714-722.

94. Ginther OJ. Major and minor follicular waves during the equine estrous cycle. J Equine Vet Sci 1993; 13: 18-25.

95. Adams GP, Matteri RL, Ginther OJ. Effect of progesterone on ovarian follicles, emergence of follicular waves and circulating follicle-stimulating hormone in heifers. J Reprod Fertil 1992; 96: 627-640.

96. Ginther OJ, Knopf L, Kastelic JP. Temporal associations among ovarian events in cattle during oestrous cycles with two and three follicular waves. J Reprod Fertil 1989; 87: 223-230.

97. Adams GP, Pierson RA. Bovine model for study of ovarian follicular dynamics in humans. Theriogenology 1995; 43: 113-120.

98. Baerwald A AG, Pierson RA. New model for ovarian follicular development during the human menstrual cycle. Fertil Steril 2003; 80: 116-122.

99. Ginther OJ, Knopf L, Kastelic JP. Temporal associations among ovarian events in cattle during oestrous cycles with two and three follicular waves. J Reprod Fertil 1989; 87: 223-230.

100. Adams GP, Matteri RL, Ginther OJ. Effect of progesterone on ovarian follicles, emergence of follicular waves and circulating follicle-stimulating hormone in heifers. J Reprod Fertil 1992; 96: 627-640.

101. Gougeon A. Qualitative changes in medium and large antral follicles in the human ovary during the menstrual cycle. Annals Biol Anim Bioch Biophys 1979; 19: 1464–1468.

102. Adams GP. The State of the Art Lecture: Maximizing ovarian potential: Comparative folliculogenesis. 46th Annual Meeting of the Canadian Fertility and Andrology Society; St. John's, Newfoundland 2000.

103. Adams GP, Jaiswal R, Singh J, Malhi P. Progress in understanding ovarian follicular dynamics in cattle. Theriogenology 2008; 69: 72-80.

104. Martinuk S, Chizen D, Pierson R. Ultrasonographic morphology of the human preovulatory follicle wall prior to ovulation. Clin Anat 1992; 5: 339-352.

105. Pierson RA, Adams GP. Bovine model for study of ovarian follicular dynamics in humans Theriogenology 1995; 43: 113-120.

106. Block E. Quantitative morphological investigations of the follicular system in women: Variations at different ages. Acta Anat (Basel) 1952; 14: 108-123.

107. Zagzebski J. Physics and Instrumentation. In: Ruby E, Sabbagha JB (eds.), Diagnostic Ultrasound Applied to Obstetrics and Gynecology. Philadelphia: Lippincott Company; 1994: 3-44.

108. Bomsel-Helmreich O, Al-Mufti W. Ultrasonography of normal and abnormal follicular development. In: Jaffe R, Pierson R, Abramowicz J (eds.), Imaging in infertility and reproductive endocrinology. Philadelphia: JB Lippincott Company; 1994: 117-128.

109. Leibman AJ, Kruse B, Mc Sweeney MB. Transvaginal sonography: comparison with transabdominal sonography in the diagnosis of pelvic masses. Am J Roentgenol 1988; 151: 89-92.

110. Gougeon A. Qualitative changes in medium and large antral follicles in the human ovary during the menstrual cycle. Annals Biol Anim Bioch Biophys 1979; 19: 1464–1468.

111. Pierson RA. Computer-assisted image analysis, diagnostic ultrasonography and ovulation induction: Strange bedfellows. Theriogenology 1995; 43: 105-112.

112. Nyborg WL, Zisken MC. Ultrasound bioeffect. In: Biological Effects of Ultrasound: Churchill Livingston, New York; 1985: 77-84.

113. Wild JJ. The use of ultrasonic pulses for the measurement of biological tissues and the detection of tissue density changes. Surgery 1950; 27: 183-192.

114. Liu X, Hart EJ, Dai Q, Rawlings NC, Pierson RA, Bartlewski PM. Ultrasonographic image attributes of non-ovulatory follicles and follicles with different luteal outcomes in gonadotropin-releasing hormone (GnRH)-treated anestrous ewes. Theriogenology 2007; 67: 957-969.

115. Zagzebski J. Pulse-Echo Ultrasound Instrumentation. In: Zagzebski J (ed.) In: Essentials of Ultrasound Physics. Philadelphia: Elsevier Health Scenices; 1996; 46-68.

116. Mendelson EB, Bohm-Velez M, Joseph N, Neiman HL. Gynecologic imaging: comparison of transabdominal and transvaginal sonography. Radiology 1988; 166: 321-324.

117. Lerner JP, Timor-Tritsch IE. Morphological evaluation of the ovary using transvaginal sonography In: Kurjak A (ed.) Ultrasound and the Ovary. New York: Taylor & Francis; 1994: 115-129.

118. Hearn-Stebbins B, Jaffe R, Brown H. Ultrasonographic evaluation of normal pelvic anatomy. In: Jaffe R, Pierson R, Abramowicz J (eds.), Imaging in infertility and reproductive endocrinology: Philadelphia: JB Lippincott Company; 1994: 1-21.

119. Zagzebski J. Properties of Ultrasound Transducer. In: Zagzebski J (ed.) Essentials of Ultrasound Physics. Philadelphia: Elsevier's; 1996: 20-45.

120. Abramowicz J, Jaffe R, Pierson R. Transvaginal color Doppler ultrasonography in the assessment of uterine and ovarian blood flow. In: Jaffe R, Pierson R, Abramowicz J (eds.), Imaging in infertility and reproductive endocrinology: Philadelphia: JB Lippincott Company; 1994: 167-178.

121. Backstrom T, Nakata M, Pierson R. Ultrasonography of normal and aberrant luteogenesis In: Jaffe R, Pierson R, Abramowicz J (eds.), Imaging in infertility and reproductive endocrinology: Philadelphia: JB Lippincott Company; 1994: 143-166

122. Pierson RA, Chizen D. Transvaginal Ultrasonographic assessment of normal and aberrant ovulation. In: Jaffe R, Pierson R, Abramowicz J (eds.), Imaging in infertility and reproductive endocrinology: Philadelphia: JB Lippincott Company; 1994: 129-142.

123. Pierson RA, Chizen D. Transvaginal diagnostic ultrasonography in evaluation and management of infertility. J Obstet Gynaecol Can 1991.

124. Baxes G. Fundamentals of Digital Image Processing. In: Digital image processing, principles and applications: New York: John Wiley & Sons 1994; 13-36.

125. Bomsel-Helmreich O A-MW (ed.). Ultrasonography of normal and abnormal follicular development. Philadelphia: JB Lippincott Company; 1994: 117-128.

126. Martinuk S CD, Pierson R. Ultrasonographic morphology of the human preovulatory follicle wall prior to ovulation. Clin Anat 1992; 5: 339-352.

127. Zalud I, Kurajak AH, Weiner Z. The corpus luteum. In: Kurjak A (ed.) Ultrasound and the Ovary. New York, London: Parthenon; 1994: 99-114.

128. Pincus G RJ, Garcia C, Rice Whira E, Pamaqua M, Rodriques I. Fertility control with oral medication. Am J Obstet Gynecol 1958; 75: 333-1346.

129. Dickey R. Managing Contraceptive Pill Patients. 8th edition. Durant: EMIS, Inc. Medical Publishers; 1997.

130. Wallach M, Grimes D. Modern oral contraception: Updates from the contraception report. Totowa: Emro; 2000

131. Singh J, Adams GP, Pierson RA. Promise of new imaging technologies for assessing ovarian function. Anim Reprod Sci 2003; 78: 371-399.

132. Singh J, Pierson RA, Adams GP. Ultrasound image attributes of the bovine corpus luteum: Structural and functional correlates. J Reprod Fertil 1997; 109: 35-44.

133. Singh J, Pierson RA, Adams GP. Ultrasound image attributes of bovine ovarian follicles and endocrine and functional correlates. J Reprod Fertil 1998; 112: 19-29.

134. Tom JW, Pierson RA, Adams GP. Quantitative echotexture analysis of bovine corpora lutea. Theriogenology 1998; 49: 1345-1352.

135. Tom JW, Pierson RA, Adams GP. Quantitative echotexture analysis of bovine ovarian follicles. Theriogenology 1998; 50: 339-346.

136. Rezaei E, Baelward AR, Pierson R A. Ultrasonographic image analysis of ovarian follicles during the human menstrual cycle: Imageing physiologic selection. Reprod Bio Endo 2009; Submitted.

137. Guillebaud. Contraception: Your questions answered. In: Edinburgh: Churchill Livingstone; 1993: 188–190.

138. Hale R. Phasic approach to oral contraceptives. Am J Obstet Gynecol 1987; 157: 1052-1058.

139. Calderoni ME, Coupey SM. Combined hormonal contraception. Adolesc Med Clin 2005; 16: 517-537.

140. Kwiecien M, Edelman A, Nichols MD, Jensen JT. Bleeding patterns and patient acceptability of standard or continuous dosing regimens of a low-dose oral contraceptive: A randomized trial. Contraception 2003; 67: 9-13.

141. Poindexter A, Reape KZ, Hait H. Efficacy and safety of a 28-day oral contraceptive with 7 days of low-dose estrogen in place of placebo. Contraception 2008; 78: 113-119.

142. Van Heusden A, Fauser B. Residual ovarian activity during oral steroid contraception. Hum Reprod Update 2002; 8: 345-358.

143. Fitzgerald C, Elstein M, Spona J. Effect of age on the response of the hypothalamo-pituitary-ovarian axis to a combined oral contraceptive. Fertil Steril 1999; 71: 1079-1084.

144. Poindexter A. The emerging use of the 20-microg oral contraceptive. Fertil Steril 2001; 75: 457-465.

145. Mishell DR Jr. Oral contraception: Past, present, and future perspectives. Int J Fertil 1992; 36 Suppl 1: 7-18.

146. Derman R. Oral contraceptives: Assessment of benefits. J Reprod Med 1986; 31 (9 Suppl): 879-886.

147. Arraztoa JA, Monget P, Bondy C, Zhou J. Expression patterns of insulin-like growth factor-binding proteins 1, 2, 3, 5, and 6 in the mid-cycle monkey ovary. J Clin Endocrinol Metab 2002; 87: 5220-5228.

148. Crosignani PG, Testa G, Vegetti W, Parazzini F. Ovarian activity during regular oral contraceptive use. Contraception 1996; 54: 271-273.

149. Young RL, Snabes MC, Frank ML. A randomized, double-blind, placebo-controlled comparison of the impact of low-dose and triphasic oral contraceptives on follicular development. Am J Obstet Gynecol 1992; 167: 678-682.

150. Killick S, Eyong E, Elstein M. Ovarian follicular development in oral contraceptive cycles. Fertil Steril 1987; 48: 409-413.

151. Killick S, Fitzgerald C, Davis A. Ovarian activity in women taking an oral contraceptive containing 20 micrograms Ethinyl Estradiol and 150 micrograms Desogestrel: Effects of low Estrogen doses during the hormone-free Interval. Am J obstet Gynecol 1998; 179: 18-24.

152. Baerwald AR, Olatunbosun OA, Pierson RA. Ovarian follicular development is initiated during the hormone-free interval of oral contraceptive use. Contraception 2004; 70: 371-377.

153. Emans SJ, Grace E, Woods ER, Smith DE, Klein K, Merola J. Adolescents' compliance with the use of oral contraceptives. JAMA 1987; 257: 3377-3381.

154. Kuhl H, Gahn G, Romberg G, Marz W, Taubert HD. A randomized cross-over comparison of two low-dose oral contraceptives upon hormonal and metabolic parameters: Effects upon sexual hormone levels. Contraception 1985; 31: 583- 593.

155. Polaneczky M, Slap G, Forke C, Rappaport A, Sondheimer S. The use of levonorgestrel implants (Norplant) for contraception in adolescent mothers. N Engl J Med 1994; 331: 1201-1206.

156. Rosenberg MJ, Meyers A, Roy V. Efficacy, cycle control, and side effects of low- and lower-dose oral contraceptives: a randomized trial of 20 micrograms and 35 micrograms estrogen preparations. Contraception 1999; 60: 321-329.

157. Spellacy WN, Kalra PS, Buhi WC, Birk SA. Pituitary and ovarian responsiveness to a graded gonadotropin releasing factor stimulation test in women using a lowestrogen or a regular type of oral contraceptive. Am J Obstet Gynecol 1980; 137: 109-115.

158. Teichmann AT, Brill K, Albring M, Schnitker J, Wojtynek P, Kustra EX. The influence of the dose of ethinylestradiol in oral contraceptives on follicle growth. Gynecol Endocrinol 1995; 9: 299-305.

159. Van Heusden AM, Fauser BC. Activity of the pituitary-ovarian axis in the pill-free interval during use of low-dose combined oral contraceptives. Contraception 1999; 59: 237-243.

160. Bracken MB, Hellenbrand KG, Holford TR, Spira A. Conception delay after oral contraceptive use: The effect of estrogen dose [Fertility following hormonal contraception (author's translation)]. Fertil Steril 1990; 53: 21-27.

161. Lanes SF, Birmann B, Walker AM, Singer S. Oral contraceptive type and functional ovarian cysts. Am J Obstet Gynecol 1992; 166: 956-961.

162. Sullivan H, Furniss H, Spona J, Elstein M. Effect of 21-day and 24-day oral contraceptive regimens containing gestodene (60 microg) and ethinyl estradiol (15 microg) on ovarian activity. Fertil Steril 1999; 72: 115-120.

163. Van Heusden AM, Coelingh Bennink HJ, Fauser BC. FSH and ovarian response: Spontaneous recovery of pituitary-ovarian activity during the pill-free period vs. exogenous recombinant FSH during high-dose combined oral contraceptives. Clin Endocrinol (Oxford) 2002; 56: 509-517.

164. Schlaff WD, Lynch AM, Hughes HD, Cedars MI, Smith DL. Manipulation of the pill-free interval in oral contraceptive pill users: The effect on follicular suppression. Am J Obstet Gynecol 2004; 190: 943-951.

165. Spona J, Elstein M, Feichtinger W, Sullivan H, Ludicke F, Muller U, Dusterberg B. Shorter pill-free interval in combined oral contraceptives decreases follicular development. Contraception 1996; 54: 71-77.

166. Hassan J, Kulenthran A, Thum YS. The return of fertility after discontinuation of oral contraception in Malaysian women. Med J Malaysia 1994; 49: 348-350.

167. Pardthaisong T, Gray R H, Gaspard U, Lambotte R, Spira A. The return of fertility following discontinuation of oral contraceptives in Thailand. Fertil Steril 1981; 35: 532-534.

168. Grimes D, Godwin A, Rubin A, Smith J, Lacarra M. Ovulation and follicular development associated with three low-dose oral contraceptives: A randomized controlled trial. Obstet Gynecol 1994; 83: 29-34.

169. Weisberg E. Fertility after discontinuation of oral contraceptives. Repro Fertil 1982; 1: 261-272.

170. Garcia-Enguidanos A, Martinez D, Calle ME, Luna S, Valero de Bernabe J, Dominguez-Rojas V. Long-term use of oral contraceptives increases the risk of miscarriage. Fertil Steril 2005; 83: 1864-1866.

171. Harlap S, Baras M. Conception-waits in fertile women after stopping oral contraceptives. Int J Fertil 1984; 29: 73-80.

172. Birtch RL, Olatunbosun OA, Pierson RA. Ovarian follicular dynamics during conventional vs. continuous oral contraceptive use. Contraception 2006; 73: 235-243.

173. Farrow A, Hull M, Northstone K, Taylor H, Ford W, Golding J. Prolonged use of oral contraception before a planned pregnancy is associated with a decreased risk of delayed conception. Hum Reprod 2002; 17: 2754-2761.

174. Fraser IS, Weisberg E. Fertility following discontinuation of different methods of fertility control. Contraception 1982; 26: 389-415.

175. Linn S, Schoenbaum SC, Monson RR, Rosner B, Ryan KJ. Delay in conception for former 'pill' users. JAMA 1982; 247: 629-632.

176. Baerwald AR, Olatunbosun OA, Pierson RA. Effects of oral contraceptives administered at defined stages of ovarian follicular development. Fertil Steril 2006; 86: 27-35.

177. Ford JH, MacCormac L. Pregnancy and lifestyle study: The long-term use of the contraceptive pill and the risk of age-related miscarriage. Hum Reprod 1995; 10: 1397-1402.

178. Hassan MA, Killick SR. Is previous use of hormonal contraception associated with a detrimental effect on subsequent fecundity? Hum Reprod 2004; 19: 344–351.

179. Gaspard U, Lambotte R, Spira A. Fertility and characteristics of ovulation after discontinuing oral contraception. Contracept Fertil Sex (Paris) 1984; 12: 1005-1010.

180. Janerich DT, Lawrence CE, Jacobson HI. Fertility patterns after discontinuation of use of oral contraceptives. Lancet 1976; 1: 1051-1053.

181. Duggavathi R, Bartlewski PM, Pierson RA, Rawlings NC. Luteogenesis in cyclic ewes: Echotextural, histological, and functional correlates. Biol Reprod 2003; 69: 634-639.

182. Vassena R, Adams GP, Mapletoft RJ, Pierson RA, Singh J. Ultrasound image characteristics of ovarian follicles in relation to oocyte competence and follicular status in cattle. Anim Reprod Sci 2003; 76: 25-41.

183. Adams GP. Comparative patterns of follicle development and selection in ruminants. J Reprod Fertil Suppl 1999; 54: 17-32.

184. Adams GP, Matteri RL, Kastelic JP, Ko JC, Ginther OJ. Association between surges of follicle-stimulating hormone and the emergence of follicular waves in heifers. J Reprod Fertil 1992; 94: 177-188.

185. Ginther OJ, Gastal EL, Gastal MO, Bergfelt DR, Baerwald AR, Pierson RA. Comparative study of the dynamics of follicular waves in mares and women. Biol Reprod 2004; 71: 1195-1201.

186. Pierson RA, Ginther OJ. Ultrasonic evaluation of the corpus luteum of the mare. Theriogenology 1985; 23: 795-806.

187. Rivera GM, Fortune JE. Proteolysis of insulin-like growth factor binding proteins -4 and -5 in bovine follicular fluid: implications for ovarian follicular selection and dominance. Endocrinology 2003; 144: 2977-2987.

188. Ireland JJ, Roche JF. Development of nonovulatory antral follicles in heifers: Changes in steroids in follicular fluid and receptors for gonadotropins. Endocrinology 1983; 112: 150-156.

189. Evans AC, Fortune JE. Selection of the dominant follicle in cattle occurs in the absence of differences in the expression of messenger ribonucleic acid for gonadotropin receptors. Endocrinology 1997; 138: 2963-2971.

190. Baerwald AR, Adams GP, Pierson RA. Characterization of ovarian follicular wave dynamics in women. Biol Reprod 2003; 69: 1023-1031.

191. Mashiach S, Dor J, Goldenberg M. Protocols for induction of ovulation: The concept of programmed cycles. In: Jones HW, Schrader C (eds), In Vitro Fertilization and Other Assisted Reproduction. Ann NY Acad Sci 1988; 541: 37-45.

192. Birtch RL, Baerwald AR, Olatunbosun OA, Pierson RA. Ultrasound image attributes of human ovarian dominant follicles during natural and oral contraceptive cycles. Reprod Biol Endocrinol 2005; 3: 12.

193. Goldzieher JW, Rudel HW. How the oral contraceptive came to be developed. JAMA 1974; 230: 421-425.

194. Shampo MA. The pill: Its history and development (The 40th Anniversary). J Pelvic Med Surg 2001; 7: 196-198.

195. Wilkie J. Combined oral contraceptives in the new millennium what pharmacists should know. In: Canadian Pharmacist Association; 2007.

196. Pierson RA, Archer DF, Moreau M, Shangold GA, Fisher AC, Creasy GW. Ortho Evra/Evra versus oral contraceptives: Follicular development and ovulation in normal cycles and after an intentional dosing error. Fertil Steril 2003; 80: 34-42.

197. Frye CA. An overview of oral contraceptives: mechanism of action and clinical use. Neurology 2006; 66 Suppl 3: 29-36.

198. Marlin J, Koering, Dougias R, Danforth, Gary D Hodgen. Early folliculogenesis in primate ovaries: Testing the role of estrogen. Biol Reprod 1991; 45: 890-897.

199. Wiegratz I, Kuhl H. Long-cycle treatment with oral contraceptives. Drugs 2004; 64: 2447-2462.

200. Fu H, Darroch JE, Haas T, Ranjit N. Contraceptive failure rates: New estimates from the 1995 National Survey of Family Growth. Fam Plann Perspect 1999; 31: 56-63.

201. Baerwald AR, Pierson RA. Ovarian follicular development during the use of oral contraception: A review. J Obstet Gynaecol Can 2004; 26: 19-24.

202. Brian L, Cohen M.B. Further studies on pituitary and ovarian function in women receiving hormonal. Contraception 1981; 24 (2): 159-172.

203. Cohen BL, Katz M. Pituitary and ovarian function in women receiving hormonal contraception. Contraception 1979; 20: 475-487.

204. Loudon N, Foxwell M, Potts D, Guild A, Short R. Acceptability of an oral contraceptive that reduces the frequency of menstruation: The tri-cyclic pill regimen. Br Med J 1977; 2: 487-490.

205. Wolfers D. Letter: The probability of conception after discontinuance of oral contraception: A note on "Oral contraception, coital frequency, and the time required to conceive". Soc Biol 1970; 17: 57-59.

206. Chasan-Taber L, Willett WC, Stampfer MJ, Spiegelman D, Rosner BA, Hunter DJ. Oral contraceptives and ovulatory causes of delayed fertility. Am J Epidemiol 1997; 146: 258-265.

207. Vessey MP, Wright NH, McPherson K, P W. Fertility after stopping different methods of contraception. Br Med J 1978; 1: 265-267.

208. Ginther OJ. Waves and Echoes. In: Ginther OJ (ed.) Ultrasound Imaging and Animal Reproduction: Fundamentals: Cross plains : Equiservices Publishing; 1995: 27-34.

209. Erickson G, Yen S. New data on follicle cells in polycystic ovaries: A proposed mechanism for the genesis of cystic follicles. Sem Reprod Endocrinol 1984; 2: 231-234.

210. Fricke P.M. FJJ, Reynolds L.P., and Redmer D.A. Growth and cellular proliferation of antral follicles throughout the follicular phase of the estrous cycle in meishan gilts. Biol Reprod 1996; 54: 879-887.

211. Wiegratz I, Kuhl H. Long-cycle treatment with oral contraceptives. Drugs 2004; 64: 2447-2462.

212. Lu Q. 3D Follicle Segmentation in Ultrasound Image Volumes of Ex-Situ Ovine Ovaries. Saskatoon: Master of Science Thesis, University of Saskatchewan 2008: pp 23-47.

213. Klipping C, Duijkers I, Trummer D, Marr J. Suppression of ovarian activity with a drospirenone-containing oral contraceptive in a 24/4 regimen. Contraception 2008; 78: 16-25.

214. Beucher S, Lantuejoul C. Use of watersheds in contour detection. In: Workshop Image Processing: Real-time edge and. motion detection/estimation; 1979: 17-21

215. Krivanek A. Ovarian ultrasound image analysis: Follicle segmentation. IEEE Trans Med Imaging 1998; 17: 935-944.

216. Muzzolini R, Yang YH, Pierson RA. Multiresolution texture segmentation with application to diagnosticultrasound image. IEEE Trans Med Imaging 1993; 12: 108-124.

217. Ireland JJ, Roche JF. Growth and differentiation of large antral follicles after spontaneous luteolysis in heifers: Changes in concentration of hormones in follicular fluid and specific binding of gonadotropins to follicles. J Anim Sci 1983; 57: 157-167.

218. Baird DT. Factors regulating the growth of the preovulatory follicle in the sheep and human. J Reprod Fertil 1983; 69: 343-352.

219. Hughes FM Jr GW. Biochemical identification of apoptosis (programmed cell death) in granulosa cells: Evidence for a potential mechanism underlying follicular atresia. Endocrinology 1991; 129: 2415-2422.

220. Hurwitz A, Adashi E. Ovarian follicular atresia as an apoptotic process. In: Adashi E, Leung P (eds.), The Ovary. New York: Raven Press; 1993: 473-486.

221. Gougeon A. Dynamics of follicular growth in the human: A model from preliminary results. Hum Reprod 1986; 1: 81-87.

222. Ireland JJ, Roche JF. Development of antral follicles in cattle after prostaglandin-induced luteolysis: Changes in serum hormones, steroids in follicular fluid, and gonadotropin receptors Endocr J 1982; 111: 2077-2086.

223. Beg MA. Follicular-fluid factors and granulosa-cell gene expression associated with follicle deviation in cattle. Biol Reprod 2001; 64: 432-441.

224. Adams GP, Dierschke GJ. Ultrasonic imaging of ovarian dynamics during the menstrual cycle in rhesus monkyes. Am J Primatol 1992; 27:13.

225. Society of Obstetricians and Gynaecologists of Canada (SOGC). Oral Contraceptive Pill (a.k.a. the Pill) In: http://www.sexualityandu.ca/about/index.aspx; 2007.

226. Inhorn MC. Global infertility and the globalization of new reproductive technologies: Illustrations from Egypt. Social Science & Medicine 2003; 56: 1837-1851.

227. Anderson FD, Hait H. A multicenter, randomized study of an extended cycle oral contraceptive. Contraception 2003; 68: 89-96.

228. Spira A. [Fertility following hormonal contraception (author's translation)]. Contracept Fertil Sex (Paris) 1983; 11: 903-907.

229. Singh J, Adams GP. Histomorphometry of dominant and subordinate bovine ovarian follicles. Anat Rec 2000; 257: 58-70.

230. Adams GP, Kot K, Smith CA, Ginther OJ. Selection of a dominant follicle and suppression of follicular growth in heifers. Anim Reprod Sci 1993; 30: 259-271.